AD-A039 578 ANALYTICS INC WILLOW GROVE PA F/G 15/4
SIMULATION OF ADVANCED INTEGRATED RECONNAISSANCE SYSTEMS. VOLUM--ETC(U)
APR 69 S W LEIBHOLZ, S F MARTIN N62269-68-C-0441
UNCLASSIFIED 1004-1 NL

1 OF 3
AD A039 578

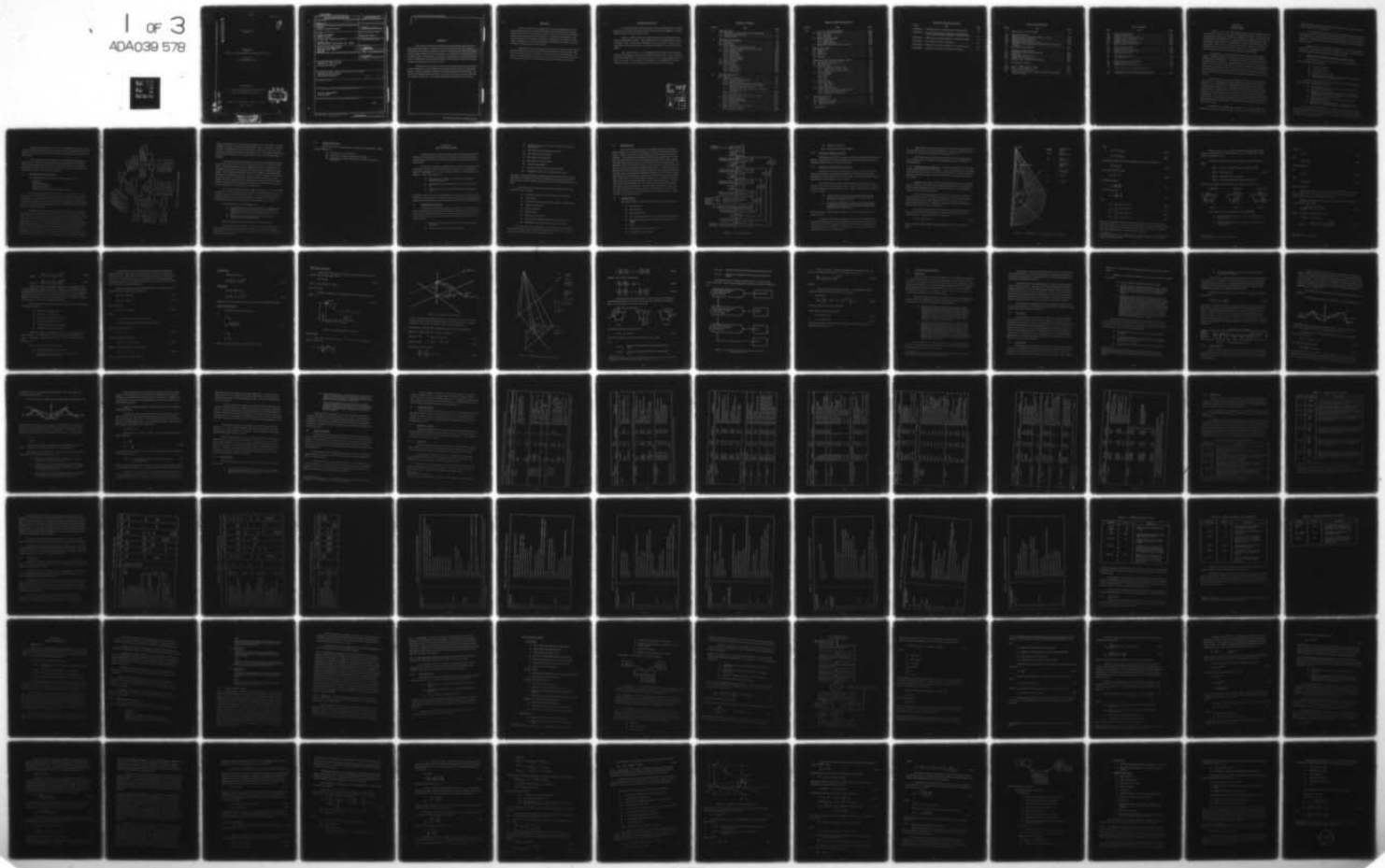

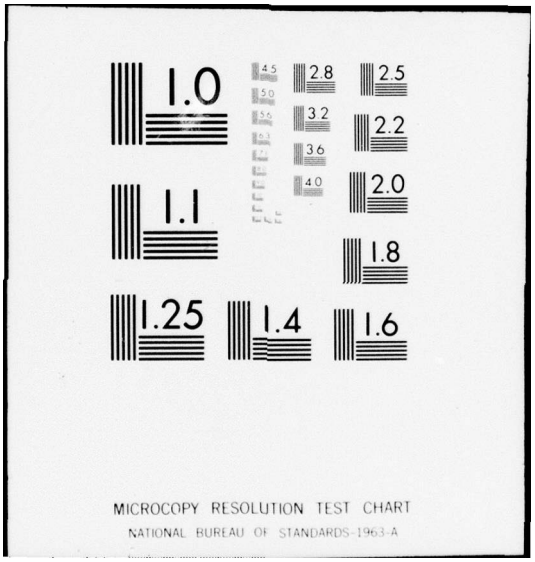
1.0
1.1
1.25
1.4
1.6
1.8
2.0
2.2
2.5
2.8
3.2
3.6
4.0
4.5
5.0
5.6
MICROCOPY RESOLUTION TEST CHART
NATIONAL BUREAU OF STANDARDS-1963-A

FINAL REPORT
1004-1

SIMULATION OF ADVANCED INTEGRATED RECONNAISSANCE SYSTEMS

VOLUME I
ANALYTICAL MODEL

SUBMITTED TO

Systems Analysis and Engineering Department
U. S. Naval Air Development Center
Johnsville, Warminster, Pennsylvania

Prepared Under Contract No. N62269-68-C-0441

April 4, 1969

Analytics
Incorporated

UNCLASSIFIED
SECURITY CLASSIFICATION OF THIS PAGE (When Data Entered)

REPORT DOCUMENTATION PAGE		READ INSTRUCTIONS BEFORE COMPLETING FORM
1. REPORT NUMBER 1004-1	2. GOVT ACCESSION NO.	3. RECIPIENT'S CATALOG NUMBER
4. TITLE (and Subtitle) Simulation of Advanced Integrated Reconnaissance Systems Volume I. Analytical Model		5. TYPE OF REPORT & PERIOD COVERED Final 6. PERFORMING ORG. REPORT NUMBER
7. AUTHOR(s) Stephen W. Leibholz Sydney F. Martin		8. CONTRACT OR GRANT NUMBER(s) N62269-68-C-0441
9. PERFORMING ORGANIZATION NAME AND ADDRESS Analytics Inc. 2500 Maryland Rd. Willow Grove, Pa. 19090		10. PROGRAM ELEMENT, PROJECT, TASK AREA & WORK UNIT NUMBERS
11. CONTROLLING OFFICE NAME AND ADDRESS Naval Air Development Center Warminster, Pa. 18974 Code 542		12. REPORT DATE 4 April 1969 13. NUMBER OF PAGES 230
14. MONITORING AGENCY NAME & ADDRESS(if different from Controlling Office)		15. SECURITY CLASS. (of this report) Unclassified 15a. DECLASSIFICATION/DOWNGRADING SCHEDULE

16. DISTRIBUTION STATEMENT (of this Report)
Approved For Public Release
Distribution Unlimited

17. DISTRIBUTION STATEMENT (of the abstract entered in Block 20, if different from Report)
Approved For Public Release
Distribution Unlimited

18. SUPPLEMENTARY NOTES

19. KEY WORDS (Continue on reverse side if necessary and identify by block number)
Tactical Reconnaissance
Computer Model

20. ABSTRACT (Continue on reverse side if necessary and identify by block number)
Over

DD FORM 1 JAN 73 1473 EDITION OF 1 NOV 65 IS OBSOLETE
S/N 0102-014-6601

UNCLASSIFIED
SECURITY CLASSIFICATION OF THIS PAGE (When Data Entered)

20

ABSTRACT

This volume describes the AIRS (Airborne Integrated Reconnaissance System) Performance Model, an analytic-simulation tool for specifying and evaluating future airborne tactical reconnaissance systems. The model is also used for studying multiple sensor systems and their interactions in the context of an integrated reconnaissance system. Performance is analyzed by computing for each sensor the detectability, identifiability, and localizability (CEP) of each target in a scenario, including the effects of interactions with other sensors.

Incorporated in the model are provisions for defining scenarios and missions. Variable parameters are used to specify the characteristics of targets, backgrounds, terrain, weather, equipment, reliability, and data integration and transmission. The model then integrates the performance of all sensors to give total system performance as a function of time-late, and evaluates the marginal contribution of each sensor.

ABSTRACT

This volume describes the AIRS (Airborne Integrated Reconnaissance System) Performance Model, an analytic-simulation tool for specifying and evaluating future airborne tactical reconnaissance systems. The model is also used for studying multiple sensor systems and their interactions in the context of an integrated reconnaissance system. Performance is analyzed by computing for each sensor the detectability, identifiability, and localizability (CEP) of each target in a scenario, including the effects of interactions with other sensors.

Incorporated in the model are provisions for defining scenarios and missions. Variable parameters are used to specify the characteristics of targets, backgrounds, terrain, weather, equipment, reliability, and data integration and transmission. The model then integrates the performance of all sensors to give total system performance as a function of time-late, and evaluates the marginal contribution of each sensor.

ACKNOWLEDGEMENTS

The Airborne Integrated Reconnaissance System (AIRS) Performance Model described in this report was developed under the direction of Mr. Stephen W. Leibholz and Mr. Sydney F. Martin of Analytics, Inc.

Messrs. Leibholz and Morris Plotkin performed the system analysis and simulation design for the model. The programming effort was performed by the staff of Analytics and Mr. Nathan Schatz (Keystone Computer Associates). Others providing substantial technical assistance to the project were Messrs. Martin and Lawrence Rafsky.

Mr. Charles Glueck, Jr. of NAVAIRDEVCEN-Johnsville, directed and contributed to the development effort for the AIRS performance model. Mr. Jay Goldfarb, also of NAVAIRDEVCEN, was the Project Manager for the overall program under which this work was done. Many members of the AIRS staff at NAVAIRDEVCEN provided substantial assistance, both technically and in the preparation of this report.

TABLE OF CONTENTS

TABLE OF CONTENTS (Continued)

TABLE OF CONTENTS (Continued)

LIST OF ILLUSTRATIONS

LIST OF TABLES

SECTION I.
INTRODUCTION

Analytics, Inc., under NAVAIRDEVCEN contract number N62269-68-C-0441, was requested to develop, in conjunction with Kettelle Associates, a simulation model for studying the performance of future tactical airborne reconnaissance systems. The immediate need for the model was in support of the Airborne Integrated Reconnaissance System (AIRS) Concept Formulation Study, called the AIRS Performance Simulation Model (in this report it is called the AIRS model). The model is, however, sufficiently general and adaptable that it may be used to study the performance of nearly any proposed tactical airborne reconnaissance system (TARS).

The AIRS model was developed because existing models did not appear capable of readily providing the types of answers required from both the AIRS and anticipated future TARS studies. These studies required a model which could measure quantitatively the ability of a range of surveillance candidate systems to see, localize, and report a wide variety of target types over broad ranges of geographical and weather environments. Further, this model had to be driven by functional rather than engineering parameters since the study orientation was toward determining the worth of future surveillance concepts rather than evaluating existing or nearly existing systems.

Existent models were found to: (1) be heavily oriented toward campaign operations (i.e., considerations of mission scheduling, squadron on-board maintenance, etc.), as in the case of the TRISECT Model developed by North American-Rockwell; (2) be based largely upon engineering design parameters rather than functional parameters; and (3) consider only a portion of the wide range of sensor, data integration, and data handling possibilities defined for AIRS and subsequent future TARS systems. These models, then, were deemed more than adequate for describing the capabilities of conventional surveillance systems which were well specified in an engineering sense but were inadequate for study of future reconnaissance concepts as exemplified by AIRS.

In developing the new AIRS model, required for the reasons outlined above, a standard modeling technique was followed. The problem, succinctly stated, was to

predict the performance of future TARS. As a necessary first step, measures of system performance were developed.

The remainder of Section I presents brief definitions of the reconnaissance performance measures which the model has been designed to provide; this is followed by a brief overview of the AIRS model as currently configured. At the conclusion of this Section, a summary of recommended modifications and extensions to the AIRS model is given.

Sections II to V present detailed discussions of the technical and programmatic aspects of the AIRS model; Section VI delineates in detail the suggested recommendations for additional modifications and extensions to AIRS.

1.1 PERFORMANCE MEASURES UTILIZED BY THE AIRS MODEL

The four primary measures of performance for a tactical airborne reconnaissance system are defined as:

(1) Target detectability

(2) Target identifiability

(3) Localizability of the target

(4) Time-late statistics (defined as the time that elapses between the collection and processing of data).

In contrast with conventional models, these parameters are computed for each of four data processing levels, namely:

(1) Real-time and near-real-time processing of reconnaissance data on board the aircraft.

(2) Keying (i.e., flagging) of data which contains relevant target information and transmission of this keyed data to the ground support station for early interpretation.

(3) Keying of relevant data but no transmission of this data to ground support station.

(4) Conventional level of processing (i.e., no keying of relevant data and no transmission to ground support station.)

The parameters of detectability, identifiability, and localizability are computed first for each target and each sensor being considered; the performances of each of the sensors vis-a-vis a given target are then aggregated to give the performance of the overall system against that target.

Targets are then grouped by types (e.g., transmitting enemy radar, moving vehicles) and integrated data prepared on the detectability, identifiability, and localizability for each sensor and for the overall reconnaissance system relative to each of the target groups.

To aid in answering such questions as how important the contribution of a given sensor is to the overall system effectiveness, an analysis of the "marginal effectiveness" of each sensor is performed. This allows the user to gain an understanding of the relative importance of each sensor, and is superior to presenting the user only with statistics on the absolute performance.

1.2 OVERVIEW OF THE AIRS MODEL

The AIRS Simulation model consists of four separate models:

SCENARIO
EXECUTIVE (EXEC)
EVALUATION (EVAL)
PHOTO-INTERPRETER AND QUEUEING (PI-Q)

The interactions among these four models are shown in Figure 1-1. The following discussion will present, in very broad terms, what each of the four models accomplishes. A more detailed discussion of each model is deferred until later sections: Section II discusses the Scenario model, Section III discusses the Executive model, Section IV discusses the Evaluation model, and Section V discusses the Photo-Interpreter and Queueing model.

The Scenario model utilizes user-provided data to form a conceptual map, or scenario, of the geographical area over which the reconnaissance mission will be flown, including substantial terrain and weather data. This map includes the locations of all targets, as well as the altitude and start and end points of each pass of the multi-pass reconnaissance mission. For each target, the user specifies the type and physical characteristics (e.g., an airfield that covers 1000 square meters of ground) as well as indicates the type of environment in which the target is located (i.e., the background surrounding the target has certain relevant characteristics such as temperature, photo-reflectivity, etc.). Whenever a target enters the field of view of a given sensor, Scenario generates data on (1) the sighting data itself (e.g., the slant

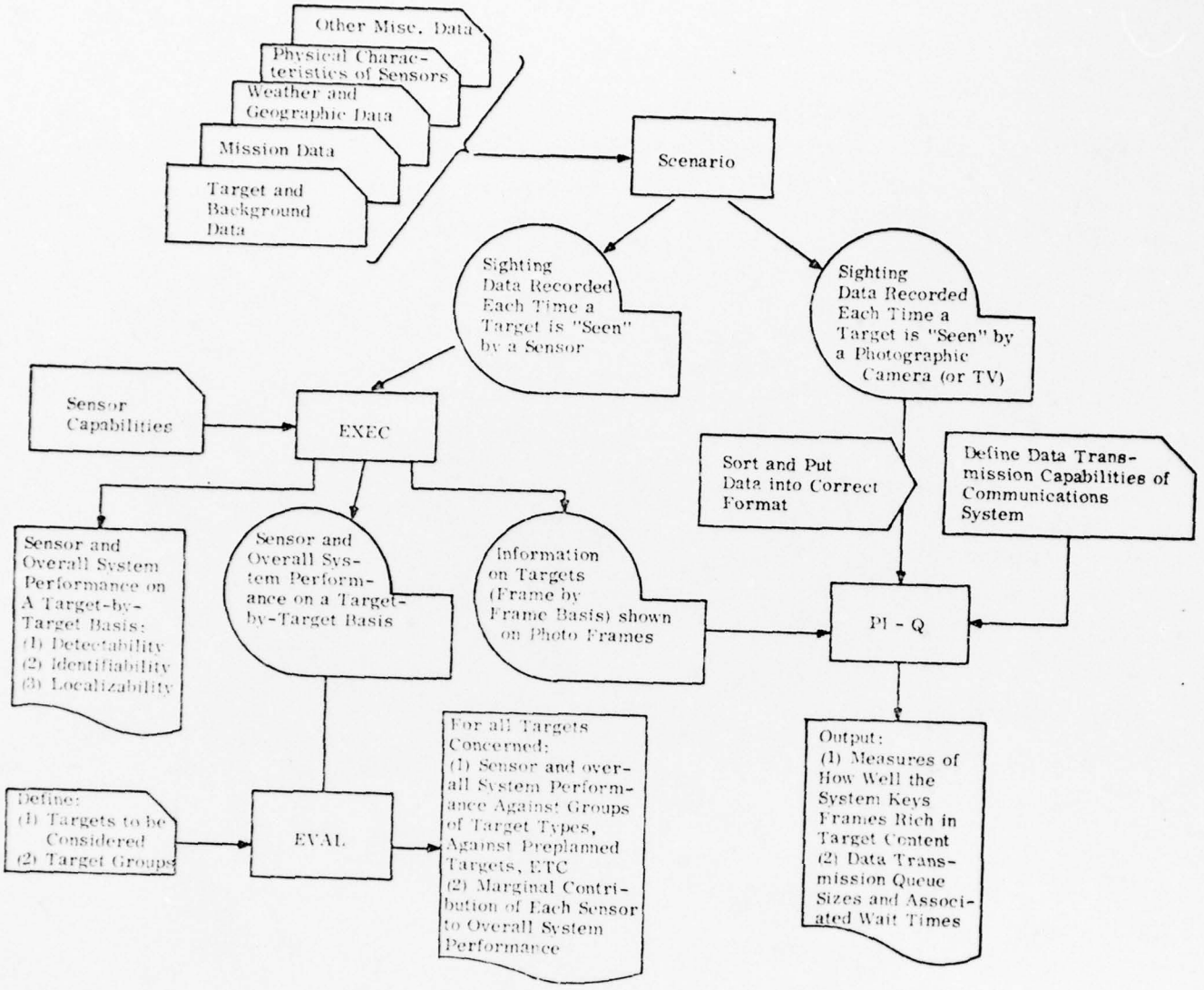

Figure 1-1. Flow Diagram of the AIRS Model

range to the target), (2) the probabilities that the target is not masked by terrain and not hidden by clouds, and (3) the probability that the sensor is operational. The first of these is straightforward, the second is computed using inputs such as rms of the terrain, prevailing visibility and precipitation rates, etc. The third is computed using data on the sensor MTBF. Note that detectability, per se, is not computed within Scenario.

The user must provide the Executive model with relevant performance data for each sensor; for example, the user must specify the thermal resolution of the IR sensor. With this information, and the sighting information computed by Scenario, the EXEC model computes the probability that a given target is detectable by a given sensor. Based on the assumption that the target is detectable, the probability that the target is identifiable is computed. One other statistic is computed for each target-sensor pair; namely, the localizability (CEP) of the target vis-a-vis the sensor. Finally, the EXEC model integrates the individual sensor performance and computes, for each target, how well the reconnaissance system as a whole performed using the criteria of detectability, identifiability, and localizability.

The EVAL model uses the output of EXEC and computes how well each AIRS reconnaissance system alternative performs against (1) particular target types, (e.g., radars), (2) various groupings of the target types (e.g., emitting enemy radars), and (3) preplanned versus non-preplanned targets. In addition, EVAL computes the marginal contribution to system performance of each sensor on the aircraft.

The PI-Q model serves a two-fold purpose:

(1) It accepts statistics supplied by the Scenario and EXEC models and uses them to estimate the capabilities of the system in selecting, for early photo-interpretation, those photographic frames which are relatively rich in target content.

(2) Estimates the length and waiting times of the queues that develop prior to data communication.

These two factors are then used to compute time-late statistics.

In summary, the user establishes, via input, a geography of interest. For specified missions, the model computes the performance of the AIRS configuration being studied, as well as the performance of each sensor in the system, against each target and each target type.

1.3 RECOMMENDATIONS

Section VI presents recommendations for improving the AIRS model. These recommendations are:

(1) Incorporation of a visual sensor.

(2) Provision for automatic topographical mapping.

(3) Modification to allow for the automatic detection of targets by the system.

SECTION II.
THE SCENARIO PROGRAM

The development of the Scenario Model is the result of the joint efforts of Analytics, Inc. and Kettelle Associates, Inc. Kettelle's contributions have been presented in their final report,[2] and the contributions of Analytics are discussed in this Section.

An overview of the Model is presented first, followed by a summary of the methodology. The discussions in these two areas draw heavily upon the Kettelle Report.[2] Paragraphs 2.3, 2.4, and 2.5 discuss the three areas of Analytics' contribution. Briefly, these areas are:

(1) Development of a model for a Forward Looking Infrared Sensor (Paragraph 2.3).

(2) Development of a model which simulates terrain (Paragraph 2.4).

(3) Implementation of an event time-line capability (Paragraph 2.5).

Paragraphs 2.6 and 2.7 discuss the detailed inputs and outputs of the Scenario Model, and because of the changes made necessary by the work of Analytics, this information supersedes the information presented in Sections IB and IC of the cited Kettelle Report.

2.1 OVERVIEW OF SCENARIO

The objective of the Scenario Program is to describe, for each sensor on board the aircraft, the time interval during which each target is in the sensor's field of view (without regard to terrain masking). Whenever a given target is within the field of view of a sensor, the Scenario Model computes the following output data, or a subset of them:

(1) Time(s) that target is in field of view of the sensor (time of detection).

(2) Ground range from the aircraft to the target.

(3) Ground range from the target to the flight line, measured perpendicularly.

(4) Slant range from the target to the aircraft.

(5) Slant range of haze traversed.

(6) Slant range of rain traversed.

(7) Slant range of clouds traversed.

(8) Camera frame numbers.

(9) Projection of target velocity onto line of sight.

(10) Probability that the target is unobscured by terrain.

The output, or subset of quantities computed, depends upon which sensor is being considered. For example, it would be meaningless to compute the projection of a target velocity onto line of sight of a sensor that has no moving target detection capability.

Before these basic outputs can be computed, the following inputs to the Scenario Model are required:

(1) Aircraft coordinates at the start of each leg of each pass.

(2) Wind velocity.

(3) Coordinates of each target (latitude, longitude, and elevation).

(4) Velocity of each target.

(5) Sensor parameters.

(6) Altitude of haze.

(7) Altitude and cloud density.

(8) Rain factor (the fraction of the terrain covered by rain).

(9) Wavelength, rms, and coherence angle of the terrain.

The above inputs are self-explanatory, with the exception of (5) and (9). The coherence angle of terrain is defined and discussed in Paragraph 2.4. Sensor parameters and other inputs are defined in Paragraph 2.6.

2.2 METHODOLOGY

A flow chart of the overall Scenario Model and the functional sequence is shown in Figure 2-1. Each box of the program is numbered for convenience of the reader. In box (1), the main (or control) program, called "Scenario", reads the input data. The outermost loop, going from box (16) through (17) to box (3), represents the passes flown by the aircraft on the mission being studied. Then, moving in the next loop, box (15), (18), (5), for each target in order, the main program sequentially calls in subroutines to compute required outputs for each sensor (box 10). (These subroutines are discussed in detail in Paragraph 2.3.) As represented by box (11), for each sensor/target combination within a given leg and pass, the main program then calls a subroutine which computes the probability of that target not being obscured from the sensor being considered by mountains or other terrain considerations. When all legs of a pass have been completed for a given sensor and target (box 13), the control program calls the next sensor for the same target. When all sensors have been interrogated (box 14), the control program then considers the next target, again using all sensors. When all targets have been covered (box 15), the control program proceeds to the next pass. This procedure is continued for all passes in the mission. The job of formulating and writing the outputs on tape is performed in the Scenario program.

2.3 SENSOR MODELS

The Scenario Model considers the following 10 basic types of sensors:

(1) Dummy Sensor.

(2) Infrared Sensor.

(3) Side Looking Radar.

(4) Side Looking Radar with capability of detecting moving targets.

(5) Forward Looking Radar with capability of detecting moving targets.

(6) ECM.

(7) Forward Looking Frame Cameras.

(8) Side Oblique Frame Cameras.

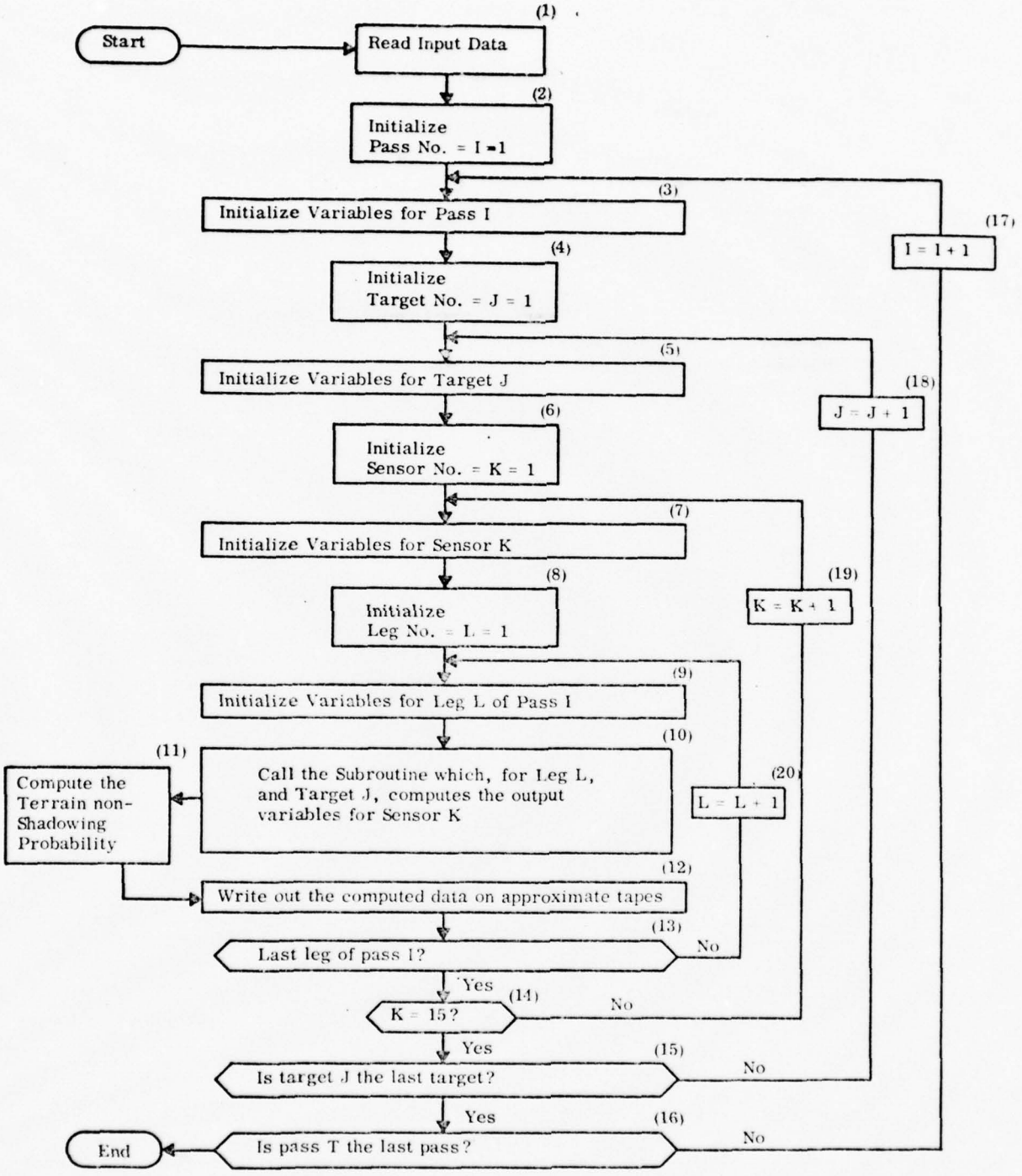

Figure 2-1. Flowchart of Scenario

(9) Oblique Pan Cameras.

(10) Forward Looking Infrared Sensor.

2.3.1 Work Done by Kettelle Associates

The Kettelle report[2] contains detailed discussions of the first nine types of sensors. Since Analytics' effort has not affected the operation of these sensors, the Kettelle material will not be repeated in this report.

2.3.2 Forward Looking Infrared Sensor (FLIR)

The FLIR sensor serves a dual purpose. First, in its elementary mode of operation, the sensor is positioned to point forward and downward to scan the ground directly in front of the aircraft. In this mode, a detection is possible whenever a target moves into the field of view of the sensor.

The second and more complex mode of operation for which FLIR was especially designed is to point the sensor toward the target after the FLIR was supplied with the coordinates of targets within its range. Target coordinates may be supplied in one of two ways:

(1) Targets may be pre-planned; that is, having been given the coordinates at the start of the mission, the system directs the FLIR at the appropriate time.

(2) Alternatively, the other two sensors which can detect targets in front of the aircraft, forward looking radar and ECM upon picking up a target, supply data from which coordinates are computed and supplied to FLIR.

The latter of these, called "slewing capability", is expected to markedly improve target detection.

In order to model this dual capability, two sensors are conceptually developed within the program; the only difference between them is in the field of view. The first has a field of view which encompasses the total area over which the FLIR may be pointed, and the second has a field of view which is that area seen by the FLIR sensor when it is in its rest position.

Whenever the main Scenario program calls upon the FLIR subroutine, the two conceptual sensors are processed sequentially. Outputs are collected for each; the Executive model will later decide which of the outputs to use.

In the following discussion, the term FLIRE (for FLIR Expanded) refers to the pointable model. Similarly, the non-pointable model is called FLIRS (for FLIR Stationary).

2.3.2.1 FLIRE-Directed Mode Analysis. The domain of FLIRE is nearly the whole forward and downward quarter of the sphere. The peripheral pointability will probably not be 90 degrees from center, nor will the maximum depression angle be 90 degrees (because, among other reasons, of the physical limitations imposed by mounting on the aircraft).

Apparently, the domain of FLIRE must comprise the horizon as an orientation aid. However, in the model, this cannot be implemented because the number of targets falling within the range of the FLIRE would be too large — an unmanageable number of records would be generated.

This consideration dictates limitation of the forward view by instituting a minimum depression angle. The model is nonetheless a realistic approximation because resolution beyond a certain slant range is too poor to be considered, i.e., would only yield useless data. Accordingly, the ground coverage of the FLIRE has the plane characteristics shown in Figure 2-2.

For conceptual ease, the aircraft remains still and the target moves. Let (X_o, Y_o) be the coordinates of the target at the start of the leg (in the aircraft coordinate system). Then the equation of the target path is

$$Y = Y_o + (X_o - X) \tan \delta \qquad (2.1)$$

where δ is defined as the difference between the heading angle, α, and the course angle, γ.

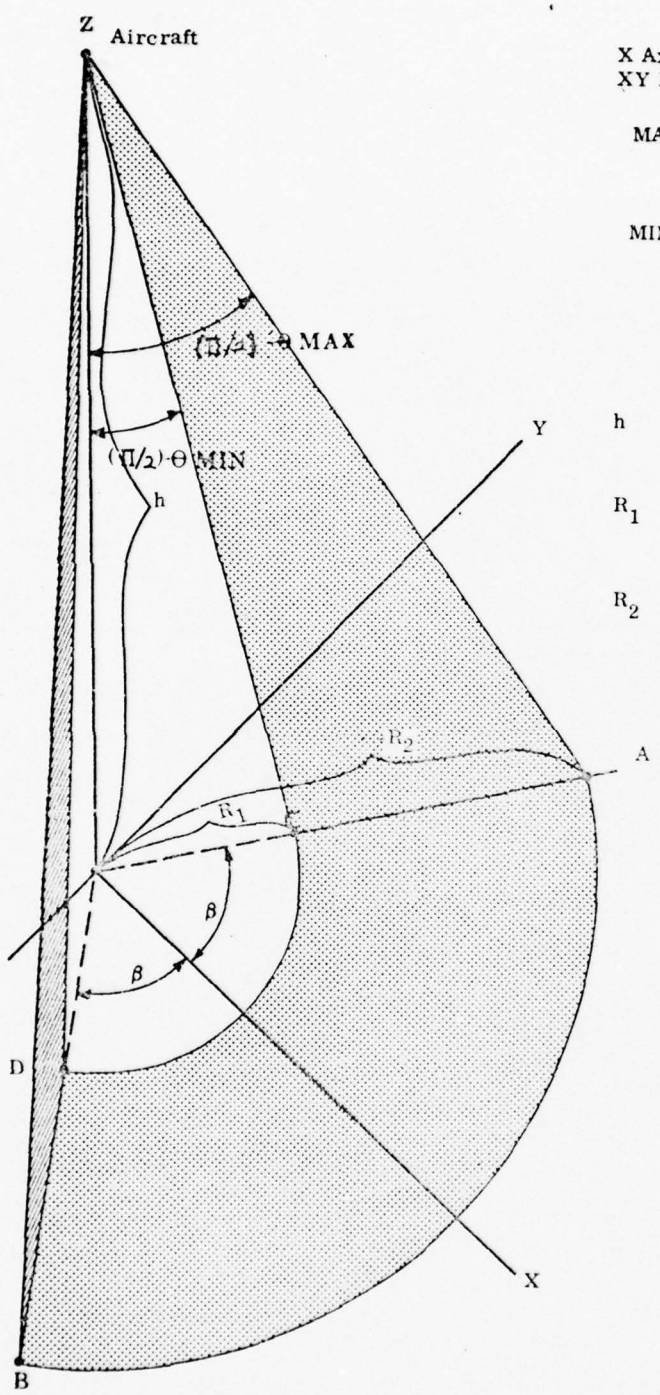

X Axis XY Plane	Airplane Heading Ground
MAX	Maximum Depression Angle
MIN	Minimum Depression Angle
	Peripheral View Angle (always positive)
h	Aircraft Height above Ground
R_1	$f(h, \theta_{MAX})$
R_2	$f(h, \theta_{MIN})$

Figure 2-2. Geometry of the Directed Mode Analysis — FLIRE

Then:

$$R_1 = h/\tan(\theta_{max}) \tag{2.2a}$$

$$R_2 = h/\tan(\theta_{min}) \tag{2.2b}$$

The equation of the circle of which arc $\widehat{AB}$ is a part (in A/C coordinates):

$$X^2 + Y^2 = R_2^2 \tag{2.3a}$$

and of which arc $\widehat{CD}$ is a part:

$$X^2 + Y^2 = R_1^2 \tag{2.3b}$$

Line $\overline{DB}$ has equation

$$X = \tan\left(\frac{\pi}{2} - \beta\right) Y \tag{2.4}$$

Line $\overline{CA}$ has equation

$$X = -\tan\left(\frac{\pi}{2} - \beta\right) Y \tag{2.5}$$

And:

$$X_A = X_B = R_2 \sin(\pi/2 - \beta) \tag{2.6}$$

$$-Y_A = Y_B = R_2 \cos(\pi/2 - \beta) \tag{2.7}$$

$$X_C = X_D = R_1 \sin(\pi/2 - \beta) \tag{2.8}$$

$$-Y_C = Y_D = R_1 \cos(\pi/2 - \beta) \tag{2.9}$$

Next, it is assumed that the target will enter the region described by ABCD; it must enter from the front, i.e., it must cross arc $\widehat{AB}$. This is not an unreasonable assumption. For example, the maximum drift angle will be about 10 degrees.* In all cases the FLIRE will be pointable more than 10 degrees off center.

*An aircraft traveling mach 1 ($\approx$1000 ft./sec.) which encounters a wind of 200 ft./sec. (about 150 miles/hr.) perpendicular to its heading has a drift angle of only about 11 degrees — arctan (200/1000).

The next step is to solve simultaneously the target path equation and the equation of the outer circle. Let the solutions be (X_1, Y_1) and (X_2, Y_2)*, and the convention adopted is $X_1 > X_2$.

The following algorithm is used to test whether or not the target enters ABDC:

Step 1: Is $X_1 > 0$? If NO, no detection is possible, if YES,

Step 2: Is $Y_A \leq Y_1 \leq Y_B$? (2.10)

Step 3: If NO, no detection is possible.

Step 4: If YES, the target enters the area of observation.

If the target enters the area of observation, one of three cases can occur:

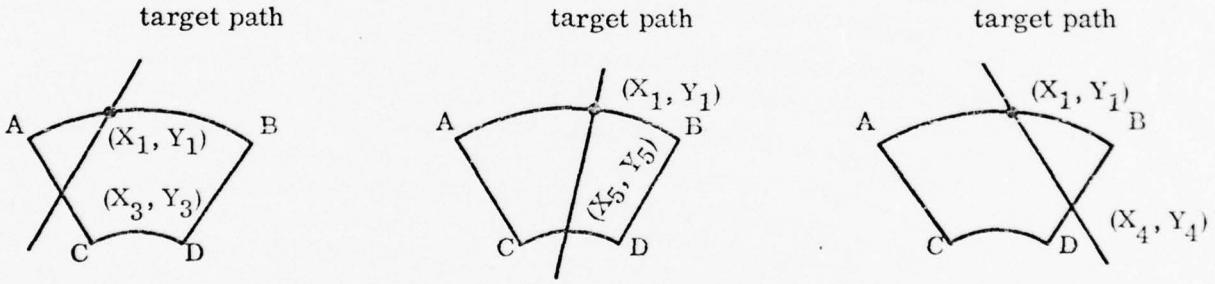

Case 1 Case II Case III

The intersection of the target path line is then formed with:

(1) The line passing through points A and C -- the intersection is called (X_3, Y_3);*

(2) The line passing through points B and D -- the intersection is called (X_4, Y_4).*

* The computation is presented in Appendix A.

Then if:

$$X_3 > 0 \tag{2.11}$$

and

$$Y_A \leq Y_3 \leq Y_c \tag{2.12}$$

Case I is observed

If:

$$X_4 > 0 \tag{2.13}$$

and

$$Y_D \leq Y_4 \leq Y_3 \tag{2.14}$$

Case III is observed.

And finally, if neither Case I nor Case III is observed, Case II must occur. If Case II exists, solve equation (2.3b) and the target path equation simultaneously. Let the solutions be $(X_5, Y_5)^*$ and $(X_6, Y_6)^*$; let $X_5 > X_6$.

The path can be defined more explicitly. For all three cases, the time, T_1, to reach the region ABDC is:

$$T_1 = \sqrt{(X_o - X_1)^2 + (Y_o - Y_1)^2}/V \tag{2.15}$$

where V is the ground velocity of the aircraft.

The time, T, in the field is:

$$\text{Case I:} \quad T = \frac{\left[(X_1 - X_3)^2 + (Y_1 - Y_2)^2\right]^{1/2}}{V} \tag{2.16a}$$

* See Appendix A for computation.

$$\text{Case II:}\quad T = \frac{\left[(X_1 - X_5)^2 + (Y_1 - Y_5)^2\right]^{1/2}}{V} \tag{2-16b}$$

$$\text{Case III:}\quad T = \frac{\left[(X_1 - X_4)^2 + (Y_1 - Y_4)^2\right]^{1/2}}{V} \tag{2-16c}$$

Having treated the family of FLIR variables, which are functions of position, as a parameter, it is now necessary to consider time as a parameter common to another family of variables. Human factors analysts working with the project have advised that it is preferable to have the FLIR output displayed as a series of fixed snapshots rather than as a continuously unrolling panorama. Therefore, the optimum display time for a single picture is considered to be D_{TO}.

One record will be generated for each such snapshot, and for each snapshot the following is required:

(1) Ground range to target in NM.

(2) Slant range to target in NM.

(3) Slant range of haze traversed in NM.

(4) Slant range through rain in NM.

(5) Depression angle to target in radians.

(6) Azimuth angle to target in radians.

Another assumption is that only two "looks" (i.e., snapshots) are taken of any given target. More specifically, the snapshots will be arbitrarily taken at $T_{EXIT} - 1$ and $T_{EXIT} - (D_{TO} + 1)$, where T_{EXIT} is the time at which the target exits from view.

There are two reasons for this assumption:

(1) It will solve the target priority problem.

(2) It will keep the number of snapshots of each target to a manageable number, namely two.

A priority problem arises because, within the simulation, each target is treated separately. Thus, target Q may be in range from time 1000 to time 2000. However, target R, in which there may be more interest, might be in view from time 1050 to 2050. Obviously, both targets cannot be traced for the complete time they are within range and viewing capability of the FLIRE. By limiting the number of looks to two, both targets can reasonably be seen.

After K seconds the aircraft has moved a distance of KV; therefore, after K seconds the new coordinates of the target are:

$$X_K = X_o - KV \cos \delta \tag{2.17}$$

$$Y_K = Y_o + KV \sin \delta \tag{2.18}$$

For the first look:

$$K = T + T_1 - 1 - D_{TO} \tag{2.19a}$$

where

T = time in view (see equations (2.16a-c)

T_1 = time to reach region of view (see equation (2.15)).

Likewise, for the final look:

$$K = T + T_1 - 1 \tag{2.19b}$$

The time of the first look (TFL) is:

$$TFL = T + T_1 - 1 - D_{TO} + T_O \tag{2.20a}$$

Similarly, the time for the second look (TSL) is:

$$TSL = T + T_1 - 1 + T_O \tag{2.20b}$$

where T_O is the time at the start of the leg.

Ground Range

Ground range (GR) is:

$$GR = \left[(X_K)^2 + (Y_K)^2 \right]^{1/2} \tag{2.21}$$

Slant Range

The slant range (R_S) is:

$$R_S = \left[GR + (h - H_T)^2 \right]^{1/2}; \tag{2.22}$$

where h is the aircraft height above MGL, and H_T is the target height above MGL.

Slant Range through Haze

The slant range through haze (R_H) is:

If

$$h > H_H$$

$$R_H = \frac{R_S (H_H - H_T)}{h - H_T} \tag{2.23}$$

If

$$h < H_H$$

$$R_H = R_S$$

where H_H is haze height and H_T is the height of the target.

Slant Range through Rain

The portion of slant range in rain (R_R) is assumed to be the product of a constant times the slant range in haze

$$R_R = (C)\, R_H \tag{2.24}$$

where C is the appropriate constant.

Depression Angle

The depression angle (f) is computed directly from the diagram shown in Figure 2-3.

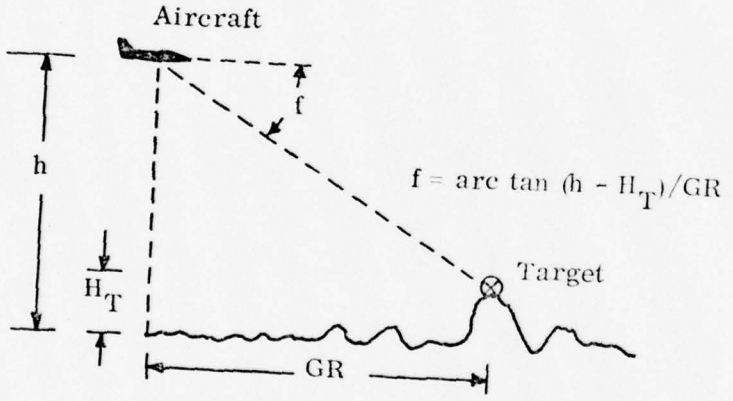

(2.25)

Figure 2-3. Depression Angle Computation

Azimuth Angle

The azimuth angle to the target, η, can be found by using the diagram illustrated in Figure 2-4.

$$\eta = \text{Arcsin}\left[\frac{Y_K}{\sqrt{X_k^{\,2} + Y_k^{\,2}}}\right]$$

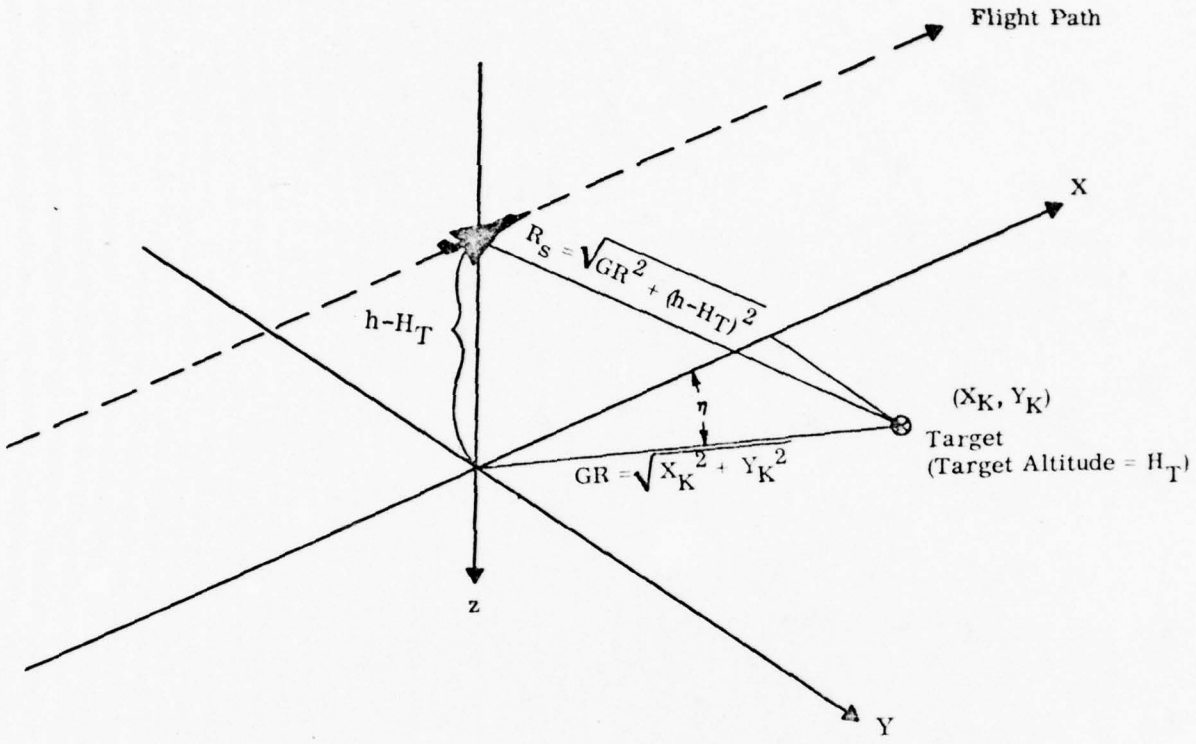

Figure 2-4. Azimuth Angle Computation

2.3.2.2 FLIRS – Unpointed Mode Analysis. In an unpointed mode, the axis of the FLIRS sensor has a depression angle θ, relative to the horizontal axis. In addition, the field of view is given by two angles, ϕ and ρ, shown in Figure 2-5.

The equations for $\overline{AB}$, $\overline{AC}$, $\overline{BD}$, and $\overline{DC}$ (see Figure 2-5) are given as follows:

Equations for $\overline{AB}$ and $\overline{CD}$ (X is a constant in both cases):

Equation for $\overline{AB}$ $$X = X_{MAX} = h/\tan(\theta-\beta) \tag{2.27a}$$

Equation for $\overline{CD}$ $$X = X_{MIN} = h/\tan(\theta+\beta) \tag{2.27b}$$

The equation for AC is given by:

$$X = \left[\frac{Y - Y_A}{Y_C - Y_A}\right](X_C - X_A) + X_A \tag{2.28a}$$

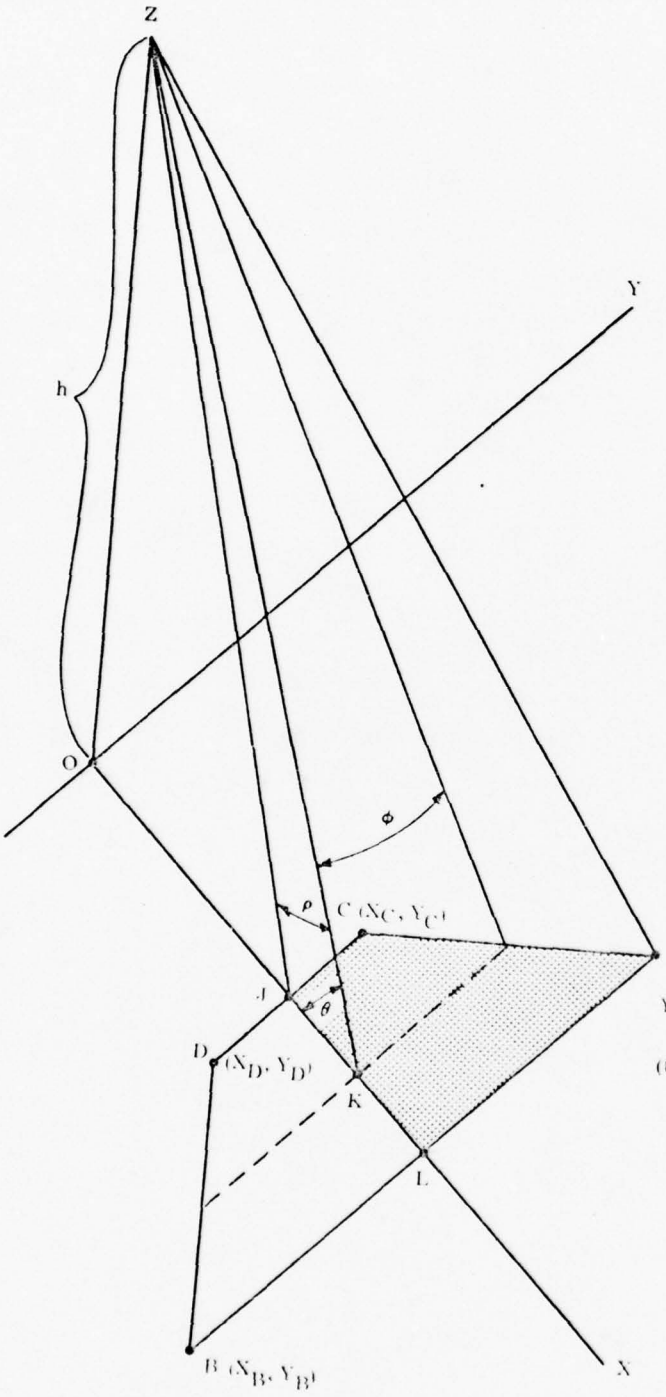

X Axis — Airplane Heading

XY Plane — Ground

ρ, ϕ — View Angles Relative to Central Beam

θ — Depression Angle Relative to Line of Flight

h — Airplain Height

$\overline{OJ} = X_C = X_D = h/\tan(\theta + \rho)$

$\overline{OL} = X_A = X_B = h/\tan(\theta - \rho)$

$Y_D = -Y_C =$

$(\tan \phi)\sqrt{(\overline{OJ})^2 + h^2}$

$Y_B = -Y_A =$

$(\tan \phi)\sqrt{(\overline{OL})^2 + h^2}$

Figure 2-5. FLIRS Parameters and Field of View

$$X - \left[\frac{X_C - X_A}{Y_C - Y_A}\right] Y = X_A - Y_A \left[\frac{X_C - X_A}{Y_C - Y_A}\right] \tag{2.28b}$$

Likewise, BD is given by the equation:

$$X = \left[\frac{Y - Y_B}{Y_o - Y_B}\right] \left[X_o - X_B\right] + X_B \tag{2.29a}$$

$$X - \left[\frac{X_o - X_B}{Y_o - Y_B}\right] Y = X_B - Y_B \left[\frac{X_o - X_B}{Y_o - Y_B}\right] \tag{2.29b}$$

It can be seen that the maximum drift is about 10 degrees*. Therefore, it is assumed that targets enter the field of view only if they enter across the leading edge, i.e., only if they cross the line segment AB.

Three cases are presented:

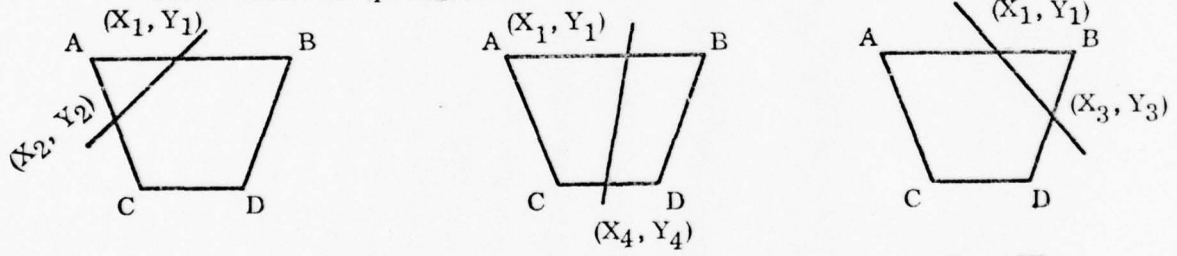

Case I Case II Case III

The equation of the target path is given by:

$$Y = Y_o + (X_o - X) \tan \delta \tag{2.30}$$

where δ is the difference between heading angle and course angle.

Let:

(X_1, Y_1)	Intersection of target path and line passing through A and B
(X_2, Y_2)	Intersection of target path and line passing through A and C

*An aircraft traveling at mach 1 (speed of sound $\cong$ 1000 ft/sec) with a side wind of 150 miles/hr., perpendicular to heading drifts only about 1 degree.

(X_3, Y_3) Intersection of target path and line passing through B and D

(X_4, Y_4) Intersection of target path and line passing through points C and D

The following algorithm (Figure 2-6) illustrates how to determine which is the correct case. (The equations yielding these coordinates are solved in Appendix B.)

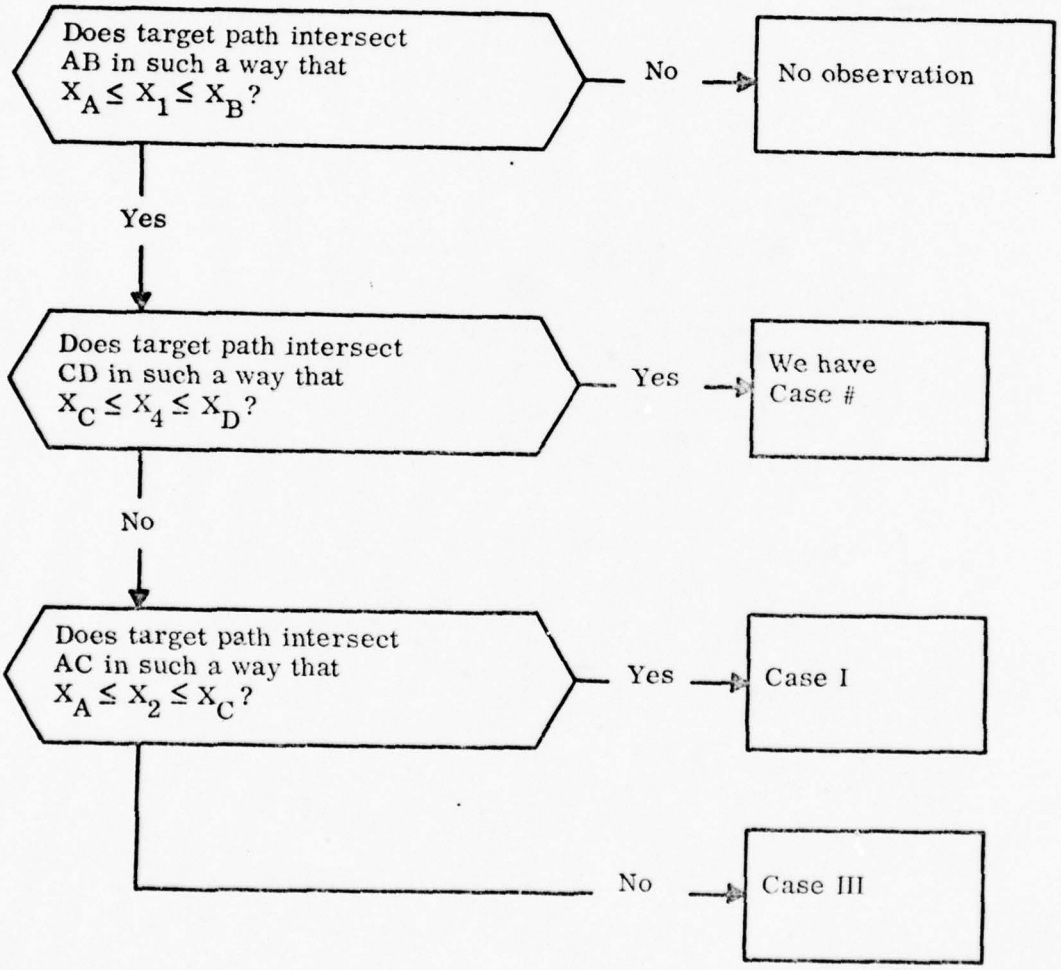

Figure 2-6. Algorithm for Determining How a Target Passes Through Field of View.

Let (X_1, Y_1) be the coordinates of the intersection on line AB; (X_E, Y_E) will be the coordinates of the exit point. The target is in view for

$$\frac{\left[(X_1 - X_E)^2 + (Y_1 - Y_E)^2\right]^{1/2}}{V} \tag{2.31}$$

seconds.

For reasons similar to those for FLIRE, it is assumed that FLIRS is given only one look at the target, namely, time T_{EXIT}-1.

Exit time is

$$T_{EXIT} = \left[\left((X_o - X_E)^2 + (Y_o - Y_E)^2\right)^{1/2}/V\right] + T_o \tag{2.32}$$

where T_O is the time of the start of the leg.

The coordinates of the look are given by

$$y = V \sin(-\delta) + Y_E \tag{2.33}$$

$$x = V \cos(\delta) + X_E \tag{2.34}$$

The relevant ranges and slant distances are computed in the same manner as in FLIRE (Paragraph 2.3.2.1).

2.4 TERRAIN SHADOWING MODEL

2.4.1 Introduction

One of the most significant degrading factors in low altitude reconnaissance is terrain shadowing: that is, the reduction in the quality of reconniassance due to an obstructed line of sight between the vehicle and a nearby target. Although not a factor affecting reconnaissance system design, the effect of terrain shadowing is to degrade the capabilities of even the best sensor systems (for a given scenario and mission), thereby tending to equalize system designs. For these reasons a terrain shadowing model has been incorporated in the AIRS simulation.

Experience with terrain shadowing involving the use of actual topographical data and geometrical algorithms to compute actual lines of sight has shown that this approach has two major disadvantages for the present problem:

(1) Typically 100 data points are required per square nautical mile of scenario (this is about 2×10^6 per mission for the scenario of interest) to fairly represent terrain.* Deterministic terrain data tapes are available from the Army Map Service for this purpose. The computations required, and the input/output demanded by the large volume of data, make it expensive in computer time to utilize the detailed terrain shadowing geometry in the AIRS model.

(2) Because the results of a geometrical terrain shadowing calculation are binary (the target is or is not obscurred), and because a trivial change in aircraft position down or across the flight path, at the altitudes of interest, is likely to completely change these results, a substantial number of Monte-Carlo calculations would have to be made for each target, frame, sensor, and pass in order to smooth out the irrelevant effects of detailed aircraft position and effect sensor timing relative to clock time. This would increase the terrain calculations beyond all reason.

Since the purpose of the AIRS simulation is to analyze alternative sensor systems, not operational missions, the wealth of results obtainable from a detailed terrain shadowing model are also not necessary.

*For example, the U.S. Army digitized terrain maps have a grid of 300 feet or approximately 400 data points per square nautical mile.

Consequently, a statistical terrain shadowing model was developed which, when suitably adjusted via three basic parameters to represent a given sample of terrain, produces estimates of the probability of terrain shadowing and its serial correlation (for multiple-look sensors).

The Terrain Shadowing Model operates in an off-line or pre-processing mode to the Scenario Model. Using the model, Monte-Carlo simulation was performed to develop a set of terrain-shadowing probability distributions, expressed as segmented polynomial curve fits to the Monte-Carlo data. These curves were then inserted as a simple subroutine into the Scenario Model. This procedure enabled the direct rapid computation of terrain shadowing probability at each step in the basic simulation without recourse to a cumbersome Monte-Carlo process.

The following paragraphs describe the development of a general method for terrain representation, a discussion of some special problems related to scaling, and the model implementation and utilization.

2.4.2 The Problem

A reconnaissance aircraft flies over a region in a series of regularly-spaced, parallel, straight-line passes in a horizontal plane. A narrow aperture surveillance device scans the region (or, alternatively, a wide aperture device successively photographs portions of the region) ahead of or to the side of the aircraft. If the terrain is not flat, low spots will be masked from observation. This paragraph is concerned with the problem of including these terrain-masking effects in a simulation. Looking forward, the desired output of the model is the probability that the target is not shadowed by terrain. The following paragraph discusses the method by which this is accomplished.

2.4.3 Basic Method

The problem of mathematically representing the terrain lies at the heart of the model. In contrast to some prior terrain shadowing models, it has been decided to use a random function to represent the terrain, and then to scale the selected function according to the measured statistics of the terrain actually employed

in the scenario. Occam's Razor* is the most useful tool for defining this terrain model.

What data are reasonably available to characterize the terrain? Three have been selected:

(1) The rms deviation of terrain height from its mean.

(2) The expected value of distance between hills; this is defined, through symmetry, as the expected value of distance between positive-going zero crossing of the terrain relative to its mean level. This corresponds to the wave length of the terrain.

(3) A terrain coherence factor representing the existence and direction of rolling terrain (e.g., the Alleghenies, as opposed to broken terrain, such as the interior of Puerto Rico), thereby characterizing the conditional probability that a target, if seen, will still be seen at a later point in the aircraft flight. This coherence factor is defined as an azimuth angle measured from the target, representing the change in "angle on bow" of the target required for two successive sightings to be statistically independent. Thus, if this factor were set at 45 degrees the aircraft would have to move through 45 degrees of azimuth relative to the target in order to obtain two statistically independent opportunities for sighting.

The first two of these data are used as the independent variables of the terrain representation (the third will be introduced later). Given the rms and the wavelength of the terrain, four additional mathematical constraints must be imposed on the random function chosen to represent the terrain:

(1) The amplitude distribution of the random function should be Gaussian.

(2) The expected distance between zero crossings of the random function must be non-zero (this is not the case with a simple random number sequence).

(3) The expected value of the slope of the terrain must be finite.

---

*Occam's Razor, a principle attributed to the English philosopher William of Ockham (14th Century), states that when a decision must be made between two apparently equivalent alternatives, the simpler alternative is always the more correct.

(4) The expected distance between reversals in the slope of the terrain must be non-zero.

Because of the resulting ease of computation one must consider the following process for terrain generation: take a random function (e.g., a random white noise where the time parameter, T, is interpreted as distance from the aircraft) and pass this function through an appropriate filter such that its output meets the constraints and exhibits the independent variables desired.

The simplest filter of this type is a linear filter (see Figure 2-7) having the transform;

$$L\ [Z(x)] = F(S) = \frac{K}{(S+\omega)^3} \tag{2.35}$$

The factor K is an amplitude scaling constant proportional to the rms terrain deviation, and the constant ω is inversely proportional to the expected distance between hilltops. That this filter must be third order can be shown relatively simply: if there is no filter, constraints 2, 3, and 4 are not satisfied although constraint 1 may be satisfied by using a Gaussian driving function. First-order filter yields a function satisfying constraint number 3. A second-order filter will cause constraint number 2 to be satisfied, and a third-order filter is required to conform to constraint number 4. (3)

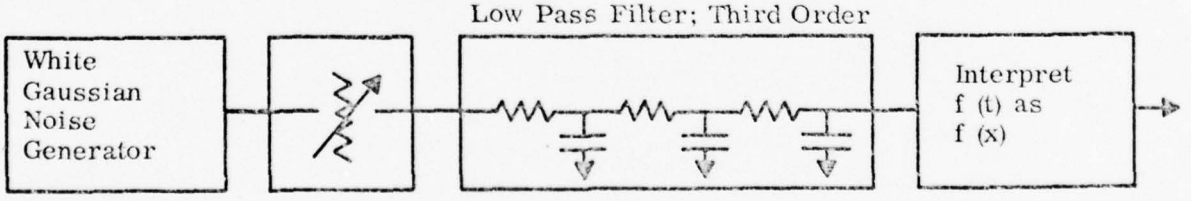

Figure 2-7. Terrain Generator Schematic

2.4.4 Terrain Analysis

Having decided on a terrain model, one could simply generate terrain within the simulation and compute explicitly the shadowing at any given time. This would, however, vitiate the entire approach, the purpose of which was to avoid irrelevancies in the calculations.

The approach selected is as follows: (1) Identify the values of the independent variables of terrain shadowing probability (i.e., rms and wavelength of the terrain); (2) Compute the probability function, giving terrain shadowing as a function of these variables. This probability function (actually a cumulative distribution function) is then embedded in the simulation and simply used when required. The resulting terrain non-shadowing probability is then carried through the simulation as a probability, not a stochastic event.

The remainder of this paragraph discusses the development of the terrain algorithm.

Let x be the horizontal distance variable and z (x) the ground elevation at x:

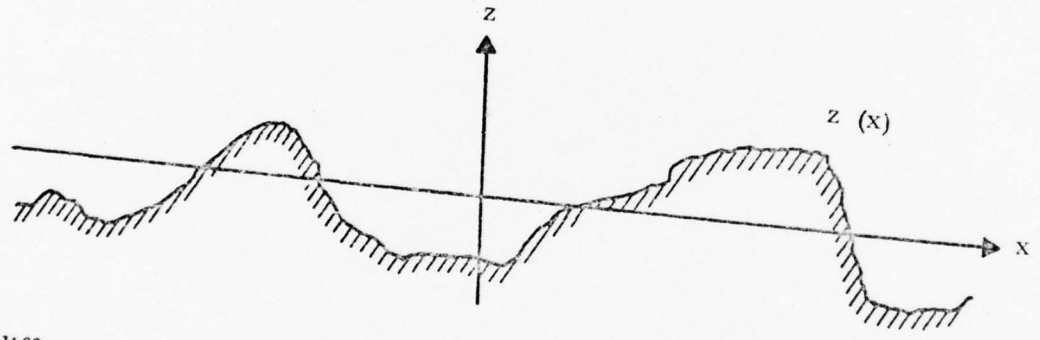

The different elevation functions z(x) occuring in different cross sections are considered to be samples generated by a stationary stochastic process.

The stochastic process which generates the terrain has an autocovariance function (by definition) of

$$R(\tau) = E\left\{z(x)\, z(x+\tau)\right\} \tag{2.36}$$

and a spatial power spectrum of:

$$S(k) = \int \cos(k\tau)\, R(\tau)\, d\tau \tag{2.37}$$

(All integrals are over the interval $(-\infty, +\infty)$ where limits are not shown.) $R(\tau)$, or equivalently S(k), has been selected to characterize the terrain to be simulated. Samples of z(x) are generated by passing white noise through a filter appropriately related

to the function S(k), as defined previously in equation (2.35). The samples z(x) are then analyzed as follows:

For each sample, an arbitrary point 0, shown in the following diagram, on

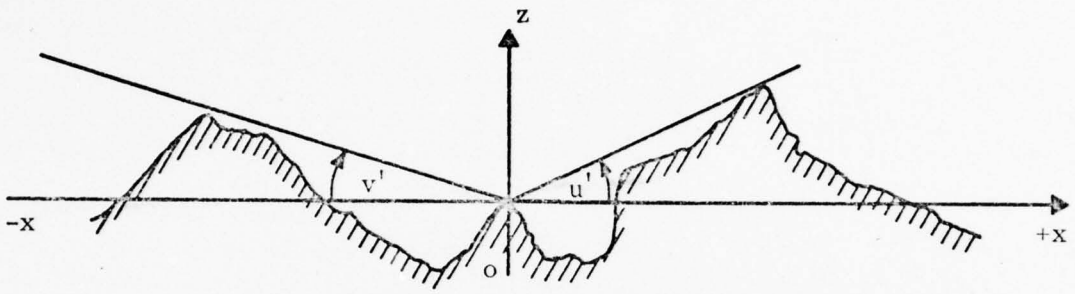

the ground surface is selected to be the origin. The visual horizon in the direction of increasing x is therefore the lowest ray from 0 in that direction that does not go below z(x); its angle above the horizon is u'. Similarly, v' is the angle above the horizontal of the visual horizon in the direction of decreasing x. For simplicity let

$$u = \tan u'$$

$$v = \tan v'$$

With respect to a target at 0, which was a randomly selected point, the pair (u, v) contains all the pertinent information about the sample z(x).

At this point a major simplification is introduced, namely to equate u and v. This is possible if the following conditions are met:

(1) The terrain generating function is statistically symmetrical with respect to reflection about the axis.

(2) The local terrain slope about the target is not determined as an independent input; i.e., its expected value is zero. This is consistent with the reasonable assumption that most targets are on relatively flat ground.

(3) The correlation of terrain shadowing, for a given target, with respect to two observations on different sides of the target (e.g., different reconnaissance legs) is ignored.

These assumptions are equivalent to asserting that the entire problem is symmetrical in the left-right sense, the fact that a target may be on a slope and therefore more visible from the east than the west is not utilized, and that the corresponding gain resulting from viewing that target from both the east and the west is not fully accounted for.

However, the target elevation (Z_o) relative to the terrain is a significant independent variable.

In other words, the two coefficients of the distribution which characterize the terrain are σ and X, the rms hill height and mean distance between positive-going zero crossings, respectively. The two independent variables of the distribution are u, the target sighting angle, and Z_o, the target elevation. Thus the desired terrain shadowing probability to be determined is

$$F(\sigma, X, Z_o, u)$$

The problem can be further simplified. By observing that the parameters can be scaled, let

$$Z^* = \frac{Z_o}{\sigma}$$
$$u^* = u \frac{X}{\sigma} \qquad (2.38)$$

This amounts to distorting the x and z axes to normalize σ and X. Thus, the function to be determined is now:

$$F(Z^*, u^*) = \text{Prob}\left[\text{Given } z^*, \text{ that the viewing angle-tangent is greater than } u^*\right] \qquad (2.39)$$

It must be pointed out that scaling, as done here, assumes that the terrain can indeed be scaled; this may not be the case, because of a problem called the "pebble problem".

The discussion so far has been concerned with the visibility from the aircraft of a point-target. The point of interest is the visibility not of a point, but of targets with finite dimensions. The purpose in replacing the targets by points was to

eliminate the target-size parameter from the masking effects. As has just been seen, the fewer the parameters that may vary, the fewer the computations and the simpler the presentation of the masking-effects model. However, the simplification can lead to problems.

A target small in size compared to its range from the reconnaissance aircraft may, for most purposes, be treated as a point, but in one important respect it may not. A point of no dimension can be concealed behind a pebble-sized obstruction close to it; an actual target cannot. If the parameter-reducing advantage of the point target assumption is to be gained, the "pebble problem" must be solved: small terrain elevations very close to the target-point must be disregarded in measuring m, u, and v.

The pragmatic solution to this problem comes about in the way that the function F (z^*, u^*) was actually calculated. The numerical calculation employed effectively quantized the terrain in units of ($\bar{X}/10$). Thus, any "pebbles" closer to the target than this quantization were ignored.

After considerable analysis it was determined that F (z^*, u^*) could not be explicitly solved, at least by the present authors. The quantity F (0, u^*) could be approximately found for $u^* << 1$, as could the relationships between k and σ; and between ω and X (equations (2.35) and (2.38), respectively). The development is found in Rice.[3] However, a Monte-Carlo procedure was still required to compute F. In doing this, the quantization errors lend to the necessity for normalizing. This was done experimentally within the computation.

2.4.5 Model Utilization

The following three-step procedure was used in actually implementing the terrain model:

(1) A series of programs were written to generate terrain samples according to the prescription of the model and on a Monte-Carlo basis to compute F (u^*, z^*) by sampling.

(2) The resulting cumulative probability histograms were used as inputs to a polynomial curve-fitting program. Based on experiments with this technique, a segmented third-order least-squares fit to the sampled data was selected.

(3) The resulting algebraic representations of the cumulative probability distribution were compared to some actual terrain data made available through another project, and normalized by further experimental runs to permit scaling to any given terrain statistics.

The final model, expressed in terms of the scaling functions and the cumulative probability distributions obtained by curve-fitting, was implemented as a subroutine within the Scenario program, directly reporting terrain shadowing probability for each simulation event without the need for additional Monte-Carlo computation. Appendix C contains a description of the implementation technique and resulting algorithm.

2.5 TIME-LINE MODEL

Human factors analysts associated with the AIRS project have indicated a need for a chronologically-ordered journal of mission events. They have specifically requested a time-line data scheme of the reconnaissance mission to portray the type (in terms of sensor response) and time of passage abeam the aircraft of each target. The purpose of the time-line is to permit statistical estimation of human factors such as crew slack time.

This capability has been designed into the Scenario Model. A tape containing target number, target type, and time of passage abeam may be generated at the option* of the program user.

As previously indicated, the symbolic identification or numbering of targets is arbitrary and may be unrelated to time, location, or any other mission parameter. Specifically, Scenario is organized about a Pass-Target-Sensor-Leg hierarchy (see Figure 2-1); this data is only coincidentally time-related.

*As discussed in Paragraph 2.7.1, the Scenario user specifies preparation of this tape by turning on Sense Switch 2 on the CDC computer console.

To obtain a hard copy of the data in time-ordered sequence, the tape produced by the Scenario Model is passed to a SORT program (CDC library routine). The time-ordered-data tape generated by SORT is used as an input to a program called LIST, which, in turn, generates the desired hard copy. Program LIST, and instructions for setting up program SORT, are given in Appendix G.*

2.6 SCENARIO INPUTS

The following information serves two purposes: to define all necessary input parameters of the Scenario program, and to provide instructions for preparation of the input deck itself. Except for changes incorporated to reflect the inclusion of a fifteenth sensor, FLIR, the following information is duplicated from pages 86-92 of the Kettelle Report. [2]

2.7 SCENARIO OUTPUTS

Much of the information in this Section was taken from the Kettelle Report, [2] It was decided to present this Section as a complete entity to avoid having the reader scan back and forth between this document and the Kettelle Report. As a result there is redundancy between the two reports.

2.7.1 Introduction

Scenario program outputs are provided on two, or optionally three, magnetic tapes. Output Tape 1 contains a descriptive record of target sightings by each of the 15 sensors turned on for a given run, and serves as input to the Executive Model.

The second tape, Output Tape 2, contains a frame-by-frame descriptive record of what each of the (up to 8) cameras on-board the aircraft surveyed. After sorting, this tape serves as input to the Photo-Interpreter Model.

The optional tape,** Output Tape, 3, lists target number, target type, and the time at which the aircraft flew past the target. This tape is sorted by time and then listed to provide a time-line record of the reconnaissance mission.

---

*This appendix is in Volume II.

**This tape is produced if Sense Switch 2 on the CDC Computer Console is turned on.

Data cards for the Scenario Model are to be prepared in the order and form described below:

Card Order	Card Description	Variable	Card Columns	Format Specification	Description
1	TITLE	I ALPHA (I)	1-80	20 (A4)	Alphabetic title for run
2	Sensor On/Off	II(1)	1-5	15	Code for each of the 15 possible sensors, designating if sensor is on for this run (set to "1" for on, "0" for off)
		II(2)	6-10	15	
		.	.	.	
		.	.	.	
		.	.	.	
		II(14)	66-70	15	
		II(15)	71-75	15	
3	Boundary restriction (all location inputs must lie within these limits)	LATMIN	1-5	15	Min. degrees latitude for run (+ for North, - for South)
		LATMAX	6-10	15	Max. degrees latitude for run
		LONMIN	11-15	15	Min. degrees longitude for run (+ for East, - for West)
		LONMAX	16-20	15	Max. degrees longitude for run
4	Index Limits	NT	1-5	15	No. of target types (- 30)
		N	6-10	15	No. of targets (- 200)
		NBKG	11-15	15	No. of backgrounds (- 15)
5	Target - One of these cards must appear for each target.	ITP(I)	1-5	I5	The index for type of target (1 through 30)
		X(I)	6-15	F10.0	Latitude (+ for North, - for South)*
		Y(I)	16-25	F10.0	Longitude (+ for East, - for West)*
		Z(I)	26-35	F10.0	Altitude code -- specified as a multiple of the rms value (see card 9)
		IPRE(I)	36-40	I5	Preplanned code (0=yes, 1=no)
		ITK(I)	41-45	I5	Code for air-to-air keying (0 = yes, 1 = no)
		IBKG(I)	46-50	I5	The index for type of background (1 through 15)

*Latitude and longitude are to be punched as XXX.YYZZ, where XXX are the degrees, YY the minutes, and ZZ the seconds. This convention applies throughout.

Card Order	Card Description	Variable	Card Columns	Specification	Description
5 (cont'd)		IWEATH(I)	51-55	I5	Rain-on-target code (1 for yes, 2 for no)
		V(I)	56-65	F10.0	Ground speed of target (knots)
		THT(I)	66-75	F10.0	Heading, in degrees clockwise from North
		NECMOFF(I)	76-80	I5	ECM code; set to "1" for on, "0" for off
(Card #5 is repeated for I = 1, 2, etc.,...., N, where N is the number of targets; see card #4)					
6	Target ECM	M(I)	1-5	I5	No. of targets of type I
		PT(I)	6-15	F10.0	Peak transmitter power (db above 1 watt)
		GT(I)	16-25	F10.0	Transmitter antenna gain (db)
		FREQ(I)	26-35	F10.0	Frequency (MHz)
		CKA(I)	36-45	F10.0	Transmitter antenna front-to-back ratio (db)
		PRF(I)	46-55	F10.0	Pulses per second
		THETA 1 (I)	56-65	F10.0	Pulse width in microseconds
		TSCPS(I)	66-75	F10.0	Target scan period (seconds)
(Card #6 is repeated for I = 1, 2, etc., ..., NT)					
7	Background	BKG(K, 1)	1-10	F10.0	Photo-reflectivity
		BKG(K, 2)	11-20	F10.0	MTISLR-backscatter coefficient
		BKG(K, 3)	21-30	F10.0	SLR-reflectivity
		BKG(K, 4)	31-40	F10.0	MTIFLR-backscatter coefficient
		BKG(K, 5)	41-50	F10.0	IR-emissivity for band 1
		BKG(K, 6)	51-60	F10.0	IR-emissivity for band 2
		BKG(K, 7)	61-70	F10.0	IR-temperature (in ^{o}K)
(Card #7 is repeated for K = 1, 2, etc., ..., NBKG)					

*Z(I) may only take on integral values between plus and minus three (including zero).

Card Order	Card Description	Variable	Card Columns	Specification	Description
8	Target/Sensor Matrix	TS(K, 1)*	1-10	F10.0	Photo-reflectivity
		TS(K, 2)	11-20	F10.0	Photo-resolution (ft.) for 90% prob. of det.
		TS(K, 3)	21-30	F10.0	MTIFLR-cross section (in m^2)
		TS(K, 4)	31-40	F10.0	SLR; MTISLR-cross section (in m^2)
		TS(K, 5)	41-50	F10.0	SLR-reflectivity
		TS(K, 6)	51-60	F10.0	SLR-resolution (m.) for 50% prob. of det.
		TS(K, 7)	61-70	F10.0	IR-area (in m^2)
		TS(K, 8)	71-80	F10.0	IR-temperature (in ^oK)
8a		TS(K, 9)	1-10	F10.0	IR-resolution (m.) for 90% prob. of detection
		TS(K, 10)	11-20	F10.0	IR-emissivity for band 1
		TS(K, 11)	21-30	F10.0	IR-emissivity for band 2
(The pair of cards 8, 8a are repeated for K = 1, 2, etc., ..., NT)					
*The index K denotes the K^{th} target type.					
9	Terrain	OMEGAL	1-10	F10.0	Wavelength of terrain (ft.)
		SIGMER	11-20	F10.0	rms of terrain (ft.)
		PHI	21-30	F10.0	Coherence angle (radians)
10	ECM	NBEAM	1-5	I5	No. of beams
		RMAX	6-15	F10.0	Max. range (NM)
		THETA 2	16-25	F10.0	Total blind angle (degrees) beneath aircraft (A/C)
11	SLR	THET 12	1-10	F10.0	Min. angle from nadir (deg.) for det.
		THET 13	11-20	F10.0	Max. angle from nadir (deg.) for det.
		RMIN 1	21-30	F10.0	Min. slant range (NM) for detection
		RMAX 1	31-40	F10.0	Max. slant range (NM) for detection
12	MTISLR	THET 22	1-10	F10.0	Min. angle from nadir (deg.) for det.
		THET 23	11-20	F10.0	Max. angle from nadir (deg.) for det.
		RMIN 2	21-30	F10.0	Min. slant range (NM)
		RMAX 2	31-40	F10.0	Max. slant range (NM)

Card Order	Card Description	Variable	Card Columns	Specification	Description
13	MTIFLR	PHIA	1-10	F10.0	Max. depression angle (deg.)
		PHIB	11-20	F10.0	Min. depression angle (deg.)
		RMINF	21-30	F10.0	Min. slant range (NM)
		RMAXF	31-40	F10.0	Max. slant range (NM)
		OMEGF	41-50	F10.0	Half angle (deg. of azimuth sweep)
		FLRFRQ	51-60	F10.0	Scan interval, in tenths of a second
14	IR	THET 32	1-10	F10.0	Max. angle from nadir (deg.) for det.
		RMAXIR	11-20	F10.0	Max. slant range (NM)
15	Photo Type	IKIND(1)	1-5	I5	Camera 1 — Code describing the type of each camera sensor: set to "0" for pan; set to "1" for side oblique frame or vertical frame; set to "2" for forward oblique frame.
		IKIND(2)	6-10	I5	Camera 2
		IKIND(3)	11-15	I5	Camera 3
		IKIND(4)	16-20	I5	Camera 4
		IKIND(5)	21-25	I5	Camera 5
		IKIND(6)	26-30	I5	Camera 6
		IKIND(7)	31-35	I5	Camera 7
		IKIND(8)	36-40	I5	Camera 8
For each of the eight cameras which are on, either card #16a or card #16b is punched. Card #16a is to be used for a pan camera, and #16b for the other types.					
16a	Pan Camera	FLENG(I)	1-10	F10.0	Focal length (inches)
		ANGS(I)	11-20	F10.0	Half-angle (deg.) subtended by film
		HFLM(I)	21-30	F10.0	Height of film (inches)
		OPR(I)	31-40	F10.0	Overlap percentage
		THTC(I)	41-50	F10.0	Angle (deg.) between A/C vertical and focal axis,
		PREVR(I)	51-60	F10.0	Darkness code (1 for day, 2 for night)

Order	Description	Variable	Card Columns	Specification	Description
16b	Frame Camera	FLENG (I)	1-10	F10.0	Focal length (inches)
		SW (I)	11-20	F10.0	Frame width (inches)*
		SL (I)	21-30	F10.0	Frame length (inches)*
		OPR (I)	31-40	F10.0	Overlap percentage
		THTC (I)	41-50	F10.0	Angle (deg.) between A/C vertical and focal axis.
		PREVR (I)	51-60	F10.0	Darkness code (1 for day, 2 for night)
(Note: The index (I) in cards #16a and 16b will vary from 1 to 8 - depending on the cameras which are on for this run.)					
17	Forward Looking Infrared	THEMA	1-10	F10.0	The maximum depression angle of the field-of-view of FLIRE
		THEMI	11-20	F10.0	The minimum depression angle of the field-of-view of FLIRE
		BETA15	21-30	F10.0	The (positive) half angle of the azimuth area that can be covered by FLIRE
		RHO15	31-40	F10.0	The (positive) half angle of the horizontal spread of the FLIRS beam
		PMI15	41-50	F10.0	The (positive) half angle of the vertical spread of the FLIRS beam
		THA15	51-60	F10.0	The depression angle of the central ray of the FLIRS beam
		DTO	61-70	F10.0	The optimal display time for a single picture of terrain taken by FLIRE
18	Weather	WINDTH	1-10	F10.0	Wind direction (deg.) - direction toward
		WINDSP	11-20	F10.0	Wind speed (knots)
		IRAIN	21-30	±10	Rain code (1 for rain, 2 for snow, 0 for no precip.)
		TRAIN	31-40	F10.0	Inches of rain (or snow)
		XO	41-50	F10.0	Prevailing visibility (statute miles)
		XOC	51-60	F10.0	Prevailing visibility in clouds (statute miles)
		XOP	61-70	F10.0	Visibility in rain (statute miles)
		XOH	71-80	F10.0	Prevailing visibility in haze (statute miles)

* Length is measured along the wiring axis; width along the a/c axis.

Card Order	Card Description	Variable	Card Columns	Specification	Description
19	Weather	PREVERE	1-10	I10	1 for day, 2 for night
		P3	11-20	F10.0	Probability of no undercast clouds
		CLOUDB	21-30	F10.0	Height (ft.) of cloud base
		CLOUDT	31-40	F10.0	Height (ft.) of cloud top
		Q	41-50	F10.0	Height (ft.) of haze level
		PPR	51-60	F10.0	Percentage of rain area
20	Flight Indices	ITT	1-5	I5	Simulation clock time at mission inception (tenths of second)
		NPASS	6-10	I5	No. of passes
		IND	11-15	I5	Index for evasion (0 for yes, 1 for no)
(The following card (#21) should appear in the data only if IND on card #20 is equal to "0".)					
21	Evasion	AMPLTD	1-10	F10.0	Amplitude of wave course (NM)
		DSCROS	11-20	F10.0	Distance between zero crossings (NM)
		ROLLMN	21-30	F10.0	Min. roll angle (deg.)
		ROLLMX	31-40	F10.0	Max. roll angle (deg.)
22	No. of Legs	NLEG(1)	1-5	I5	The number of legs for each pass.
		NLEG(2)	6-10	I5	Each pass must have at least 2 legs.
		.	etc.	etc.	The last leg is always a turn, or flight to base, during which time all sensors are off.
		.	.	.	
		.	.	.	
		NLEG(NPASS)	.	.	
23	Flight Plan	XX(I,J)	1-10	F10.0	Latitude* at start of leg J of pass I
		YY(I,J)	11-20	F10.0	Longitude* at start of leg J of pass I
		HH(I,J)	21-30	F10.0	Altitude (ft.) for leg J of pass I
		IT(I,J)	31-40	I10	Time (tenths of sec.) to fly leg J of pass I
(Card #22 is repeated for I = 1, J = 1, 2, etc., ..., NLEG (1), then for I = 2, J = 1, 2, etc., ..., NLEG (2); until I = NPASS.)					

*See footnote on page 2-30.

Card Order	Card Description	Variable	Card Columns	Specification	Description
24	Navigation	ANAVHD	1-10	F10.0	Heading error (radians)
		ANAVSP	11-20	I10	Speed error code - "0" if ANAVSP is in knots; "1" if ANAVSP is a % of the true speed.
		ANAVSP	21-30	F10.0	Speed error (based on code above)
		ANAVPS	31-40	F10.0	Initial position error (NM)
		ANAVPR	41-50	F10.0	Position error rate (NM/hr.) from checkpoint
		ITCP	51-60	I10	Time of checkpoint intervals (tenths of second)
		ANAVHT	61-70	F10.0	Altitude error (ft.)
25	Reliability	AMTBF(1)	1-10	F10.0	
		AMTBF(2)	11-20	F10.0	
		AMTBF(3)	21-30	F10.0	
		.	.	.	
		.	.	.	
		.	.	.	
		AMTBF(7)	61-70	F10.0	The mean time (in hours)
		AMTBF(8)	71-80	F10.0	between failures for each
25a		AMTBF(9)	1-10	F10.0	of the 15 sensors.
		AMTBF(10)	11-21	F10.0	
		.	.	.	
		.	.	.	
		.	.	.	
		AMTBF(14)	51-60	F10.0	
		AMTBF(15)	61-70	F10.0	

Notice: All the preceding cards must appear in a deck for each run with 2 exceptions:

1) The #16 card will not be required for a camera which is off; i.e., the card is not required if the value punched for that sensor on card #2 is "0".
2) Card #21 will not be required unless it is an evasion run; i.e., unless the value of IIND on card #20 is set to "0".

2.7.2 Output Tape 1

This tape, written on logical tape unit 11, contains binary records of 73 words each. The first record contains header information as indicated in Table 2-1. Following the header record is a series of records which describe target sightings. They are ordered by pass, target, sensor, and time.

For each target-pass combination, a record for the Dummy Sensor is always produced which contains time information. This information is used in evaluating the other sensors.

Immediately following the Dummy Sensor record are three records, the format of which is shown in Table 2-2, for the FLIR Sensor which are generated whether or not the sensor domain encompasses the target being considered on the current pass. The first two of these records contain information on target sightings consistent with the assumption that the sensor was slewed or that the target was preplanned (see Paragraph 2.3.2.1). The third contains similar information consistent with the assumption that the sensor was not slewed and/or that the target was not preplanned.

TABLE 2-1. RECORD 1 OF OUTPUT TAPE 1

WORDS	CONTENT
1-3	Dummy words arbitrarily set to zero.
4-23	An 80-character alphanumeric label which describes this particular run.
24-38	Fifteen indices, one for each of the 15 sensors. If the value of the index is 1, the sensor is included in this run; if the value is 0, the sensor is not included.
39	The number of pass-target combinations described on this tape. Its value is simply the number of passes times the total number of targets being simulated.
40-47	Eight indices, one for each of the 8 photographic sensors. The value of an index describes the type of photographic sensor: 0 = pan camera; 1 = side oblique plane camera; 2 = forward oblique plane camera.
48-73	Filler to maintain uniform record length.

TABLE 2-2. TARGET SIGHTING RECORDS

WORD	VARIABLE	DEFINITION
1	ITARG	A five digit number. The first two are the pass number and the last three are for target number.
2	ITYPE	This two digit index identifies the Sensor. Table I-1 lists the sensors and their associated indices.*
3	ITIME	This gives the time of the sighting in tenths of a second, as measured from mission start time.
4-33	G(1) G(2) . . . G(15)	These words contain geometric parameters describing target-aircraft relationships, e.g., slant range. (See Table 2-3.)**
34-43	P(1) P(2) . . . P(5)	These variables contain probabilities relating to the sighting, e.g., probability equipment is up, probability of cloud cover. (See Table 2-3.)**
44-53	W(1) W(2) . . . W(5)	These variables contain weather statistics relevant to the sensor being considered, e.g., visibility through rain. (See Table 2-3.)**
54-73	T(1) T(2) . . . T(10)	These variables contain pertinent information on the target and its surrounding, e.g., target and background temperatures. (See Table 2-3.)***

*Table I-1 is located in Appendix I, Volume III, a classified document.

**The content of these arrays vary depending upon the sensor type being considered.

***This array varies depending upon the target being considered.

For most of the other sensors, a single record is produced, if and only if the target was actually detected. For the ECM and Photo sensors there may be more than one record generated for a given pass-target-sensor-leg combination. In the case of the cameras, a separate record is generated for each camera frame during the time the target is in view. For ECM, a distinct record is created for each separate beam. Since the number of such records is variable, a flag is used to signal the end of the set. The flag is a record made distinct by filling the fourth and fifth words of the record with a large, floating-point, negative number.

Table 2-2 shows the form of each of the target records. The G(I), P(I), W(I), and T(I) arrays are defined for each of the sensor types in Tables 2-3a and 2-3b.

After all target records for the run have been generated, a closing record is generated which serves not only as an end-of-file, but also contains data. The variable ITARG (see Table 2-2) is set to 99999 to indicate end-of-file. Variables G(4) to G(11) contain the final frame counts for each of the eight cameras.

2.7.3 Output Tape 2

Output Tape 2 contains a frame-by-frame descriptive record of what each of the (up to 8) cameras on board the aircraft surveyed. After sorting, the tape serves as input to the Photo-Interpreter model.

This tape, written on logical tape unit 12, contains binary coded decimal records, each being 135 characters in length. The first record is the header. Table 2-4 is a description of the data content of this record.

Following the header is a series of photoframe records. Each time a target appears within a frame of a camera, a separate record is generated; e.g., if target A appears on frames 100 to 107 of camera B, eight separate records will be generated. These records are written on the tape in the order they are produced, i.e., on a pass-target-photosensor-leg basis.

As stated in Paragraph 2.2, each pass of the mission is processed sequentially. Within each pass, each target is treated in turn; for each target, each sensor is sequentially considered; for each sensor, all legs in the pass are

TABLE 2-3a. SCENARIO - VARIABLE OUTPUT LIST

		Dummy	IR	SLR	SLR MTI	FLR MTI	ECM	Photo	FLIR
Time target is broadside to aircraft	(0.1 sec.)	G(1)							
Range - ground offset	(NM)	G(2)	G(1)	G(1)	G(1)		G(1)		G(1)
Slant offset range	(NM)	G(3)	G(2)	G(2)	G(2)		G(4)	G(3)	G(2)
Frame count for camera 1		G(4)							
Frame count for camera 2		G(5)							
Frame count for camera 3		G(6)							
Frame count for camera 4		G(7)							
Frame count for camera 5		G(8)							
Frame count for camera 6		G(9)							
Frame count for camera 7		G(10)							
Frame count for camera 8		G(11)							
Aircraft height above mean ground level	(ft.)			G(3)	G(3)	G(2)	G(3)		
Target height above MGL	(ft.)		G(3)	G(4)	G(4)	G(4)			G(3)
Aircraft ground speed	(K)			G(7)					
Aircraft speed	(K)						G(2)		
Target velocity-radial ground projection	(K)			G(6)		G(1)			
Target velocity slant range projection	(K)				G(6)				
Slant range of rain traversed	(NM)				G(5)	G(9)	G(9)		
Slant range haze	(NM)		G(5)					G(4)	G(5)
Slant range clouds	(NM)		G(6)						G(6)
Depression angle to target	(rad.)		G(7)						
Minimum ground range for detect. target	(NM)					G(4)			
Maximum ground range for detect. target	(NM)					G(5)			
σ^2 of terrain height above mean	(ft^2)		G(4)	G(5)	G(7)	G(8)			
Target sightings expected - clear of terrain						G(6)			
σ^2 of unobstructed sightings						G(7)			
Code - nadir - target within Θ_2							G(7)		
Value of Θ_2							G(8)		
Target height							G(10)		

TABLE 2-3a. SCENARIO - VARIABLE OUTPUT LIST (contd.)

		Dummy	IR	SLR	SLR-MTI	FLR MTI	ECM	Photo	FLIR
Navigational error in heading	(rads)	P(1)							
Navigational σ^2 in heading	(rad^2)		P(3)						P(3)
Navigational error in speed	(Kn)	P(2)							
Navigational σ^2 in altitude	(ft^2)		P(4)						P(4)
Navigational CEP	(NM)	P(3)							
Probability that terrain is not shadowed			P(1)	P(1)	P(1)	P(1)	P(1)	P(1)	P(1)
Probability that equipment is up			P(2)	P(2)	P(2)	P(2)	P(2)	P(2)	P(2)
Target type code		T(1)							
Target area	(m^2)		T(1)						P(1)
Radar cross section	(m^2)			T(1)	T(1)	T(1)			
Peak power transmitted (1w.)	(db)						T(1)		
Reflectivity of target (photo)								T(1)	
Code for preplanned targets		T(4)							
Target temperature	(^oK)		T(2)						T(2)
Radar reflectivity				T(2)					
Backscatter coefficient					T(2)	T(2)			
Transm. ant. -main lobe gain	(db)					T(2)			
Resolution req'd for 90% prob. of det.	(ft.)		T(3)				T(2)		T(3)
Resolution req'd for 50% prob. of det.	(m.)			P(3)					
Code for key for air to air commun.		T(3)							
Frequency	(mHz)						T(3)		
Reflectivity of background				T(4)				T(3)	
Target E for band 1			T(4)						T(4)
Target E for band 2			T(5)						T(5)
Background E for band 1			T(6)						T(6)
Background E for band 2			T(7)						T(7)
Background temperature	(^oK)		T(8)						T(8)
Antenna front to back ratio (XM)	(db)						T(4)		
Pulses per second							T(5)		
Pulse width	(msec.)						T(6)		
Target scan period	(secs.)						T(7)		

TABLE 2-3a. SCENARIO - VARIABLE OUTPUT LIST

	Dummy	IR	SLR	SLR-MTI	FLR MTI	ECM	Photo	FLIR
Visibility through haze (sm)		W(1)						W(1)
Visibility through clouds (sm)		W(2)						W(2)
Undercast clouds - prob. of none		W(3)						W(3)
Precipitation rate (rain or snow) (in/hr)			W(1)	W(1)	W(1)	W(1)		
Weather type index - clear, rain, snow (0, 1, 2)			W(2)	W(2)	(W2)			
Precipitation on target code (yes = 1, no = 2)			W(3)	W(3)	W(3)	W(2)		
Visibility prevailing (sm)							W(1)	
Visibility in rain (sm)							W(2)	
Day/night (1, 2)							W(3)	

TABLE 2-3b. VARIABLE OUTPUT LISTS BY SENSOR TYPE*

Dummy Sensor	
G(1)	- time at which the target lies broadside of the aircraft (in tenths of a second).
G(2)	- ground offset range in NM. The positive direction is to the right.
G(3)	- slant offset range in NM. This parameter is always positive.
G(4)	- frame count for camera 1.
G(5)	- frame count for camera 2.
G(6)	- frame count for camera 3.
G(7)	- frame count for camera 4.
G(8)	- frame count for camera 5.
G(9)	- frame count for camera 6.
G(10)	- frame count for camera 7.
G(11)	- frame count for camera 8.
G(12) to G(15)	- not used.
P(1)	- navigational error in heading (radians).
P(2)	- navigational error in speed (knots).
P(3)	- navigational CEP (NM).
P(4) and P(5)	- not used.
W(1) to W(5)	- not used.
T(1)	- the target type code.
T(2)	- a code designation for preplanned targets (set to "0" if preplanned, set to "1" if not).
T(3)	- a code denoting if the target is keyed to air-to-air communications (set to "0" if keyed, set to "1" if not).
T(4) to T(10)	- not used.

*With the exception of the section of this table on the forward looking infrared sensor, this table is taken verbatim from the Kettelle Report.[2]

TABLE 2-3b. VARIABLE OUTPUT LISTS BY SENSOR TYPE (Contd.)

Infrared Sensor	
G(1)	- ground range to target (when passing broadside) in NM.
G(2)	- slant range to target in NM.
G(3)	- target height above mean-ground-level (MGL) in feet.
G(4)	- variance of the terrain height about its mean in $(\text{feet})^2$.
G(5)	- slant range of haze traversed in NM.
G(6)	- slant range through clouds in NM.
G(7)	- depression angle to the target in radians.
G(8) to G(15)	- not used.
P(1)	- terrain shadowing probability.
P(2)	- probability that the equipment is up.
P(3)	- variance in heading error in $(\text{radians})^2$; arising from navigational subsystem.
P(4)	- variance in altitude error in $(\text{feet})^2$; arising from navigational subsystem.
P(5)	- not used.
W(1)	- prevailing visibility through haze in statute miles.
W(2)	- prevailing visibility through clouds in statute miles.
W(3)	- probability of no undercast clouds.
W(4) and W(5)	- not used.
T(1)	- target area in $(\text{meter})^2$.
T(2)	- target temperature in ^{o}K.
T(3)	- resolution in meters required for 90% probability of detection.
T(4)	- target emissivity for band 1.
T(5)	- target emissivity for band 2.

TABLE 2-3b. VARIABLE OUTPUT LISTS BY SENSOR TYPE (Contd.)

Infrared Sensor (Contd.)	
T(6)	- background emissivity for band 1.
T(7)	- background emissivity for band 2.
T(8)	- background temperature in ^{o}K.
T(9) and T(10)	- not used.
Side Looking Radar	
G(1)	- ground range to target (when passing broadside) in NM.
G(2)	- slant range to target in NM.
G(3)	- aircraft height above MGL in feet.
G(4)	- target height above MGL in feet.
G(5)	- variance of the terrain height about its mean in $(feet)^2$.
G(6)	- radial ground projection component of target velocity in knots.
G(7)	- aircraft ground speed in knots.
G(8)	- rain height.
G(9) to G(15)	- not used.
P(1)	- terrain shadowing probability.
P(2)	- probability that the equipment is up.
P(3) to P(5)	- not used.
W(1)	- precipitation rate of rain or snow in inches per hour.
W(2)	- precipitation index ("0" for none, "1" for rain, "2" for snow).
W(3)	- a code denoting if precipitation is falling upon the target ("1" for yes, "2" for no).
W(4) and W(5)	- not used.

TABLE 2-3b. VARIABLE OUTPUT LISTS BY SENSOR TYPE (Contd.)

Side Looking Radar (Contd.)	
T(1)	- radar cross section in $(meter)^2$.
T(2)	- radar reflectivity.
T(3)	- the resolution in meters required for 50% probability of detection.
T(4)	- background reflectivity.
T(5) to T(10)	- not used.
Side Looking Radar (MTI)	
G(1)	- ground range to target (when passing broadside) in NM.
G(2)	- slant range to target in NM.
G(3)	- aircraft height above MGL in feet.
G(4)	- target height above MGL in feet.
G(5)	- slant range of rain traversed in NM.
G(6)	- absolute value of target speed (in knots) projected along the slant range vector.
G(7)	- variance of the terrain height about its mean in $(feet)^2$.
G(8) to G(15)	- not used.
P(1)	- terrain shadowing probability.
P(2)	- probability that the equipment is up.
P(3) to P(5)	- not used.
W(1)	- precipitation rate of rain or snow in inches per hour.
W(2)	- precipitation index ("0" for none, "1" for rain, "2" for snow).
W(3)	- a code denoting if precipitation is falling upon the target ("1" for yes, "2" for no).
W(4) and W(5)	- not used.

TABLE 2-3b. VARIABLE OUTPUT LISTS BY SENSOR TYPE (Contd.)

Side Looking Radar (MTI) (Contd.)	
T(1)	- radar cross section of the target in $(meter)^2$.
T(2)	- backscatter coefficient.
T(3) to T(10)	- not used.
Forward Looking Radar (MTI)	
G(1)	- absolute value of target speed projected along the slant range vector in knots.
G(2)	- aircraft height above MGL in feet.
G(3)	- target height above MGL in feet.
G(4)	- minimum ground range, in NM, at which target is detectable.*
G(5)	- maximum ground range, in NM, at which target is detectable.*
G(6)	- expected number of target sightings unmasked by terrain.
G(7)	- variance of the number of unobstructed sightings.
G(8)	- variance of the terrain height about its mean in $(feet)^2$.
G(9)	- slant range of rain traversed in NM.
G(10) to G(15)	- not used.
P(1)	- terrain masking probability.
P(2)	- probability that the equipment is up.
P(3) to P(5)	- not used.
W(1)	- precipitation rate of rain or snow in inches per hour.
W(2)	- precipitation index ("0" for none, "1" for rain, "2" for snow).

*See equations (3.5.1) and (3.5.2) of Section IA of the Kettelle Report. (2)

TABLE 2-3b. VARIABLE OUTPUT LISTS BY SENSOR TYPE (Contd.)

Forward Looking Radar (MTI) (Contd.)	
W(3)	- a code denoting if precipitation is falling upon the target ("1" for yes, "2" for no).
W(4) and W(5)	- not used.
T(1)	- radar cross section of the target in $(meter)^2$.
T(2)	- backscatter coefficient.
T(3) to T(10)	- not used.
ECM Sensor	
G(1)	- ground distance of target from flight line in NM.
G(2)	- aircraft speed in knots .
G(3)	- aircraft height above MGL in feet.
G(4)	- slant range to target in NM.
G(5)	- time of the look in tenths of a second.
G(6)	- not used.
G(7)	- code: set to "1" if target passed directly underneath the aircraft (within θ_2 degrees of nadir, where θ_2 is an input value); set to "0" otherwise.
G(8)	- the value of θ_2 in radians (used to determine G(7)).
G(9)	- slant range of rain traversed in NM.
G(10)	- target height in feet.
G(11) to G(15)	- not used.
P(1)	- terrain shadowing probability.
P(2)	- probability that the equipment is up.

TABLE 2-3b. VARIABLE OUTPUT LISTS BY SENSOR TYPE (Contd.)

Forward Looking Infrared Sensor (Contd.)	
G(9) to G(15)	- not used.
P(1)	- terrain shadowing probability.
P(2)	- probability that the equipment is up.
P(3)	- navigational variance in heading in $(\text{radians})^2$.
P(4)	- navigational variance in altitude in $(\text{feet})^2$.
P(5)	- not used.
W(1)	- prevailing visibility through haze in statute miles.
W(2)	- prevailing visibility through clouds in statute miles.
W(3)	- probability of no undercast clouds.
W(4) and W(5)	- not used.
T(1)	- target area in $(\text{meter})^2$.
T(2)	- target temperature in ^{o}K.
T(3)	- resolution in meters required for 90% probability of detection.
T(4)	- target emissivity for band 1.
T(5)	- target emissivity for band 2.
T(6)	- background emissivity for band 1.
T(7)	- background emissivity for band 2.
T(8)	- background temperature in ^{o}K.
T(9) and T(10)	- not used.

TABLE 2-4. RECORD 1 OF OUTPUT TAPE 2

Character	Format	Description
1-4 5-12 13-18	I4 I8 I6	These records are arbitrarily set to zero.
19-98	20A4	An 80 character alphanumeric label which describes the run.
99-114	8I2	Eight two-character on-off indices for the 8 photo sensors: 1 = on; 0 = off.
115-119	I5	A number, used as a program control, which is the multiplication of the number of passes in the mission by the number of targets considered.
120-135	8I2	Eight two-character integers indicating the type of each photo-sensor: 0 = pan camera; 1 = side oblique plane camera; 2 = forward oblique plane camera.

analyzed. Each time a target enters the field of view of a sensor, a record containing information about the sighting is generated. Hence, the targets are not ordered with respect to time.

Output Tape 2 is sorted by camera, frame, and target, and passed to a program called TAPEQNT (see Paragraph 5.5.1) which computes the number of targets seen on each camera frame. The resulting tape contains records of the form shown in Table 2-5; these records always appear after the header record.

The last record on the tape is an end-of-file indicator, and contains a value of 99 for the camera index. It is a control record and does not contain information.

2.7.4 Output Tape 3

Output Tape 3 lists target number, target type, and the time at which the aircraft flew past the target. This tape is sorted by time and then listed to provide a time-line record of the reconnaissance mission.

TABLE 2-5. SIGHTING RECORDS FOR OUTPUT TAPE 2

Character	Format	Description
1-4	I4	Two-digit index of the camera to which this record pertains.
5-12	I8	The camera frame number being considered.
13-18	I6	A five-digit number to identify the target (the last 3 digits) and the pass (first 2 digits) to which this frame pertains.
19-30	F12.6	The probability that this target is not masked by terrain.
31-42	F12.6	The probability that this target is viewed through clouds in this frame.
43-47	I5	The total number of targets seen in this frame (from TAPEQNT program).

The user has the option of generating this tape on logical tape unit 13. The records are binary coded decimal and are 60 characters long.

Each time a target is passed broadside, a record is generated; the contents of which are described in Table 2-6. Records are generated on a pass-target-sensor basis, and are not coded chronologically. Output Tape 3 is sorted* by time and, with the aid of a program called LIST, is listed as hard copy output. This output is then a time-line of target passage.

* Sorting is accomplished by sorting output tape 3 using the standard CDC library sort routine. Setup of this routine is discussed in Appendix G.

TABLE 2-6. RECORD FORMAT OF OUTPUT TAPE 3

Variable	Format	Description
ITARG	I20	A five digit designation of the target number (last 3 digits) and the pass number for the current target.
ITP (ITAR)	I20	An integer designating the type of target being passed.
ITIME	I20	An integer designating the time, in tenths of seconds, from mission start time at which the target is passed abeam.

SECTION III.
THE EXECUTIVE MODEL

3.1 INTRODUCTION

The purpose of the Executive program is to determine with what probability each target being considered is detected, identified, and localized by (1) each of the sensors on board the reconnaissance aircraft, and (2) by the overall reconnaissance system, i.e., by integrating the results of all sensors.

This is done for each of four processing levels:

Level 1. Real-time and near-real-time processing of data on board the aircraft.

Level 2. Data keying and transmission to a ground station.

Level 3. Data keying but no transmission to a ground station.

Level 4. No data keying and no transmission to a ground station.

In real-time processing the reconnaissance operator observes on display terminals a subset of the area being viewed by the sensors. The operator analyzes the displayed information for target content, and, when possible, identifies the target. When important targets are detected he can signal the ground station directly.

The only purpose of the keying function in Level 1 is to mark important data for later processing. For example, the airborne observer may not wish to signal the ground station but he may wish to note suspected significance within a frame. He would then "push a button" to key the frame. In the case of a preplanned target, the frame is keyed automatically when the picture is taken. Whether automatically or manually performed, keying would alert the Photo-Interpreter (PI) operator to the frames most likely to contain target information.

In Level 2, the system automatically selects "data packages" for immediate transmission to ground. This action has the effect of reducing system time-late for critical reconnaissance data not able to be evaluated on board the aircraft.

Level 3 assumes that the data has been keyed but is not transmitted. Nevertheless, system performance, especially time-late, is improved because PI operators examine keyed data first, that is, the data that is relatively target rich.

In Level 4 data is collected on board and brought back to the ground for analysis, as evidenced in current conventional reconnaissance systems (e.g., RA-5C).

Paragraph 3.2 contains a discussion of how to determine with what probability each target can be detected, identified, and localized, based on the quantity and quality of the information provided by a particular sensor. (Scenario determines if a target is in the field of view of a sensor, but it is not determined by Scenario if the target is detectable.)

Paragraph 3.3 discusses how data for each sensor is combined into statistics for the overall performance of the system in relation to each target being considered.

The Executive computer program is briefly discussed in Paragraph 3.4. Detailed discussions of the program inputs and outputs form Paragraphs 3.5 and 3.6, respectively. Collectively, Paragraphs 3.4, 3.5, and 3.6 form an abbreviated user's guide for the program.

Paragraph 3.7 describes how a user can study the effectiveness of one sensor at a time without exercising the entire model, thus providing an optimization tool for single sensors.

3.2 MODELS FOR EACH SENSOR

The subsequent paragraphs discuss the technical aspects of each sensor model. A few definitions are given of the performance criteria for each sensor.

- Detectability -
  Conditional:

  Conditional detectability is the probability that the sensor sees the target assuming: (1) the sensor equipment is operable; (2) the target is not masked by terrain; (3) the target is not obscured by clouds.

Total:

Total detectability is the probability that the sensor sees the target taking into account consideration of terrain, weather, and equipment up probabilities.

- Identifiability -
  Conditional:

  Given that the target has been detected conditionally, the conditional identifiability is the probability that the target can be identified.

  Total:

  This is the product of total detectability and conditional identifiability, i.e., the probability of identifying a target considering terrain, weather, and equipment-up conditions.

- Localizability -
  Conditional:

  This is the CEP of the target position given by the sensor in the absence of cloud cover, terrain masking, and equipment failure.

  Total:

  This is the CEP given by the sensor when terrain, weather, and failure statistics are considered.

3.2.1 Overview of Sensor Models

3.2.1.1 Photo-TV Model. A single model is used for Photo, TV, and LLTV, even though both the results and their analysis levels are different. Basically, the models assume that the f-stop setting, V/H factors, etc., are appropriate and in range, and concentrate on image quality degradation. If target-background contrast is reduced by atmospheric scattering, a check is made as to whether there is enough contrast remaining for a usable image. In the case of illuminated night photography, the assumption is made that the exposure has been correctly set to produce a maximally dense acceptable negative at the aircraft nadir, and a check is made to see if an acceptable negative density is produced at the target range. Resolution is computed next and corrected for range, slant angle, and contrast-induced degradation. From the corrected resolution value, target detection and identification probabilities are computed, using curve-fits to observational data. The resolution required for identification is assumed to be five times the resolution required for detection; both are degraded by cloud undercast.

Photos are labeled as to whether or not they were keyed by alerting for segregation of total detection and identification probabilities into analysis levels. TV and LLTV are only effective at Level 1 (unless recorded), while photos are potentially effective at Levels 1, 2, 3, and 4.

For the optical sensors, positioning CEP's are considered negligible compared with navigation errors and are therefore ignored.

3.2.1.2 Infrared Sensor Model (IR). The IR model generally follows the same pattern as the photo model, except that one look, at most, is provided per target, and the system is self-keying. Targets are characterized by cross section and temperature, normalized to an assumed 18 centigrade degrees background. Using IR sensitivity equations, a detectability is estimated after the target output relative to background is attenuated and scattered by distance, atmosphere, and clouds. At present, the cloud attenuation is a rough estimate, because in-cloud visibility is hard to predict. Identification is only roughly possible with IR in most cases (except that targets will be classified as to radiative output) unless a refined spectroscopically sensitive IR system is proposed. In general, the target size will be sufficiently smaller than the resolution spot size, making geometrical identification impossible. Positioning errors, on the other hand, are significant for IR because the target altitude is not known to certainty. Therefore, position error estimates must be made and incorporated with navigation errors. Alerting via IR assumes a target sufficiently hot as observed, to key a gaussian square-law detector, while IR imagery assumes displays and film recording.

3.2.1.3 Radar Model. The basic radar model is applicable to the Side Looking Radar, the Moving Target Information Side Looking Radar, and the Moving Target Information Forward Looking Radar.

These radar models follow classical lines, including atmospheric and rain degradation affects as well as rain clutter where appropriate for the radar band to be employed. The Moving Target Information (MTI) and positioning channels are considered separately. A simple ground clutter model is employed, with ground clutter rejection expressed as a single number in db. MTI data are obscured by MTI clutter.

3.2.1.4 ECM Model. The ECM model follows a classical pattern except that, in general, several independent looks are available. The ECM pickups are approximated by N independent rays (N is generally equal to the number of ECM receiver antennas) rather than a correlated continuum of inputs. The only significantly complex submodel is the passive ranging model. It assumes approximately an optimal (minimum variance) estimation of range from passive observations, and combines these results with navigational errors to get an ECM-CEP.

3.2.1.5 Forward Looking Infrared Sensor (FLIR). The FLIR model is similar to that of the IR, except that multiple looks at a target may or may not occur.

If a target is preplanned, or if FLIR is slewed by other sensors, FLIR is given two looks at the target. Slewing occurs when a forward looking sensor (i.e., MTI FLR, ECM) sees a target and provides FLIR with the coordinates.

3.2.2 Infrared Model (IR)

In simplified terms, for each of the four levels of processing, the IR model accepts the Scenario outputs and, for the target being considered, computes:

(1) The IR sensor detectability of the target on the current leg and pass.

(2) The conditional probability that, once detected, the target is identified.

(3) The error (CEP) in localizing the target.

However, since the IR sensor is actually two independent IR receivers, a high and a low band, each of the three quantities are computed separately for each band and then combined to yield the overall sensor detectability, identifiability, and CEP statistics.

The inputs to the IR model are of two kinds: (1) those provided by the Scenario program, and (2) those provided by the user.

INPUTS FROM SCENARIO

GEOGRAPHIC:

- Ground range when passing broadside in NM.
- Total slant range to the target in NM.
- Target height above MGL in feet.
- Variance of terrain height about its mean in feet.
- Slant range through (1) haze and (2) clouds in NM.
- Probability that target is not masked by terrain.
- Depression angle to the target.

WEATHER DATA:

- Prevailing visibility through (1) haze and (2) clouds in NM.
- Probability of no undercast clouds.

TARGET/BACKGROUND DATA:

- Target area in square meters.
- Temperature of target and background in ^{o}K.
- Resolution in meters required for 90% probability of detection
- Target and background emissivities for both bands 1 and 2

SENSOR AND NAVIGATIONAL SYSTEM DATA:

- Probability that IR equipment is up.
- Navigational variance in heading in radians squared.
- Navigational variance in altitude in radians squared.

USER INPUTS*

- Angular resolution for bands 1 and 2 in radians.
- Highest and lowest wavelength of both bands 1 and 2 in microns.

*Parameters such as rise time and scan rate are assumed to be appropriate.

Infr	
T(6)	
T(7)	
T(8)	
T(9)	
Side	
G(1)	
G(2)	
G(3)	
G(4)	
G(5)	
G(6)	
G(7)	
G(8)	
G(9)	
P(1)	
P(2)	
P(3)	
W(1)	
W(2)	
W(3)	
W(4)	

- Thermal resolution of bands 1 and 2 in ^{o}K.
- Variance in angular measurements (bands 1 and 2) in radians squared.
- IR system file gamma
- Minimum detectable logarithimic contrast.

These inputs are drawn together in the following manner:

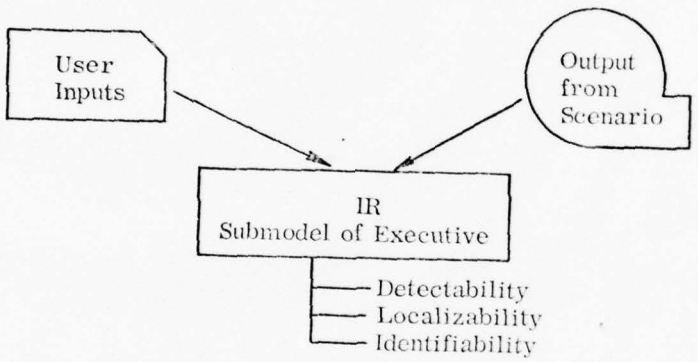

Paragraph 3.2.2.1 shows how the IR submodel, using the inputs given above, can predict detectability. Identifiability is discussed in detail in Paragraph 3.2.2.2; a discussion of the localization is the subject of Paragraph 3.2.2.3.

3.2.2.1 Detectability. As might be expected, the starting point in computing detectability is the computation of the power radiated per unit area into the atmosphere by both the target and its background. This is done by first computing the power radiated by a black body and then multiplying by the appropriate emissivities.

Next, having been provided as input the relevant geographic data (e.g., slant range to the target), weather information (e.g., cloud cover and depth, haze condition), and other such data as the probabilities that the IR is operable and that the target is not masked by terrain, one can compute the target and background powers per unit area actually received at the IR by considering the effects of:

(1) Scattering.

(2) Attenuation of signal.

(3) Noise and clutter.

These received powers are then adjusted by the area of target and background observed, thus changing the data from power per unit area received to power received.

Finally, one forms the ratio of the power received from the target to the power received from the background. This contrast ratio may then be used to predict the detectability.

Figure 3-1 is a flowchart of the computation of detectability. The elements of the flowchart are elaborated in Paragraphs 3.2.2.1.1 through 3.2.2.1.4, which comprise, respectively:

(1) Computation of the power radiated by the target and the background.

(2) Computation of the power received at sensor (target and background).

(3) Computation of the noise power received at the sensor.

(4) Computation of the overall detectability.

3.2.2.1.1 Power Radiated by Background and Target. A black body of temperature T degrees Kelvin radiates (into a hemisphere) $W_\lambda(\lambda)$ watts per square meter at the wavelength λ (in microns) where

$$W_\lambda(\lambda) = \left[\frac{3.7405 \times 10^8}{\lambda^5}\right]\left[e^{(14387.9/\lambda T)} - 1\right]^{-1} \qquad (3.1)$$

This equation is taken from reference.[4]

The power radiated by such a body in the band (λ_1, λ_2) is the integral of equation (3.1):

$$W(T) = \int_{\lambda_1}^{\lambda_2} W_\lambda(\lambda)\, d\lambda \qquad \text{watts/square meter} \qquad (3.2)$$

It is assumed that the detector sensitivity curve in each band is rectangular. If not, W_λ would have to be multiplied by $S(\lambda)$, the sensitivity curve, and the results

Side Lo (MT	
T(1)	
T(2)	
T(3) to	
Forwa Radi	
G(1)	
G(2)	
G(3)	
G(4)	
G(5)	
G(6)	
G(7)	
G(8)	
G(9)	
G(10)	
P(1)	
P(2)	
P(3) t	
W(1)	
W(2)	

• See

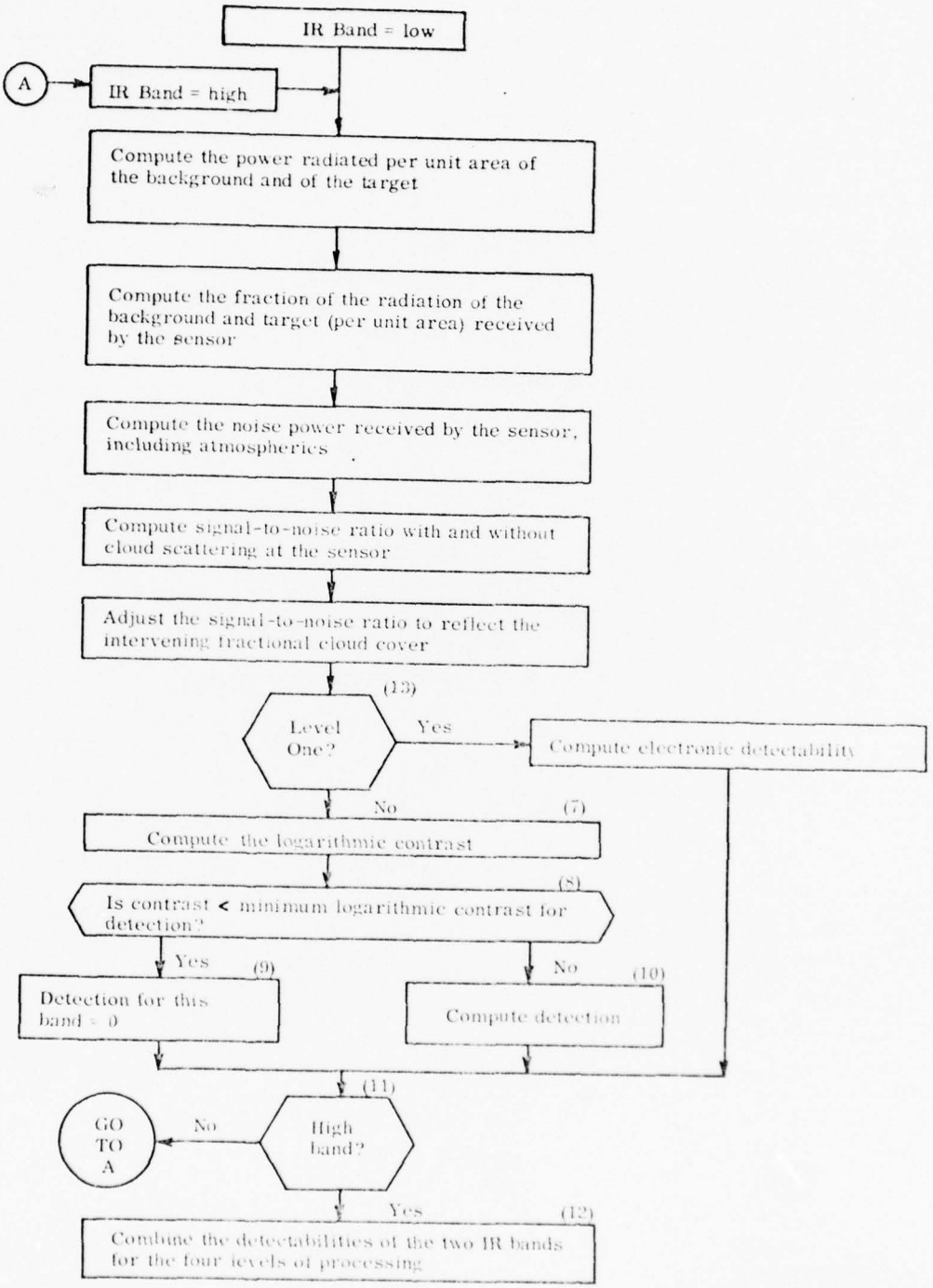

Figure 3-1. Flowchart of Infrared Sensor

numerically integrated. Under the stated assumption, using the three-point Gaussian Mechanical Quadrature,* equation (3.2) may be evaluated to yield:

$$W(T) = \frac{D}{9} [5\, W_\lambda (X_1) + 8\, W_\lambda (X_2) + 5\, W_\lambda (X_3)] \qquad (3.3)$$

where

$$D = (\lambda_2 - \lambda_1)/2$$

$$S = (\lambda_2 + \lambda_1)/2$$

$$C = 0.77459667$$

$$X_1 = S - D \cdot C$$

$$X_2 = S$$

$$X_3 = S + D \cdot C.$$

This formula (as proved by Gauss) is guaranteed to have at least the same accuracy as could be obtained by replacing the integrand (equation 3.1) with the best fitting (over the range λ_1, λ_2) fifth degree polynomial. (It was felt unnecessary to fit a higher order polynomial to the equation.)

The power radiated by the targer per unit area is then:

$$E_T\, W\, (T_T)$$

and of the background

$$E_B\, W\, (T_B)$$

where E_T and E_B are the emissivities of the target and the background, respectively; $W\, (T_T)$ is the black body radiation at the target temperature and $W\, (T_B)$ is the black body radiation at the temperature of the background.

*Gauss demonstrated that a fifth degree polynomial may be exactly integrated by knowing only the values of the function at three particular points. This technique is explained and referenced in Handbook of Mathematical Functions, reference (14).

3.2.2.1.2 Power Received at the Sensor from the Target and Background. Several parameters must be defined in order to compute the power received at the sensor.

Let:

A_S = effective sensor aperture in square meters.

A_T = target area in square meters (a spherical target is assumed).

R = slant range to the target in meters

δ = the angular resolution of the system in radians.

Then the area, normal to the radius vector, which is exposed to the system at one time is:

$$A_N = \delta^2 R^2 \tag{3.4}$$

The detector, when on target,* sees a target area of A_1, where A_1 is given by:

$$A_1 = \text{Minimum of } A_T \text{ and } A_N. \tag{3.5}$$

Similarly, A_2, the projected background area seen by the sensor, is given by:

$$A_2 = \text{Maximum of } 0 \text{ and } (A_N - A_T). \tag{3.6}$$

By assuming that the background is an isotropic, flat radiator, Lambert's Law can be used -- only the equivalent area normal to the radius vector need be considered.

*It is assumed that at some point the complete target is in the field of view of the detector.

The fractional radiated power captured by the system from a target (P_T) and background (P_B) is then:

$$P_T = \frac{A_S}{\pi R^2}\left[E_T A_1 W(T_T) + E_B A_2 W(T_B)\right] \tag{3.7}$$

$$P_B = \frac{A_S}{\pi R^2}\left[E_b A_N W(T_B)\right] \tag{3.8}$$

where E_t and E_b are the target and background emissivities, respectively.

Ordinarily, the received power would be multiplied by a broad-band absorption factor for each band to determine the effects of absorption. However, inspection of all relevant chapters of the ONR Handbook of Military Infrared Technology[4] indicates that at wavelengths of interest such absorption would be small. Further, since absorption reduces both P_T and P_B its effects tend to cancel at higher signal-to-noise (S/N) ratios.

However, the scattering effect of haze or clouds cannot be ignored. The approximate effect, for a well collimated receiver beam, is to reduce the contribution of $W(T_T)$ in equation (3.7). This is equivalent to adding in background, so that the result:

$$P_{Ti} = \left[\alpha_i A_1 E_T W(T_T) + \alpha_i A_2 E_B W(T_B) + (1 - \alpha_i) A_N E_B W(T_B)\right] A_s / \pi R^2 \tag{3.9}$$

$$(i = 1, 2)$$

Where

P_{T1} = the power received at the sensor from the target when clouds intervene

P_{T2} = the power received at the sensor from the target when clouds do not intervene

α_1 = the total scattering when clouds are present

α_2 = the total scattering when clouds are not present

The rest of this paragraph is devoted to computing α_1 and α_2.*

*Scattering of reflected sunlight is ignored since below 10μ the system is ineffective through clouds, while above 8μ the sunlight contribution is very small.

The ONR reference[4] shows, further, that for $1 \leq \lambda \leq 10\mu$ the atmospheric haze scattering is small out to 10km and highly inconsistent with respect to haze thickness. Thus any physical model of haze scattering would be conjectural. However, there is a relationship between IR and optical scattering outside the obsorption bands. For visible light[4] the scattering coefficient, σ_v, is

$$\sigma_V = \frac{3.9}{V} \qquad (\text{meters}^{-1})$$

where V is the meteorological visibility in meters. Taking the mean wavelength of visible light, $\lambda = 0.55\mu M$, the IR wavelength can be scaled to this value.

The IR scattering (σ) is found by first defining a constant γ. *

$$\gamma = 0.058 V^{1/3} \tag{3.10}$$

and then assuming, as is generally the case, that:

$$\sigma = (C\lambda)^{-\gamma}$$

$$\sigma/\sigma_V = \left(\frac{\lambda}{.55}\right)^{-\gamma} \tag{3.11}$$

$$\sigma = \left(\frac{3.9}{V}\right)\left(\frac{\lambda}{0.55}\right)^{-\gamma}$$

where V is now the optical visibility. Haze scattering and cloud scattering can be computed by replacing σ with σ_c or σ_H and V with V_c or V_H in equations (3.10) and (3.11).

Hence, total scattering for the case where there are both clouds and fog is:

$$\alpha_1 = e^{-(\sigma_h X_h + \sigma_c X_c)} \tag{3.12a}$$

where:

X_h = slant range through haze

X_c = slant range through cloud or fog cover

*A worst case is assumed. Figure 6-37 of the ONR Handbook[4] was chosen. However, Figure 6-33 is more optimistic.

If no clouds intervene (a probabilistic event)

$$\alpha_2 = e^{-\sigma_h X_h} \tag{3.12b}$$

These two values for α_1 and α_2 are inserted into equation (3.9) yielding two values of P_T. Value α_1 yields P_{T1} when inserted into equation (3.9) and α_2 yields P_{T2}. P_{T1} is simply the power received at the sensor from the target when clouds are present; P_{T2} is the power received from the target in the absence of clouds.

3.2.2.1.3 Noise Power Received at the Sensor. In addition to the degradation in detectability resulting from the target-relative temperature of the target background, the internal noise of the system affords another limitation. This internal noise can be of at least two varieties:

(1) Thermal noise caused by the ambient temperature of the detector.

(2) Shot noise caused by the condition that relatively few quanta are received (per resolution time interval) at the receiver; hence, being of similar energy and random (Poisson) timing, sampling noise is induced at the detector.

To determine the effects, or relative importance, of (1) and (2) more detail is required of the IR system design than is ordinarily available at the requirements level. These include the effective aperture of the optical system, the number of detectors, all geometric details of the optical system, the detector ambient temperature, and temperature rise per unit radiated power input.

Instead of trying to compute the physical contributions to noise it is necessary to work from the other end: from a specification that the thermal resolution is ΔT (given in ^{o}C). An equivalent noise power, of the size corresponding to ΔT thermal resolution, is estimated and equated to the equivalent noise power.

For the purpose just stated, it is sufficient to consider the case where the resolution cell is at the same temperature, T. As E_T is insensitive to temperature, the change in power, P, caused by a small change, ΔT, in T is (from the Stefan-Boltzman equation, differentiated with respect to T):

$$\Delta P = 4\ P\Delta T/T \tag{3.13}$$

The desired goal is to express the change ΔP in received power corresponding to the given thermal resolution ΔT. By equation (3.13), ΔP depends not only on ΔT, but on P and T also. P in turn, depends on the attenuation and scattering coefficients. It is no problem since the thermal resolution ΔT must also, from physical reasoning, depend on these factors. Then ΔP depends only on T:

$$\Delta P(T) = 4\Delta T\ P\ (T)/T.$$

This has two implications. First, to define the thermal resolution as a constant ΔT independent of temperature seen is unrealistic. If the resolution limit is due to internal noise, ΔP would be independent of temperature, and if it was due to background radiation noise, it would be proportional to $\sqrt{P(T)}$. Equation (3.13) shows that neither of these is correct. Second, if some constant value of T, e.g., the coolant temperature (T_o) is taken, the noise power, N, is given by:

$$N = [4\,\Delta T P\ (T_o)/T_o]\ b \qquad (3.14)$$

b = constant of proportion

for establishing the noise level, and thereafter N is considered to be independent of T; then the noise is attributed to internal detector noise. If treating it as a background radiation noise is desirable, the noise should be proportional to P:

$$N = [4\Delta T \sqrt{P(T)P(T_b)}/T_o]\ b \qquad (3.15)$$

Therefore, the best procedure is to compute the equivalent change in input power due to radiant background, at some standard temperature (say 18°C) and emissivity (say 1.0); this corresponds to a change of T*.

Then the estimated noise power, N, is:

$$N = \frac{A_S A_N}{\pi R^2}\ [W(318^\circ K + \Delta T) - W(318^\circ K)]$$

where ΔT is measured in °K for consistency of units.

*The assumption here, in effect, is that ΔT is a vendor's claim made under optimistic conditions, just like, e.g., receiver sensitivity. At present T is taken to be 318°K, although the choice is non-critical.

3.2.2.1.4 Detectability Computation. For infrared, detectability is handled as two separate cases: in the first case, Level 1, electronic detection and threshold triggering are assumed; the model for this detection closely follows radar lines. In the second case, Levels 2 through 4, photographic or display imagery are presumed, and an imagery-detection model is used.

In each of the two cases, detectability computations are made for each of the two bands, and for each of the alternative hypotheses that target is/or is not obscured by clouds. For one band, the detectability results from the two alternative calculations are combined via linear weighting where the weights are determined by the fractional undercast. This result is then combined with a like result from the other band on a conjunction basis, i.e., if either band "sees" the target, it has been detected.

3.2.2.1.4.1 Electronic Detection Model. Several sensors are modeled assuming RF-type electronic detection to convert received signals to data, via a square-law detector with thresholding. This includes the MTI radars, the ECM, and Level 1 processing in the IR subsystem. (Electronic detection is not included in the SLR imagery model because internal noise is not considered a significant factor when coherent integration is employed.) Signal-to-noise characteristics of a detector, while sensitive to false alarm rates and integration times, are not particularly sensitive to the linearity characteristics of the detector, rarely varying more than one db. Therefore, the assumption that the detector is of the square-law type, without regard to the fact that it may actually be otherwise (e.g., a linear-log detector), is reasonable.

The problem is as follows: given a signal of unknown amplitude, and a threshold decision as to whether or not the signal is present at any given time, what is the probability of detection of that signal when the threshold has been adjusted to a given and acceptable false alarm rate? If the signal shape is known (as indeed it is if a hard-edge source is assumed) one might just as well assume that it is a sinusodial signal with judicious filtering. (This point is commented on in the reference cited below.) In common practice, the noise is assumed to be additive, gaussian, and of limited bandwidth. This question poses the well known tradeoff problem of Type I errors (non-detection) versus Type II errors (false alarm). The

problem is solved in Skolnik, Section 2.5.[5] A curve-fit to the solution for a false alarm rate of 10^{-8} per integration interval is given in Betars:[6]

$$PDC = -0.320691 + S/N\left[0.027154 + S/N\,(0.0018809 - 4(10^{-5})\,(S/N))\right] \quad (3.16)$$

constrained to $0 \leq PDC \leq 1$, where S/N is the unitless signal-to-noise ratio (not db) and PDC the corresponding conditional detectability. Subroutine PDET implements this equation in the simulation program. Adjustments for other values of false alarm rates are handled internally within each sensor model as follows: An input variable IFALS represents the exponent in the desired false alarm rate, that is

$$X = 10^{-IFALS} \quad (3.17)$$

where X is the desired false alarm rate per unit integration time. Subroutine PDET is first entered to compute the detection probability PD8 for the nominal value of $X = 10^{-8}$. This quantity is used to adjust the signal-to-noise ratio by the following curve-fitting equation:[12]

$$C = (IFALS-8)\,(0.0679-PD8\,(0.0021)) \quad (3.18a)$$

$$[S/N]' = (S/N)\,(10^{-C}) \quad (3.18b)$$

and subroutine PDET is entered a second time with the adjusted value of signal-to-noise ratio, $[S/N]'$, to compute the adjusted probability of detection. The result is then returned to the appropriate sensor model for further processing.

3.2.2.1.4.2 Detectability

(1) Level 1. At this level, for alerting, electronic detection is assumed (see Paragraph 3.2.1.4.1).

Within a given IR band, the signal received is simply the difference between the target power received and the background power received. Therefore:

$$(S/N)_{\alpha_1} = \left|P_{T1} - P_B\right| / N \quad (3.19a)$$

$$(S/N)_{\alpha 2} = \left|P_{T2} - P_B\right| / N \quad (3.19b)$$

where $(S/N)_{\alpha_1}$ is the signal-to-noise ratio when clouds are present and $(S/N)_{\alpha_2}$ is the signal-to-noise ratio when clouds are not present. P_B is given in equation (3.8), and N in equation (3.15). P_{T1} is found by substituting equation (3.12a) into (3.9); P_{T2} by substituting (3.12b) into (3.9).

Substituting equation (3.19a) into equation (3.16) yields the conditional probability of detection when clouds are present; denote this quantity by $PDC^1_{\alpha_1}$ where the superscript denotes Level 1. A substitution of (3.19b) into (3.16) will yield the conditional probability of detection when clouds are not present, $PDC^1_{\alpha_2}$.

(Note that $PDC^1_{\alpha_1}$ and $PDC^1_{\alpha_2}$ must each be computed twice — once for IR band 1 and once for IR band 2.)

Combining the two bands to determine the conditional detectability for the overall sensor (denoted by PDT) yields, where R is fraction of undercast clouds:

$$PDT = R \left[1 - (1-PDC'_{\alpha_1}) \quad 1-PDC^2_{\alpha_1}) \right] + (1-R) \left[1-(PDC'_{\alpha_2}) \right] \left[(1-PDC^2_{\alpha_2}) \right] \tag{3.20}$$

The total detectability, PD, is then given by:

$$PD = PDC\ (P_1)\ (P_2)\ (K_{(1)}) \tag{3.21}$$

where

P_1 = the terrain non-shadowning probability

P_2 = the equipment

$P(1)$ = the decision
(0 = no, 1 = yes) as to the availability of the IR sensor at Level 1.

(2) Levels 2, 3, and 4. With these levels (all assumed to have the same detectability) there is an imagery problem and the noise N acts like a random fluctuation under which a contrast must be detected. Extrapolating from the Photo-Visual Model:

The contrast

$$C = \gamma \left| \log_{10}\left(\frac{P_T + N}{P_B + N}\right)\right| \tag{3.22}$$

where γ is the system film gamma.

If $C < C_o$, the conditional detectability, PDC, is zero. (C_o is a user input and is the minimum contrast at which detection is possible.) Otherwise, letting P_O be the required resolution for 90 percent probable detection at high contrast:

$$PDC = e^{\left[-0.1 \frac{A_N}{P_O^2}\right]}$$

where A_N is given in equation (3.4). This equation for PDC represents an empirical curve fit to $\frac{(S/N)}{\text{data}}$ contained in reference (12).

This equation for PDC must be modified to take in account the ground cell size corrected for contrast degradation, yielding:

$$PDC = e^{\left[-0.1 \frac{U}{P_O^2}\right]} \tag{3.23}$$

where U is given by (from reference (12))

$$U = \frac{A_N}{\left(1 - e^{-2C}\right)^2}$$

Equation (3.23) must be computed twice for each band, once for each value of α (as given in equation (3.12)). Let $PDC_{i\alpha_1}$ be the value of PDC from equation (3.23) when α_1 is used and band i is being considered. $PDC_{i\alpha_2}$ is analogous for α_2.

Then let

$$PDC'_1 = 1-(1-PDC_{1\alpha_1})\ (1-PDC_{2\alpha'_2})$$

$$PDC'_2 = 1-(1-PDC_{1\alpha_2})\ (1-PDC_{2\alpha_2})$$

$$PDC_{TOTAL} = R(PDC'_1) + (1-R)\ (PDC'_2)$$

And finally, the conditional detectability for the sensor (Levels 2, 3, and 4) is given by

$$PDC_{TOTAL} = 1 - (1 - PDC'_1)\ (1 - PDC'_2)$$

As usual, the total detectability, PD, is given by

$$PD = PDC_{TOTAL}\ P_1\ P_2\ K_{(1)}$$

where, as in equation (3.21):

P_1 = the terrain non-shadowing probability

P_2 = the equipment up probability

$K_{(1)}$ = the decision (0 = no, 1 = yes) as to whether the IR sensor is available in processing Levels 2, 3, and 4.

3.2.2.2 Identifiability. Let $P_{Ii}^{(L)}$ be the conditional identifiability based upon band i in Level L.

Because conditional identifiability (conditioned on detection), on a per-target basis, is not well understood, approximations must be used.

For Level 1, an input parameter S_o is defined to be an "identifiability threshold." Then

$$P_{I1}^{(1)} = P_{I2}^{(1)} = \begin{cases} 0 & \text{If } Pd < S_o \\ 1 & \text{If } Pd \geq S_o \end{cases}$$

It is assumed that, as in the photograph model (see Paragraph 3.2.7.2) five times the resolution needed for detection is needed for identification. This assumption is discussed in reference (12). Then from the conditional probability equation:

$$P(A|B) = P(A \wedge B)/P(B) \tag{3.24}$$

$$P_{Ii}^{(2)} = P_{Ii}^{(3)} = P_{Ii}^{(1)} = e^{-2.4\frac{U^2}{P_T}} \tag{3.24a}$$

for i = 1, 2.

The overall sensor conditional identifiability, PI_L, (Level L), is given by

$$PI_L = 1 - \left(1 - P_{I1}^{(L)}\right)\left(1 - P_{I2}^{(L)}\right) \tag{3.24b}$$

3.2.2.3 Localizability. A CEP value is computed for each of the two IR bands. The CEP for the overall sensor is defined as equal to the least of the band CEP's. The following paragraphs discuss how the CEP is computed for each band.

In the lateral direction, ground distance estimation errors, incorrect assumption of target height, and granularity errors are the most significant. Other sources of lateral error are not considered since they appear to be negligible.

At this point the variables used in this discussion are defined:

H = the true target height above the ground (not AMGL)

R = the true ground range to target

H_o = the true aircraft height above mean ground level (AMGL)

TH = the true target height AMGL

H' = the true difference between the aircraft and target height AMGL

θ = the true depression angle to the target

$\hat{R}$ = the estimated ground range to the target

$\hat{\theta}$ = the measured depression angle to the target

$\hat{H}$ = the estimation of H

Figure 3-2 illustrates the use of these variables.

First, the error in lateral direction (perpendicular to flight path) is considered. This consists of two parts: the error due to lack of knowledge of the target's vertical distance component relative to the aircraft, and the error due to uncertainty in the measured depression angle of the target.

The true ground distance to the target, R, is given by

$$R = (H_o - TH)\cot\theta = H'\cot\theta \tag{3.25}$$

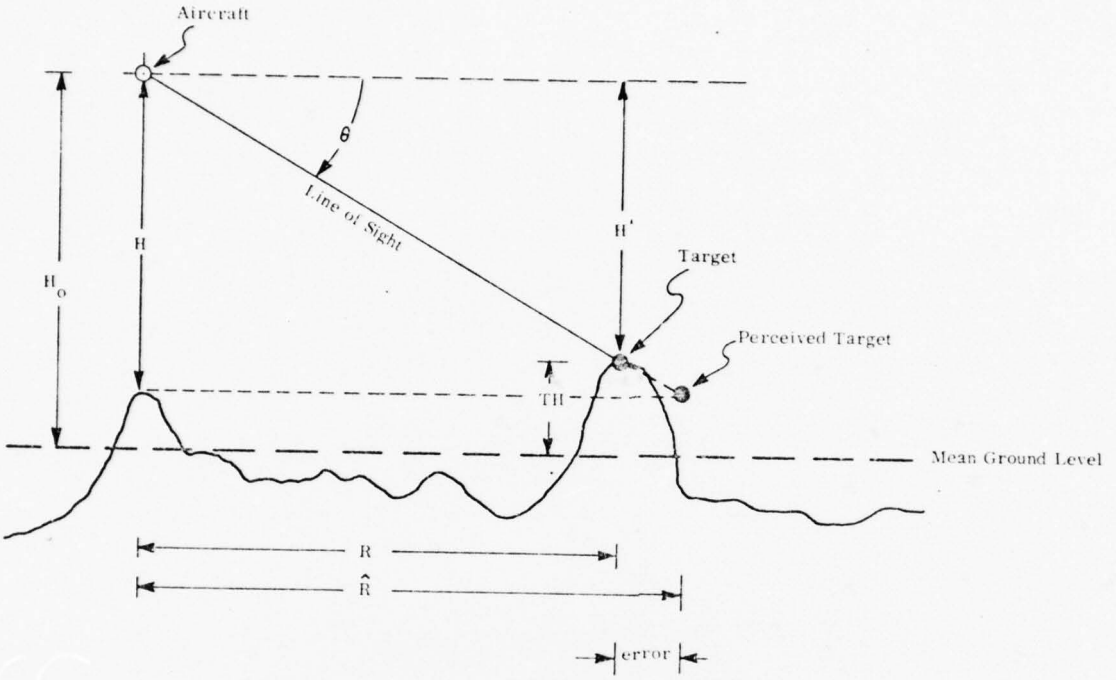

Figure 3-2. Illustration of Lateral IR Position Error

On the other hand, the system infers a ground range $\hat{R}$ based on measured aircraft height, $\hat{H}$, and the measured depression angle $\hat{\theta}$:

$$\hat{R} = \hat{H} \cot \hat{\theta} \tag{3.26}$$

The error in the measured aircraft height contains two random components, namely

(1) δZ — the error due to the fact that the aircraft nadir is not at mean ground level

(2) δH — a height error arising from imperfect altitude measurement

Mathematically:

$$\hat{H} = H_o + \delta Z + \delta H \tag{3.27}$$

The error in the depression angle consists of a random angular measurement error, $\delta\theta$. Then

$$\hat{\theta} = \theta + \delta\theta \tag{3.28}$$

Substituting equations (3.28) and (3.27) into equations (3.26) yields

$$\hat{R} = (H_o + \delta Z + \delta H) \cot (\theta + \delta\theta)$$

The argument of the cotangent function can be expanded by a Taylor's series; neglecting terms of third and higher order:

$$\cot (\theta + \delta\theta) = \cot\theta - \delta\theta \csc^2\theta \tag{3.29}$$

Incorporating this expansion, the equation for R becomes

$$\hat{R} = (H_o + \delta Z + H) (\cot\theta - \delta\theta \csc^2\theta) \tag{3.30}$$

The lateral error variance, σ_x^2 is then given by

$$\sigma_x^2 = E\left[\hat{R} - R\right]^2 = E\left[(H_o + \delta Z + \delta H) (\cot\theta - \delta\theta \csc^2\theta) - (H_o - TH) \cot\theta\right]^2 \tag{3.31}$$

Since the error terms are assumed independent and the random error symmetric, the solution is

$$\sigma_x^2 = \left[TH^2 + \sigma_Z^2 + \sigma_H^2\right] \cot\theta + H_o^2 \sigma_\theta^2 \csc^4\theta$$

where

σ_Z^2 is the variance of the terrain about its mean

σ_H^2 is the variance in the aircraft height above mean ground level as measured by the system

σ_θ^2 is the variance of depression angles as measured by the system

The last term is relatively small, and since $H >> TH$, no significant error is introduced by using the approximation

$$H_o \cong R \tan\theta$$

Hence,

$$\sigma_x^2 = \left[TH^2 + \sigma_Z^2 + \sigma_H^2 \right] \cot^2\theta + \sigma_\theta^2 \frac{R^2}{\sin^2\theta \cos^2\theta} \tag{3.32}$$

This sigma calculation, being wholly correlated among the bands, should be computed only once. If, however, the system is diffraction-limited and σ_θ^2 varies between bands, then the higher value of σ_θ^2 is chosen.

Longitudinally, the granularity error and the heading error contributions are considered. It is assumed that V/h is effectively within limits and that the speed error may be ignored. Then

$$\sigma_y^2 = \frac{R^2 (\sigma_\theta^2 + \sigma_{\theta_1}^2)}{\cos^2 \theta_1} \tag{3.33}$$

where

$\sigma_{\theta_1}^2$ is the variance in heading.

And finally, the CEP for each band is given, conventionally, as

$$CEP = 1.178 \sqrt{(\sigma_x)(\sigma_y)} \tag{3.34}$$

The CEP for the overall sensor is taken to be the minimum of the CEP's computed for each band.

3.2.3 Side Looking Radar Imagery Model (SLR)

The purpose of this model is to compute, for a given target, the detectability and identifiability probabilities and the CEP of localization based upon information provided by the SLR sensor.

As in the case of the IR, the inputs to the SLR submodel are of two varieties: (1) those supplied directly by the user, and (2) those supplied by the Scenario Program. As shown below, these parameters are fed into the SLR submodel within EXEC and are used to compute the three main outputs.

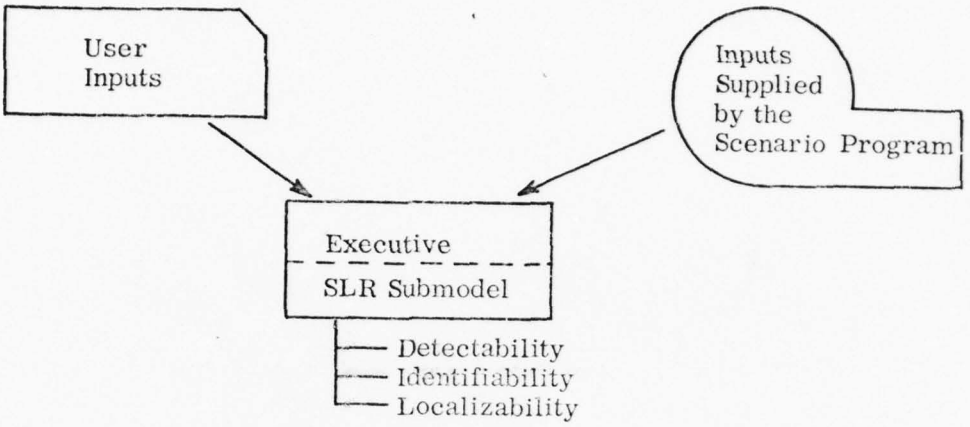

More specifically, the inputs are:

INPUTS PROVIDED BY SCENARIO

GEOGRAPHIC

- Ground range to target at time of abeam passage
- Slant range to target at time of sighting
- Aircraft height above mean ground level
- Target height above mean ground level
- Aircraft speed (ground)
- Variance of terrain height about its mean
- Radial ground projection of target velocity
- Probability that, at the time of sighting, the target is not masked by terrain

WEATHER DATA

- Precipitation rate (inches per hour) of rain or snow
- Type of precipitation (i.e., rain, snow or none)

TARGET/BACKGROUND DATA

- Radar cross section of target
- Radar reflectivity of target and background

SENSOR DATA

- Resolution required for 50 percent probability of detection
- Probability that equipment is in an up state at time of sighting

USER SUPPLIED DATA

- Range resolution
- Cross range resolution
- Depression angle of SLR
- Radar wavelength
- Film gamma
- Resolution (in lines/mm or line pairs) of film or display
- Minimum detectable logarithmic contrast
- Width of film
- Minimum and maximum slant ranges covered by film (a subset of the total range which is in the field of view of the SLR)
- Width of range displayed
- The variance of the perceived azimuth angle to the target (for use in computing localization errors)

The following paragraphs contain a discussion of the technical manner in which detection, identification, and localization are treated for the SLR.

3.2.3.1 Detectability. Side Looking Radar presents an imagery problem similar to that of photography. The signal and system gain characteristics are such that detectability in terms of classical radar-type considerations (vis-a-vis noise and attenuation) would be essentially 1.0 for a "white" target against a "gray" background. The operational view of the model in terms of detectability is described below.

The signal returns generated by the target, background, and precipitation backscatter are additively and coherently processed (n at a time) through an appropriate phase-controlled filter to yield film images. If the target size is significantly

larger than the radial projection of the ground resolution cell, the energy returned in the filled cells is the sum of:

(1) Target reflectivity return.

(2) Precipitation clutter in the three dimensional resolution cell.

If the target is smaller than the projected ground resolution the energy returned in the filled cells is the sum of:

(1) Target's radar cross section return.

(2) Background return in that part of resolution cell not covered by target

(3) Precipitation clutter in the resolution cell.

The background adjacent to the target reflects energy as the sum of:

(1) Background reflectivity and the return cell size.

(2) Precipitation clutter in the resolution cell.

Since only imagery on a film or CRT is of concern, effects due to radar figure of merit, inverse fourth power spreading, atmospheric attenuation, antenna pattern and assorted constants will cancel out when target-background contrast is considered. From this point on, then, the problem is one of contrast and resolution on the visual image and only the appropriate equivalent cross sections per unit area (i.e., the equivalent reflectivities) need be considered.

3.2.3.1.1 The Cell Reflectivities. Let the target cross section be σ_τ and its reflectivity be r_τ. The target's visual cross section is then σ_τ/r_τ, neglecting glint.

Let the target depression angle be ϕ.

Let h and j be, respectively, the range and cross-range resolution of the radar in meters. Note that it is an approximate characteristic of focused coherent radars that the effective azimuth resolution varies inversely proportional to range, and that the quantity j is independent of range.

Then the ground resolution cell area, A_r, can be found with the aid of Figure 3-3. In Figure 3-3, the second part is a cross section of the first:

ρ = ground range to target

R = slant range to target

h = range resolution

j = cross range resolution

Z' = the ground projection of h

$A_r = (j)\, Z'$

A_r can be found as a function of ρ, R, and h by noting* that

$$Z' \,(2\rho + Z') = h\,(2R + h)$$

$$Z'^2 + 2\rho Z' - h\,(2R+h) = 0$$

$$Z' = \frac{-2\rho \pm \sqrt{4\rho^2 + 4h\,(2R+h)}}{2}$$

$$Z' = \left(\sqrt{\rho^2 + h\,(2R+h)} - \rho\right) \tag{3.35}$$

Hence,

$$A_r = j\left(\sqrt{\rho^2 + h\,(2R+h)} - \rho\right) \tag{3.36}$$

*A well known theorem from plane geometry states that $(\overline{AE})\,(\overline{BE}) = (\overline{CE})\,(\overline{DE})$ where $\overline{AB}$ and $\overline{CD}$ are intersecting chords of the same circle.

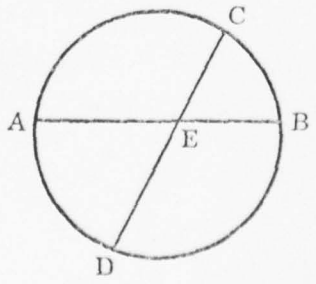

AD-A039 578 ANALYTICS INC WILLOW GROVE PA F/G 15/4
SIMULATION OF ADVANCED INTEGRATED RECONNAISSANCE SYSTEMS. VOLUM--ETC(U)
APR 69 S W LEIBHOLZ, S F MARTIN N62269-68-C-0441
UNCLASSIFIED 1004-1 NL

2 OF 3
ADA039 578

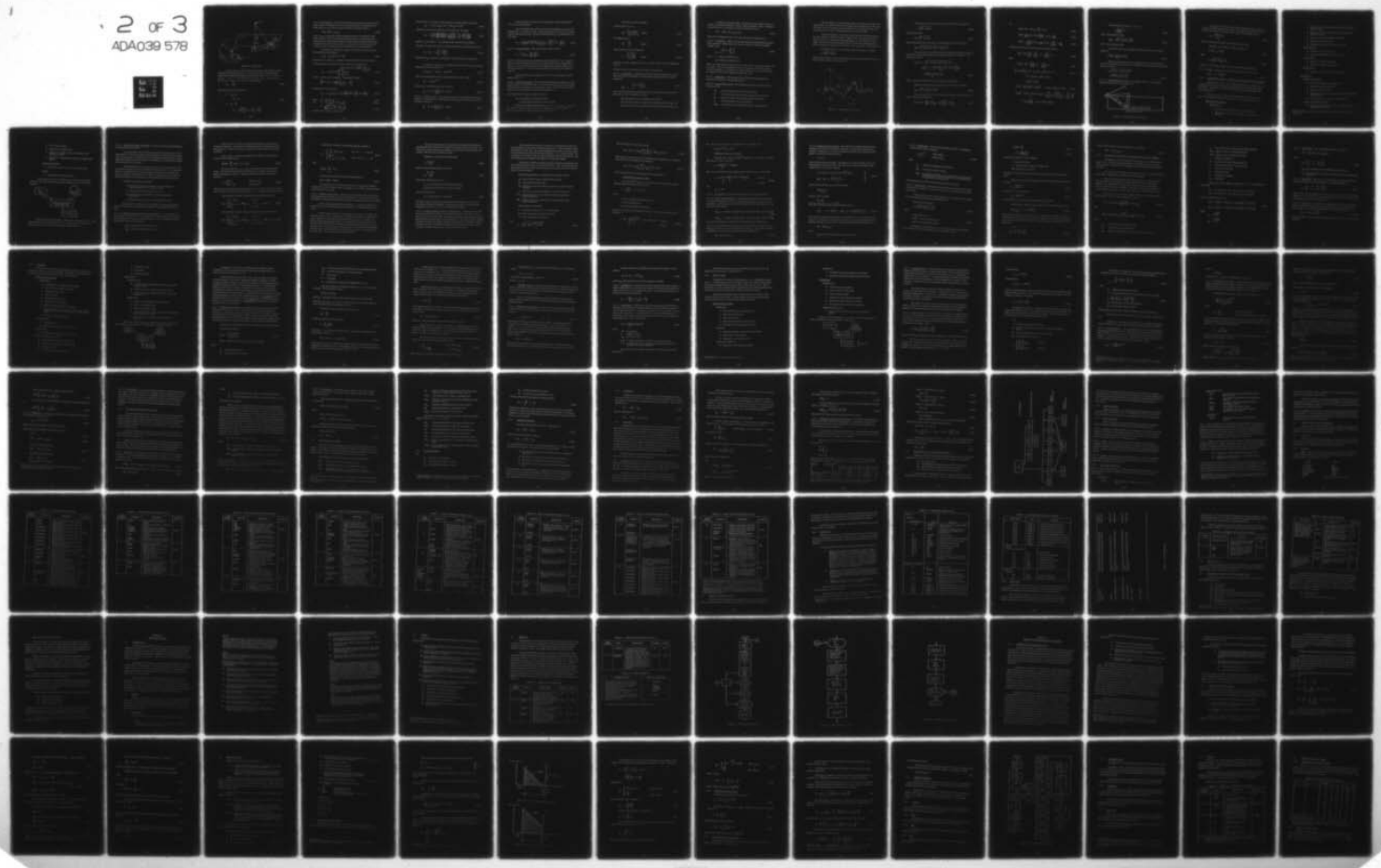

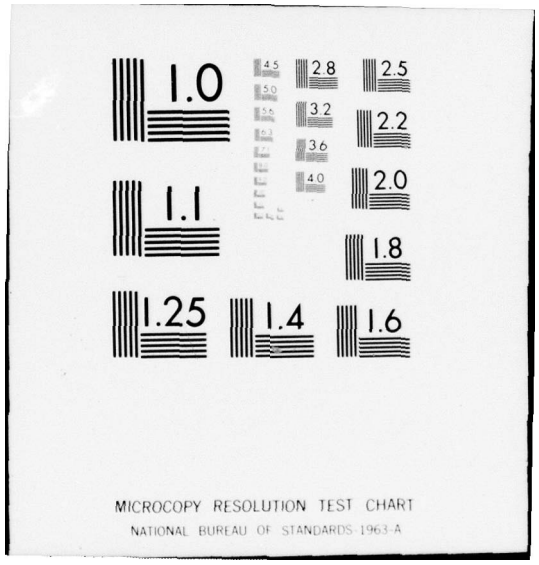
1.0
1.1
1.25
1.4
1.6
1.8
2.0
2.2
2.5
2.8
3.2
3.6
4.0
4.5
5.0
5.6
6.3
MICROCOPY RESOLUTION TEST CHART
NATIONAL BUREAU OF STANDARDS-1963-A

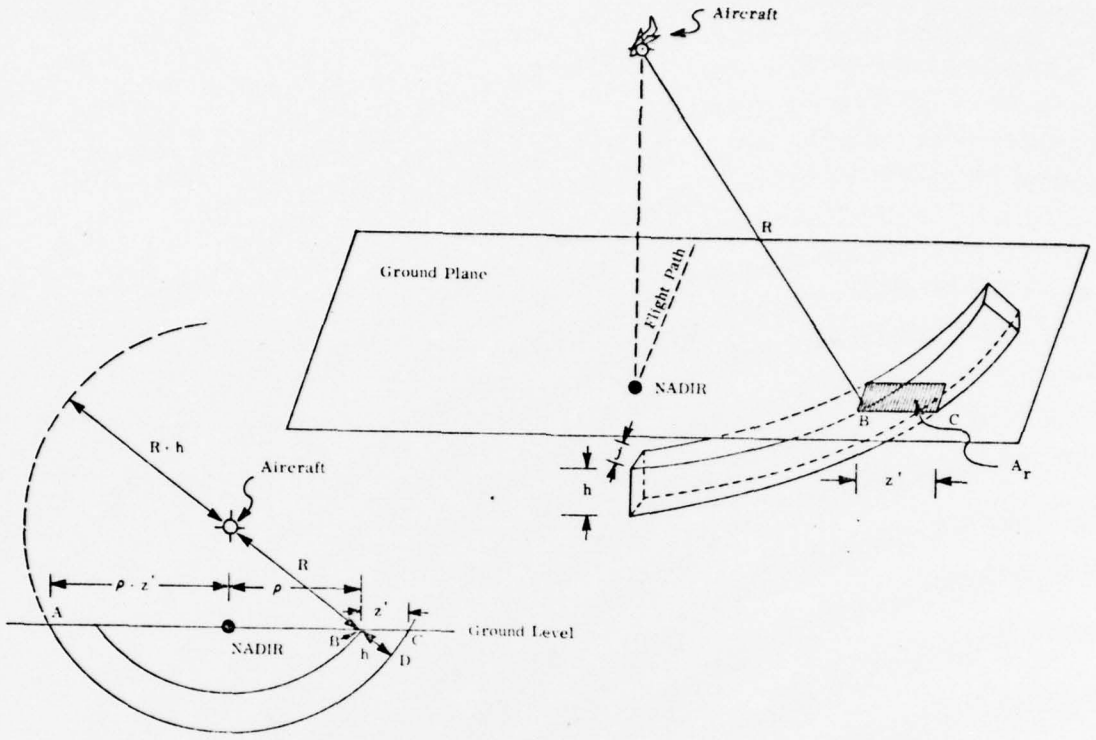

Figure 3-3. Ground Cell

Let X_T and X_b be, respectively, the equivalent reflectivities of a radar cell centered on and off the target. Let r_T and r_b be the corresponding radar reflectivities (sometimes designated as σ_o in the literature). (X_b is taken to be r_b). Let A_T be the equivalent target area, identified as the ratio of cross section to reflectivity.

$$A_T = \frac{\sigma_T}{r_T} \tag{3.37}$$

Then from the foregoing discussion:

If $A_T \geq A_r$

$$X_T = r_T \tag{3.38}$$

If $A_T < A_r$

$$X_T = r_T \left(\frac{A_T}{A_r}\right) + r_b \left(1 - \frac{A_T}{A_r}\right)$$

3.2.3.1.2 Rain Clutter. Let R be the slant range to the target and H be the aircraft height, AMGL. The reflection from rain in a period of time corresponding to one radar range cell at R is from a volume covered by a depression angle ϕ:

$$\arcsin \frac{H}{R} \geq \phi \geq \phi_{min} \tag{3.39}$$

where ϕ_{min} is given by the minimum depression angle for which the $\csc^2$ beam pattern is valid. The $\csc^2$ beam pattern is assumed, and is conventional since, within the pattern, all equivalent targets at a given relative altitude, but any range, return the same energy to the receiver. It is assumed the beam power density is $(w)\csc^2\phi$, where w is a generic constant related to power and antenna gain.

In a volume $dV = hR^2 \Delta\psi d\phi$, where h is the range resolution and $\Delta\psi$ is the azimuth beam width, there is

$$\sigma_R \, dV = \sigma_R \, hR^2 \Delta\psi \cos\phi \, d\phi \tag{3.40}$$

backscatter area, where σ_R is defined as the backscatter area per unit volume.

Then the antenna sees rain-clutter power (where H_r is height of rain)

$$C_R = w\sigma_R hR^2 \Delta\psi \int_{\substack{\max\{\phi\min,\ \arcsin,\ \frac{H-H_r}{R}\} \text{ if } H_r < H \\ \phi_{min} \text{ if } H_r \geq H}}^{\phi_{min}} \csc^4\phi \, d\phi \tag{3.41}$$
$$\arcsin H/R$$

where w is still a generic constant. This integral is benign:

$$\int \csc^4\phi \, d\phi = -\frac{\cos\phi}{3\sin\phi}\left[\frac{1}{\sin^2\phi} + 2\right] \tag{3.42}$$

and so equation (3.41) becomes

$$C_R = (w\sigma_R hR^2 \Delta\psi/3)\left\{A - \left(\sqrt{(R^2/H^2) - 1}\right)\left(2 + (R^2/H^2)\right)\right\} \tag{3.43}$$

where $A = \min\{B, C\}$ (3.44)

and $B = \cot\phi_{min}\left(2 + \csc^2\phi_{min}\right)$; (3.44a)

$$C = \sqrt{\frac{R}{(H - H_r)^2} - 1}\left(2 + \frac{R^2}{(H - H_r)^2}\right) \tag{3.44b}$$

It remains to consider w and σ_R; first w.

On the ground, at range R the ground clutter is, using the symbols used above,

$$C_G = w \csc^4 \phi \, \sigma_G \, h R \, \Delta\psi = w R^5 \, \sigma_G \, h \, \Delta\psi / H^4 \tag{3.45}$$

where the w is the same in equations (3.41) and (3.43). Therefore,

$$C_R = C_G \left(\frac{\sigma_R}{\sigma_G}\right)\left(\frac{H^4}{R^3}\right)\left(\frac{1}{3}\right)\left\{A - \sqrt{\left(\frac{R^2}{H^2}\right) - 1}\left(2 + \left(\frac{R^2}{H^2}\right)\right)\right\} \tag{3.46}$$

and here σ_G is actually "r", the appropriate ground backscatter coefficient.

Therefore, the rain clutter causes an effective increase in total clutter from C_G to

$$C_G + C_R = C_G \left(1 + \frac{C_R}{C_G}\right) \tag{3.47}$$

The quantity C_G is identified, as appropriate, with either target or background.

It remains to evaluate σ_R. Referring to page 542 in reference (5), the given empirical curves may be fitted to:

$$\log(\sigma_R) = \alpha + \beta \log P = \log(\alpha' P)^{\beta} \tag{3.48}$$

where P is the precipitation rate in equivalent mm/hr. of water. Then

$$\sigma_R = \alpha'(R=2) \cdot P^{\beta} \tag{3.49}$$

By the curve, derived from reference (5), this is

$$\sigma_R = K \cdot 10^{-3} \left(\frac{81}{\lambda^4}\right) P^{1.6} \ \mathrm{cm}^2/\mathrm{m}^3 \tag{3.50}$$

where P = rainfall in mm/hr. The quantity K is unity for rainfall and 0.22 for snow (Ref (5)). To make this into a dimensionless product $\sigma_R H$, H must be given in meters (in this term only) and

$$\sigma_R = K \cdot 10^{-7} \left(\frac{81}{\lambda^4}\right) P^{1.6} \ \mathrm{m}^2/\mathrm{m}^3 \tag{3.51}$$

H and R must be in meters and λ in centimeters, because the coefficient 10^{-7} is an empirical constant.

Since normalized radar returns have been used throughout, C_R can now be identified with X_p, the equivalent precipitation backscatter per unit area. In this case, using the stated normalization, C_G must be identified with σ_G. Assembling the previous results,

$$X_p = K\left(\frac{81}{\lambda^4}\right)\left(\frac{10^{-7} P^{1.6} H}{r}\right)\left(\frac{H^3}{3R^3}\right)\left\{A - \sqrt{\frac{R^2}{H^2} - 1}\left(2 + \frac{R^2}{H^2}\right)\right\} \qquad (3.52)$$

3.2.3.1.3 Target Contrast. The target contrast is given simply by

$$C = \gamma \left| \log_{10} \frac{X_T + X_p}{X_b + X_p} \right| \qquad (3.53)$$

where γ is the system gamma, including film gamma, typically it is 0.8. Note that there is an additional improvement in C if the precipitation return is assumed incoherent, i.e., the projected raindrop speed in range is large compared to $\frac{\lambda}{\tau}$, where τ is the integration time. For now, it is pessimistically assumed that precipitation is coherent.

If the target contrast is insufficient, i.e., if $C < C_o$, the target is not detectable; PDC = 0.

3.2.3.1.4 Effective Resolution. The interaction which degrades resolution as a function of contrast is not known for SLR. It is assumed that the general process of degradation of resolution proceeds as in photographic systems, for which there is available a curve fitted to actual film data as given in Paragraph 3.2.7.

Let Y be the effective system resolution in meters.

Let L_1 be the film resolution in lines/mm

L_1' be the display resolution in total line pairs.

Let D_1 be the width of film in meters per line. Let R_{min}, R_{max} be the width of range displayed in the display in meters, and R_1' is the width of range displayed (in meters).

The effective output resolution is

for film (Levels 2, 3, 4)

$$Q_1 = \frac{R_{max} - R_{min}}{D_1 \times 10^3 \times L_1} \quad \text{meters} \tag{3.54}$$

for display (Level 1)

$$Q_1' = \frac{R_1'}{L_1'} \quad \text{meters} \tag{3.55}$$

Then the effective system resolution is

$$Y = \frac{\sqrt{A_r + (Q_o)^2}}{1 - e^{(-2C)}} \quad \text{meters} \tag{3.56}$$

where $Q_0 = Q_1$ when considering Levels 2, 3, and 4, and $Q_0 = Q_1'$ when considering Level 1.

Note the correction for the projection of range in computing Ar.

3.2.3.1.5 Detectability. Assuming the conditions imposed by equation $C > C_o$ (i.e., $PDC \neq 0$), the basic detectability is estimated by an empirical data curve fit (12) given below:

$$PDC = e^{\left[-0.69 \frac{Y^2}{Y_T^2}\right]} \tag{3.57}$$

where Y_T is the 50 percent probable radar detection resolution requirement for the target type, Y is from equation (3.56) above.

Note that equation (3.57) is computed twice; namely:

(1) For Level 1, using the value of Y from equation (3.56) when $Q_0 = Q_1'$

(2) For Levels 2, 3, and 4 using the value of Y from (3.56) when $Q_0 = Q_1$.

To obtain the total detectability, this factor must be multiplied by P_T, the terrain non-shadowing probability, and P_{up}, SLR-up probability, and by an indicator K_L which is 0 (or 1) as the SLR is not (or is) available at Level L.

$$PD = (PDC)\ (P_T)\ (P_{up})\ (K_L) \tag{3.58}$$

Again, PD is computed once for Level 1 and once for the remaining levels.

3.2.3.2 Identifiability. Since, for SLR, about three times the detectability resolution is required for identification (12), we have, using the conditional probability equation (3.24),

$$P_I = e^{\left[-5.5\ \frac{Y^2}{Y_T^2}\right]} \tag{3.59}$$

where: Y is given in equation (3.56)

Y_T is defined in equation (3.57)

Again, two values of PI are computed: one value for Level 1, and one value for Levels 2, 3, and 4. When PI is computed for Level 1, the value of Y is found in equation (3.56) by letting $Q_o = Q_1'$; similarly, the value of PI for Levels 2, 3, and 4 is found by using the value of Y from equation (3.56) when $Q_o = Q_1$.

3.2.3.3 Localizability. This is expressed as a CEP measure comprising two components, lateral error and longitudinal error.

3.2.3.3.1 Lateral Position Error. The definitions given below are used in the following discussion:

TH = the true target height above mean ground level

H = the true aircraft elevation above mean ground level (meters)

SR = the slant range to the target being considered (meters)

ψ = the bearing angle to the target (radians)

$\sigma^2(\xi)$ = the variance of the terrain height about its mean (meters^2)

The SLR actually measures the slant range to the target (by counting signal return delay), but, unlike the IR, does not measure the depression angle to the target. Therefore, as far as the SLR can tell, the target may be located at any point on the circumference of a circle of radius SR with the aircraft at the center.

As shown in Figure 3-4, the actual target location is at the intersection of the circle of diameter SR and the ground. However, the system does not know the target elevation, so it cannot give the ground distance, ρ, to the target correctly. Rather, the system assumes (as shown in Figure 3-4) that the target height is the same as the ground directly below the aircraft. This is the source of the lateral error.

Referring to Figure 3-4, the ground range to the target, ρ, is simply

$$\hat{\rho} = \sqrt{SR^2 - (H-Z)^2}$$

Note that Z is a random variable which shows how the ground height directly below the aircraft differs from the mean ground level.

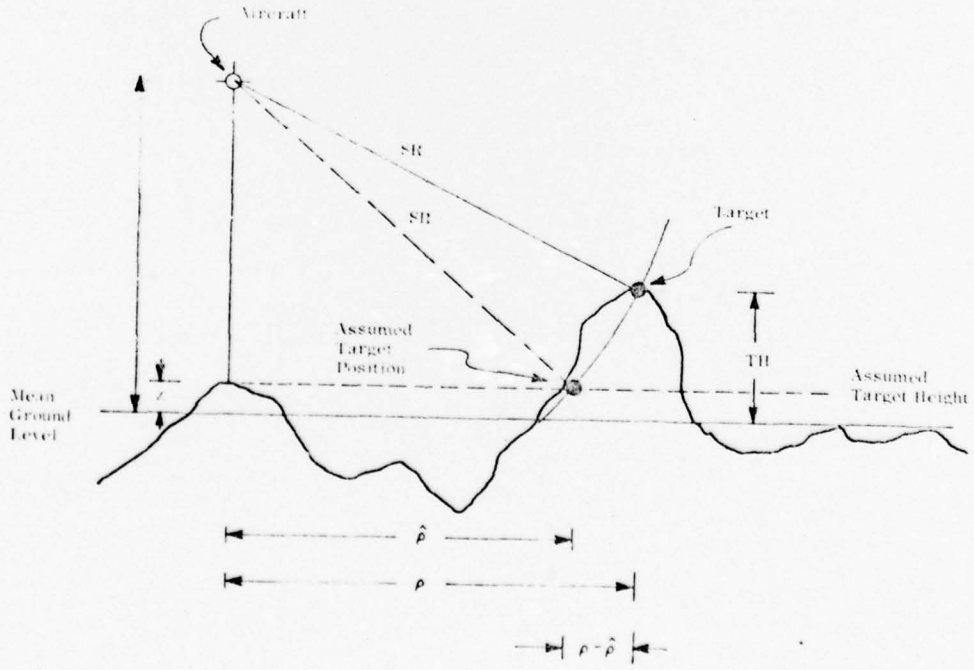

Figure 3-4. Lateral SLR Position Error

On the other hand, the true ground range to the target, ρ, is given by

$$\rho = \sqrt{SR^2 - (H-TH)^2} \tag{3.60}$$

solving for SR yields

$$SR = \sqrt{\rho^2 - (H-TH)^2} \tag{3.61}$$

Substituting equation (3.60) with (3.61), and writing $\hat{\rho}$ as a function of Z gives

$$\hat{\rho}(Z) = \sqrt{\rho^2 - (2H)(TH) + (TH)^2 + H(2Z) - Z^2}$$

For any given value of Z this would give the true $\hat{\rho}$ and would be the error in localization. Rather than introduce the nonsignificant numerical values of z, it is preferable to discuss

$$\begin{aligned} E(\hat{\rho} - \rho) &= E\sqrt{\rho^2 - 2H(TH) + TH^2 + 2HZ - Z^2} - \rho \\ &\approx E\left\{\rho\left(1 - \left[\frac{2H(TH) - TH^2 - 2HZ + Z^2}{2\rho^2}\right]\right)\right\} - \rho \\ &= -\frac{2H(TH) - TH^2 + \sigma^2(Z)}{2\rho} \end{aligned} \tag{3.62}$$

which is the mean localization error in direction of target bearing.

Equation (3.62) must now be evaluated. As a first step, notice that

$$\hat{\rho}(o) = \sqrt{\rho^2 - 2H(TH) + (TH)^2} \tag{3.63}$$

Next, the value of $\hat{\rho}(Z)$ can be computed by utilizing a Taylor expansion, as shown by the following equations:

$$\hat{\rho}(Z) = \hat{\rho}(0) + Z\left[\frac{d}{dZ}\hat{\rho}(Z)\right]_{Z=0} + \frac{Z^2}{2!}\left[\frac{d^2}{dZ^2}\hat{\rho}(Z)\right]_{Z=0} + \cdots \tag{3.64}$$

or

$$\hat{\rho}(Z) = \hat{\rho}(0) + Z\,\hat{\rho}'(0) + \frac{Z^2}{2}\,\hat{\rho}''(0) + \ldots \tag{3.65a}$$

$$\hat{\rho}'(Z) = \frac{1}{2\hat{\rho}(Z)}(2H - 2Z) = \left(\frac{H-Z}{\hat{\rho}(Z)}\right) \quad ; \quad \hat{\rho}'(0) = \frac{H}{\hat{\rho}(0)} \tag{3.65b}$$

$$\hat{\rho}''(Z) = -\frac{H-Z}{(\hat{\rho}(Z))^2}\,\hat{\rho}'(Z) - \frac{1}{\hat{\rho}(Z)}; \quad \hat{\rho}''(0) - \frac{H^2}{(\hat{\rho}(0))^3} - \frac{1}{\hat{\rho}(0)} \tag{3.65c}$$

Substituting equations (3.65b) and (3.65c) for equation (3.65a):

$$\hat{\rho}(Z) = \hat{\rho}(0) + \frac{ZH}{\hat{\rho}(0)} - \frac{Z^2}{2\hat{\rho}(0)}\left(1 + \frac{H^2}{(\hat{\rho}(0))^2}\right) + \ldots \tag{3.66}$$

Then

$$E\,\hat{\rho}(Z) = \hat{\rho}(0) - \frac{\sigma^2(Z)}{2\hat{\rho}(0)}\left(1 + \frac{H^2}{(\hat{\rho}(0))^2}\right) + \ldots \tag{3.67}$$

$$\left[E\; c\hat{\rho}(Z))^2\right] = E\,(\rho^2 - 2H(TH) + (TH)^2 + 2HZ - Z^2) \tag{3.68}$$

$$= \rho^2 - 2H(TH) + (TH)^2 - \sigma^2(Z)$$

$$= (\hat{\rho}(0))^2 - \sigma^2(Z)$$

$$\sigma^2(\hat{\rho}) = E\left((\hat{\rho}(Z))^2\right) - (E\,\hat{\rho}(Z))^2 = \quad \text{(From 3.65b) and (3.65c)} \tag{3.69}$$

$$(\hat{\rho}(0))^2 - \sigma^2(Z) - (\rho(0))^2 + \sigma^2(Z)\left(1 + \frac{H^2}{(\hat{\rho}(0))^2}\right) - \left\{\frac{\sigma^2 Z}{2\hat{\rho}(0)}\left[1 + \frac{H^2}{(\hat{\rho}(0))}\right]\right\}$$

$$= \sigma^2(Z)\frac{H^2}{(\hat{\rho}(0))^2} + \text{Terms in } \sigma^4 \text{ and higher.}$$

Summarizing, the variance, in $\hat{p}(z)$ is

$$\frac{H^2 \sigma^2 (z)}{(\hat{\rho}(0))^2} \tag{3.70}$$

where, from equation (3.63b):

$$\hat{\rho}(0) = \sqrt{\rho^2 - 2H(TH) + (TH)^2} \tag{3.71}$$

and ρ = the true ground range.

It is already known (from equation (3.61)) that the mean error in lateral position is

$$-\frac{\sigma^2(\xi) - 2H(TH) + (TH)^2}{2\rho} \tag{3.72}$$

The root mean square (rms) error squared is not the variance because of the bias introduced by the mean error $\neq 0$. Taking this into account, the rms of lateral u error, is given by

$$u = \sqrt{\text{variance} + (\text{mean error})^2}$$

$$= \sqrt{E(\hat{\rho}^2) + \left[E(\hat{\rho} - \rho)\right]^2} \tag{3.73}$$

3.2.3.3.2 Longitudinal Position Error. The doppler effect causes a systematic longitudinal position error (see Figure 3-5).

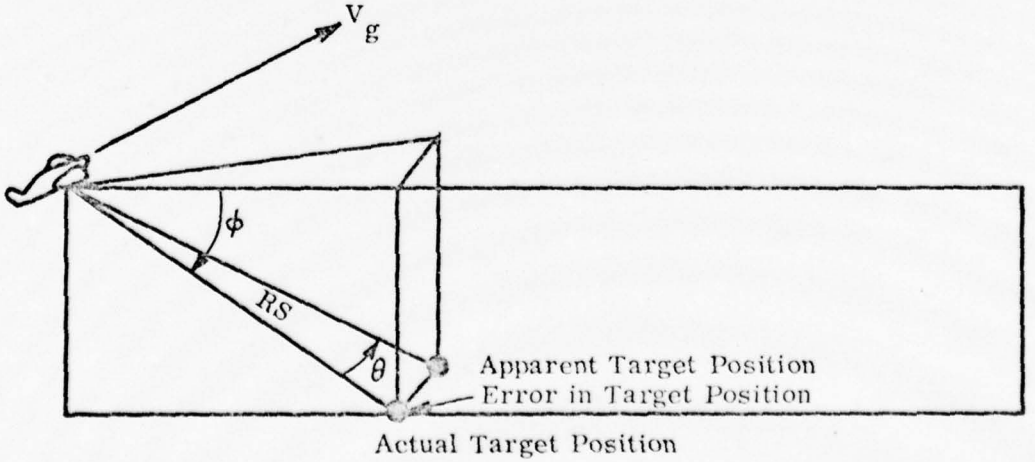

Figure 3-5. Doppler Effect Position Error

Let V_D be the radial ground-projection component of target velocity, and let V_g be the aircraft ground speed (knots). It is assumed that all photos are corrected by the measured drift angle. If it is small, the systematic error is

$$\Delta_1 = \frac{RSV_D \cos \phi}{V_g} \tag{3.74}$$

where ϕ is the depression angle to the target (see Figure 3-5).

The drift error introduces a random displacement

$$\sigma^2 (\Delta_2) = \sigma^2 (\theta) \rho^2 \tag{3.75}$$

Then

$$V = \sqrt{\Delta_1^2 + \sigma^2 (\Delta_2) + Ar} \tag{3.76}$$

where Ar is the ground resolution cell area as defined in equation (3.36).

3.2.3.3.3 CEP. Combining the lateral and longitudinal errors, the CEP is

$$CEP = 1.178 \sqrt{(U)(V)} \tag{3.77}$$

3.2.4 Forward Looking Radar with Moving Target Detection Capability (MTIFLR)

MTIFLR is considered a sensor although FLR imagery is valuable only as a navigational aid, because the latter's low resolution makes it an ineffective backup for the SLR. Nevertheless, as a source of moving target information (MTI), this unit is quite useful.

There are two types of inputs to the MTIFLR model. The first class of inputs are supplied by the Scenario Program; the second is supplied by the user:

INPUTS FROM SCENARIO

GEOGRAPHIC

- Aircraft and target height above mean ground level
- Minimum and Maximum ground range at which target is detectable

- Expected number of target sightings unmasked by terrain: also the variance
- Absolute value of the target velocity projected along the slant range vector
- Variance of the terrain height about its mean
- Slant range of rain traversed
- Probability that target is not masked by terrain

WEATHER DATA

- Precipitation rate of rain or snow
- Type of precipitation (none, rain, or snow)

TARGET DATA

- Radar cross section of the target
- Backscatter coefficient of the target

SENSOR DATA

- Probability that the equipment is operational

USER INPUTS

SENSOR PARAMETERS

- Size of the rectangular resolution cell
- Radar wavelength in centimeters
- Maximum depression angle
- Threshold velocities above which a target can (1) be detected (2) be identified
- Processing levels in which the MTIFLR operates

TARGET/BACKGROUND DATA*

- Signal-to-clutter and signal-to-noise for standard target under standard conditions

*The terms standard target and standard background will be defined later in this paragraph.

- Size of standard target
- Slant range to standard target
- Difference in altitude between A/C and target under standard conditions
- Reflectivity — backscatter coefficient for standard background

NAVIGATIONAL DATA

- Standard deviation of the perceived azimuth angle.

OTHER

- False alarm rate (noise induced)

These inputs flow into the MTIFLR submodel of the Executive Model where they are used to compute detectability, identifiability, and localizability statistics:

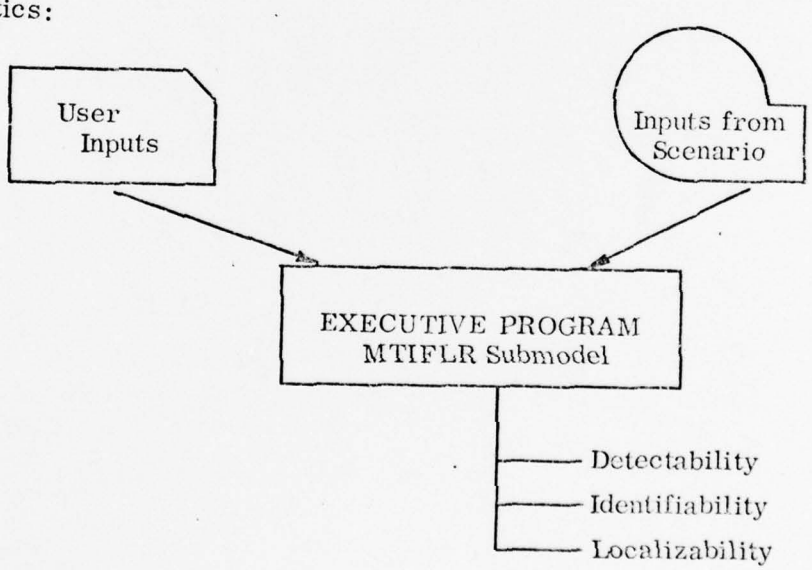

Factors influencing detectability are discussed in Paragraph 3.2.4.1. Target detectability is the topic of Paragraph 3.2.4.2. Paragraphs 3.2.4.3 and 3.2.4.4 discuss, respectively, the target identifiability and localizability.

3.2.4.1 Factors Influencing Detectability. In order to properly model detectability, several factors must be known.

A very important concept with this sensor is that the target may be "seen" more than once. (This is in contrast with such sensors as the IR, which sees a target only at abeam passage.) Statistically, it is assumed that the sensor is given a number of discrete, independent looks at the target. Detectabilities are computed for each look and then integrated over all looks.

The detectability for a given look is found by first ascertaining if the radial component of the target velocity is sufficiently large to be detected. Then, assuming that it is, a careful analysis is made of the signal returned from the target to the sensor; in particular, the effects of noise, clutter, and attenuation are modeled. If the signal degraded by all these factors is still sufficiently large, detection occurs.

The following paragraphs will discuss:

(1) Statistical treatment of the number of independent looks (see Paragraphs 3.2.4.1.1 and 3.2.4.1.2).

(2) Velocity filter model (Paragraph 3.2.4.1.3)

(3) Signal-to-Clutter and Signal-to-Noise Ratio (Paragraph 3.2.4.1.4).

(4) Attenuation due to rain or snow (Paragraph 3.2.4.1.5).

Paragraph 3.2.4.2 illustrates how detectability is actually computed once the above factors are known, both for single looks and for the integration over all looks.

3.2.4.1.1 Number of Looks and Associated Viewing Angles. A "look" is defined as one radar scan, provided the target is within the radar's geometrical limits. Sweep-to-sweep integration, however, is handled separately. Several variables used in the following discussion are defined below:

R_{max} = maximum slant range of the sensor

R_{min} = minimum slant range of the sensor

The next step is to find the expected value of the square of the number of unobstructed sightings. This variable is called EXSQC and is computed in one of two alternative ways. Let $\Delta\psi$ be the coherence angle of terrain masking, $\Delta\psi$ is an input parameter.

If $\psi_2 - \psi_1 \leq \Delta\psi$, the looks are assumed to be completely correlated with respect to terrain shadowing and

$$\text{EXSQC} = \sum_{i=1}^{NL} (2(NL) - 2i + 1)\, PM_i \tag{3.89}$$

If, on the other hand, $\psi_2 - \psi_1 > \Delta\psi$, a somewhat more complex situation exists. The looks are divided into two independent sets, the looks within a set are held to be completely correlated. The sets are formed by defining a variable N' defined by:

$$N' = \left\{ \begin{array}{ll} NL/2 & \text{if NL is even} \\ (NL + 1)/2 & \text{if NL is odd} \end{array} \right\} \tag{3.90}$$

Then the first set consists of those looks before N', i.e., the set J such that $1 \leq J \leq N'$, and the second set consists of those looks after N', i.e., the set K such that $N' \leq K \leq NL$.

The probability of exactly i unobstructed sightings in the first set is

$$P_{i1} = \left\{ \begin{array}{ll} 1.0 - PM_{N'} & \text{if } i = 0 \\ PM_{(N' - i + 1)} - PM_{(N' - i)} & \text{if } i = 1, \ldots, (N' - 1) \\ PM_1 & \text{if } i = N' \end{array} \right. \tag{3.91}$$

The probability of exactly i unobstructed sightings in the second set is

$$P_{i2} = \left\{ \begin{array}{ll} 1.0 - PM_{NL} & \text{if } i = 0 \\ PM_{(NL - i + 1)} - PM_{(NL - i)} & \text{if } i = 1, \ldots, (NL - N' - 1) \\ PM_{(1 + N')} & \text{if } i = NL - N' \end{array} \right. \tag{3.92}$$

The probability of exactly i unobstructed sightings altogether is

$$P_i = \begin{cases} \sum_{j=0}^{i} P_{j1} P_{(i-j)2} & \text{for } i = 0, 1, \ldots, (NL-N') \\ \sum_{j=i-N'}^{NL-N'} P_{(i-j)1} P_{j2} & \text{for } i = NL-N'+1, \ldots, NL \end{cases} \tag{3.93}$$

Then

$$EXSQC = \sum_{i=1}^{NL} i^2 P_i' \tag{3.94}$$

The variance of the number of unobstructed sightings is

$$VAR = EXSQC - (EXC)^2 \tag{3.95}$$

The expected value and variance of the number of unobstructed sightings (equations 3.94 and 3.95) will be used in Paragraph 3.2.4.2.2 when computing multiple look detectability for a target.

3.2.4.1.3 Doppler Velocity Filter. MTI applies only to targets with a velocity whose radial component is in excess of some fixed threshold value. The radial velocity must be computed and then checked against this threshold to determine if detection is possible.

Let the radial component of target velocity, i.e., the Doppler velocity, be denoted by V_r, and let the threshold value be given by V_t — an input parameter to the model.

The first step is to find V_r. If the target is at long range, it is likely to be masked by terrain. If it is at close range its radial velocity contains a multiplicative factor, namely the cosine of the depression angle; as the target comes closer, the cosine of the depression angle tends to zero. To take into account the extent of overlap between the region of terrain visibility and the region of large enough cosine (depression angle), more computation and programming is required than can be afforded. Therefore, only a single instant is examined to determine whether or not velocity is MTI-detectable. This computation is conducted as follows.

Let V_y be the target velocity component in the direction perpendicular to the flight path; V_y is positive if the distance from the flight path is increasing. Similarly, let V_x be the target velocity component in the direction of the flight path; it is positive if the aircraft is overtaking the target.

Compute an average target azimuth angle:

$$\psi = \frac{\psi_1 + \psi_2}{2.0} \tag{3.96}$$

and an average depression angle to the target

$$\phi = \frac{\phi_1 + \phi_2}{2.0} \tag{3.97}$$

where (from Paragraph 3.2.4.1.1):

ψ_1, ψ_2 are the first and last azimuth angles and,

ϕ_1, ϕ_2 are the first and last depression angles.

The radial component is

$$V_r = \left| \cos \phi \, (V_y \sin \psi + V_x \cos \psi) \right| \tag{3.98}$$

The radial velocity component is tested against the threshold V_t. If $V_r < V_t$, no detection is possible; the probability of detection is set equal to zero and no other computations are made. If $V_r \geq V_t$, the computations continue.

3.2.4.1.4 Signal-to-Clutter and Signal-to-Noise Ratios. A classical approach for determining the signal-to-clutter and signal-to-noise ratios of the radar system involves computation over the radar range equations using basic characteristics such as effective system bandwidth and receiver noise figures. For signal-to-clutter analysis, a detailed knowledge of the clutter rejection select capabilities is required. Alternatively one may select "specification standards" and scale them to the real-world environment. The latter approach was employed for the simulation.

These specification standards, as given in, say manufacturer's literature, are with respect to some standard target and environment. If the specification claims X db signal-to-clutter ratio, this must be described with respect to a unit area target at some extreme range with defined clutter reflectivity, i.e., a standard target. The parameters of the standard target are used to determine the radar parameters, as the most useful approach available in the absence of a known radar design.

The procedure adopted is necessary because the designs of the detector and of the clutter rejection circuitry are not fixed or known. Thus, the approach of using input specified signal-to-clutter (S/C) and signal-to-noise (S/N) ratios for a standard target and range is adopted.

The following definitions are established for the standard target:

σ_o = size of standard target, in square meters (radar)

R_o = slant range of standard target

H_o = difference in altitude between aircraft and target under standard conditions

r_o = reflectivity, backscatter coefficient, of standard background

S/C_o = signal-to-clutter ratio in decibels for standard target under standard conditions

S/N_o = signal-to-noise ratio in decibels for a standard target under standard conditions

Other definitions used include:

r = backscatter coefficient of the background

TH = target elevation above mean terrain level

σ = radar crosssection of the target

Let

$$R = \sqrt{(H - TH)^2 + \left(\frac{Y_a + Y_b}{2}\right)^2} \qquad (3.99)$$

Then the signal-to-clutter ratio is (in db)

$$S/C = S/C_o + 10 \log_{10}\left[\frac{\sigma r_o R_o}{\sigma_o r R}\right] - 10(\log_{10}(X_p+1)) \qquad (3.100)$$

where X_p is the precipitation clutter correction (see Paragraph 3.2.3.1.2) and the signal-to-noise ratio (assuming a $\csc^2$ beam) is

$$S/N = S/N_o + \log_{10}\left[\frac{H_o^4 \sigma}{\sigma_o (H - TH)^4}\right] - 10 \log_{10} Q \qquad (3.101)$$

where Q is the precipitation attenuation and is found as follows:

Precipitation Attenuation for Rain

From Skolnik[5] (Figure 12.11) empirical curves are fitted to yield the following attenuation equation for $\lambda \leq 10$ cm.

$$\alpha = \frac{0.37g}{\lambda^{2.65}} - 3.7 \times 10^{-8} g \lambda^4$$

where:

α is the attenuation coefficient in db/NM

λ is the wavelength in cm

g is the precipitation rate in mm/hr.

Let D be the distance traveled through rain in NM. Then A, the overall attenuation coefficient, is:

$$A = \alpha D = \begin{cases} \left(\frac{0.37\, gD}{\lambda^{2.65}}\right) - 3.75 \times 10^{-8} g D \lambda^4 & \lambda \leq 10\text{cm} \\ 0 & \lambda > 10 \text{ cm} \end{cases} \qquad (3.102a)$$

The twoway multiplicative attenuation for radar Q, is

$$Q = \left(10^{-A/10}\right)^2 = 10^{-A/5}$$

Precipitation Attenuation for Snow

Using the same data from Skolnik[5] (Equation 12.34) and a method analogous to the rain case,

$$\alpha = \frac{0.00648\ g^{1.6}}{\lambda^4} + \frac{0.00416\ g}{\lambda}$$

where g is now defined as the precipitation rate in mm/hr of water. Then, again

$$A = \alpha D = \begin{cases} \dfrac{0.00648\ g^{1.6} D}{\lambda^4} + \dfrac{0.00416\ g\ D}{\lambda} & \lambda \leq 10\ \text{cm} \\ 0 & \lambda > 10\ \text{cm} \end{cases} \qquad (3.102b)$$

and

$$Q = 10^{-A/5}$$

3.2.4.2 Detectability. Detectability is assumed to be the same for all levels.

3.2.4.2.1 Single Look Detectability. Using data in Skolnick, [5] the electronic detection model of Paragraph 3.2.2.1.4.1 is used (equation (3.16)) to compute detection probability, considering signal-to-noise and signal-to-clutter ratios separately. Simply restating this equation:

$$PDC_{S/N} = -0.320691 + (S/N)\left(0.027154 + (S/N)\left(0.0018809 - 4(10^{-5})\ (S/N)\right)\right) \qquad (3.103)$$

$$PDC_{S/C} = -0.320691 + (S/C)\left(0.027154 + (S/C)\left(0.0018809 - 4(10^{-5})\ (S/C)\right)\right)$$

S/N and S/C are unitless (not db) signal-to-noise and signal-to-clutter ratios.

As shown, this equation must be performed twice, once for the signal-to-noise case ($PDC_{S/N}$) and once for the signal-to-clutter case ($PDC_{S/C}$). The results are multiplied together to yield PD, the single-look conditional detectability.

$$PD = PDC_{S/N}\ PDC_{S/C} \qquad (3.104)$$

3.2.4.2.2 Multiple Look Detectability. The problem in computing the multiple look detectability is to take into account the effect of $\Delta\psi$, the coherence angle in terrain masking. Thinking of ϵ as the number of unobstructed looks and η as the keying probability, the following relationship exists:

$$\eta = f(\epsilon)$$

Both ϵ and η are random variables. The mean of ϵ, $\bar{\epsilon}$, and its variance, $\sigma^2(\epsilon)$, are known (equations (3.94) and (3.95)). The mean of η is examined by taking a Taylor expansion about ϵ in the above equation:

$$\left.\begin{aligned} \eta &= f(\bar{\epsilon}+\Delta\epsilon) = f(\bar{\epsilon}) + \Delta\epsilon f'(\epsilon) + \frac{\Delta\epsilon^2 f''(\epsilon)}{2} + \ldots \\ E(\eta) &= f(\bar{\epsilon}) + 0 + \frac{\sigma^2(\epsilon) f''(\bar{\epsilon})}{2} + \ldots \end{aligned}\right\} \quad (3.105$$

That is, $\sigma^2(\epsilon)$ shifts the mean of η by the amount

$$\frac{\sigma^2(\epsilon) f''(\bar{\epsilon})}{2}$$

from the "naive" estimate

$$\hat{\eta} = f(\bar{\epsilon})$$

In this case $f(\varepsilon) = 1-(1-PD)^{\varepsilon}$
Thus, the conditional multiple look detectibility, PD_T, is

$$PD_T = 1 - (1 - PD)^{\bar{\epsilon}} \left(1 + \left[\text{Log}_e (1 - PD)\right]^2 \left[\frac{\sigma^2(\epsilon)}{2}\right] \right) \quad (3.106)$$

where PD is the single look detectability from equation (3.104). The values of $\bar{\epsilon}$ and $\sigma^2(\epsilon)$ are, as indicated, the expected value and variance of the number of unobstructed sightings (equations (3.94) and (3.95). The total multiple look detectability, PD', is

$$PD' = PD_T (P_{UP})$$

where

P_{UP} is the probability that the sensor is operable

3.2.4.3 Identifiability. Data on MTI identifiability is sparse. The following "cookie-cutter" approach is adopted.

$$P_I = \begin{cases} 1.0 & \text{if } PD_T \geq PD_{To} \\ 0.0 & \text{if } PD_T < PD_{To} \end{cases} \qquad (3.108)$$

where:

P_I = conditional probability of identifiability

PD_T = the multiple look detectability

PD_{To} = a threshold detectability (a user input parameter reflecting the fact that if the detectability probability is not sufficiently high, no identification can be expected)

This approach can be improved when useful data becomes available.

3.2.4.4 Localizability. Localizability is expressed as a CEP statistic that can be divided into two components: a lateral error, and error introduced by target height uncertainties.

The computation for the lateral position error is exactly the same as in the case of the Side Looking Radar (see Paragraph 3.2.3).

Simply stating the results:

$$U = \sqrt{E(\hat{\rho}^2) + \left[E(\hat{\rho} - \rho)\right]^2} \qquad (3.109)$$

where:

U is the lateral error

$E(\hat{\rho}^2)$ = variance of lateral error

$E(\hat{\rho} - \rho)$ = the mean lateral error (3.110)

The range error due to the size, h, of the (rectangular) ground resolution cell is (assuming that aircraft altitude errors are relatively small)

$$\sigma^2 (SR) = \frac{h^2}{12} \tag{3.111}$$

$$\sigma^2_\rho = \left(\frac{h^2}{12}\right)\left(\frac{SR^2}{\rho^2}\right) \tag{3.112}$$

due to range resolution. In these equations

ρ = true ground range

h = the size of the rectangular resolution cell

SR = slant range to the target

The factor 1/12 is simply the variance of a rectangular probability distribution of width 1.

Then, the rms error due to height uncertainties and total standard deviation in range is

$$\sigma_\rho = \sqrt{\sigma^2_\rho + U^2} \tag{3.113}$$

The total cross range resolution is

$$\sigma_\omega = (SR)\, \sigma(\theta) \tag{3.114}$$

where $\sigma^2(\theta)$ is the variance of the measured angle to the target.

Combining these statistics, for a single look, the localizability is given by

$$CEP_{(1\ look)} = 1.178 \sqrt{\sigma_\rho \cdot \sigma_\omega} \tag{3.115}$$

This equation for $CEP_{(1\ look)}$ must, however, be corrected for the choice of a representative SR. Since the target is moving, no smoothing can be done unless sophisticated target tracking is undertaken. It is best to wait for the range, R, to minimize. When this occurrs

$$\rho = Y_a$$

$$SR = \sqrt{\rho^2 + (H - TH)^2} \tag{3.116}$$

and the expected number of successful looks is 1. Therefore,

$$CEP = CEP_{(1\ look)} \tag{3.117}$$

3.2.5 Side Looking Radar with Moving Target Detection Capability (MTISLR)

The MTISLR is treated in exactly the same manner as the MTIFLR (Paragraph 3.2.4). The inputs (one additional input — the ground range to the target at abeam passage — is provided to the MTISLR by Scenario) and the desired outputs are the same.

As in the case of the MTIFLR, several factors must first be computed before detectability, identifiability, and localizability can be predicted.

First, the radial component of the target velocity, V_r, must be computed and checked against a threshold value, V_t (the value below which no detection is possible). The equations for computing this are identical to those in Paragraph 3.2.4.1.3 and are therefore not repeated. If $V_k \geq V_t$, a variable XD is defined to be 1 and computations continue. If, on the other hand, $V_r < V_t$, XD is defined to be 0.

The next step is to compute the signal-to-clutter (S/C) and signal-to-noise (S/N) equations. These are (from Paragraph 3.2.4.1.4):

$$S/C = S/C_o + (10)\text{Log}_{10}\left(\frac{\sigma r_o R_o}{\sigma_o r R}\right) - (10)\text{Log}_{10} X_p \tag{3.118a}$$

and

$$S/N = S/N_o + (10)\text{Log}_{10}\left(\frac{\sigma H_o^4}{\sigma_o (H - TH)^4}\right) - (10)\text{Log}_{10} Q \tag{3.118b}$$

where:

σ_o = cross section of the standard target

R_o = slant range to the standard target

H_o = difference of altitude between aircraft and standard target

r_o = ground backscatter coefficient of standard background

S/C_o = signal-to-clutter for standard target (db)

S/N_o = signal-to-noise for standard target (db)

r = backscatter coefficient

TH = target elevation above mean ground level

H = aircraft elevation above mean ground level

σ = cross section of target

R = target slant range

Q = precipitation attenuation

X_p = rain clutter

Q and X_p have been computed in Paragraph 3.2.4.1. Two definitions are now needed:

Pd_1 = the detectability when signal-to-clutter is considered

Pd_2 = the detectability when signal-to-noise is considered

Then, from Paragraph 3.2.2.1.4:

$$Pd_1 = -0.320691 + 0.027154S_1 + 0.00188964S_1^2 - 4\,(10^{-5})\,S_1^3$$

$$Pd_2 = -0.320691 + 0.027154S_2 + 0.00188964S_2^2 - 4(10^{-5})\,S_2^3 \qquad (3.119)$$

where:

$$S_1 = 10^{\left(\frac{S/C}{10}\right)}$$

$$S_2 = 10^{\left(\frac{S/N}{10}\right)}$$

3.2.5.1 Detectability. The overall target detectability is given by

$$PD = (Pd_1)\,(Pd_2)\,(XD)\,(P_{up})\,(P_T)$$

where

$$XD = \begin{cases} 1 & \text{If} \quad V_r \geq V_t \\ 0 & \text{If} \quad V_r \leq V_t \end{cases} \tag{3.120}$$

P_{up} is the probability that the MTISLR equipment is up, and

P_T is the probability the target is not masked by terrain (see Paragraph 3.2.4.1.2).

3.2.5.2 Identifiability. The concept of a "cookie-cutter" model is adopted in the same manner as in the case of the MTIFLR. P_I, the identifiability is:

$$P_I = \begin{cases} 1 & \text{If} \quad PD \geq PD_o \\ 0 & \text{If} \quad PD < PD_o \end{cases} \tag{3.121}$$

where PD_o is a user-established threshold parameter for detectability. This simply reflects the fact that unless the detectability probability exceeds a certain value (PD_o) no identification can reasonably be expected.

3.2.5.3 Localizability. Localizability is computed the same as in the case of the MTIFLR, with the exception that the doppler shift term in the MTIFLR equation is zero. Simply stating results (see Paragraph 3.2.4.4 for the computation),

$$CEP = 1.178 \sqrt{(\sigma_\rho)\,(\sigma_\omega)} \tag{3.122}$$

where σ_ρ is the rms error because of height uncertainties, and σ_ω is the cross range resolution.

3.2.6 ECM Model

As in the case of the other seven submodels, the inputs to the ECM are of two kinds: (1) those provided (via tape output - Paragraph 2.7.2) by the Scenario program, and (2) those prepared by the user. These inputs are:

INPUTS FROM SCENARIO

GEOGRAPHIC

- Ground distance to target at abeam passage
- Aircraft speed and height above MGL
- Slant range to the target
- Time of the look
- Target height above MGL
- Slant range of rain traversed
- Angle from nadir to target (A/C as apex)
- A key which indicates threshold angle from nadir to target — if angle is less than this value, target is assumed "under" aircraft
- Terrain non-masking probability

WEATHER DATA

- Precipitation rate
- Kind of precipitation (none, rain, or snow)

SENSOR DATA

- Probability ECM equipment up at time of look

TARGET/BACKGROUND DATA

- Peak transmitted power in db above 1 watt
- Transmitter antenna gain - main lobe in db
- Frequency in MHz
- Transmitter front to back ratio in db

- Pulses per second
- Pulse width
- Target scan period

USER INPUTS

AVIONICS DATA

- Variance of A/C position (from actual) as given by the avionics system
- Variance of velocity as given by avionics systems
- Angular measurement precision relative to beam width (typically 1/6)

SENSOR DATA

- Number of receiving beams (usually antennas)
- Receiver bandwidth (in MHz)
- Receiver noise figure (in db)
- Threshold frequency (in MHz) above which it is possible to set an angular fix on target
- Table of receiver antenna gain plus line losses vs. frequency

These inputs are used as shown in the following diagram to produce the three outputs of (1) detectability, (2) identifiability, and (3) localizability.

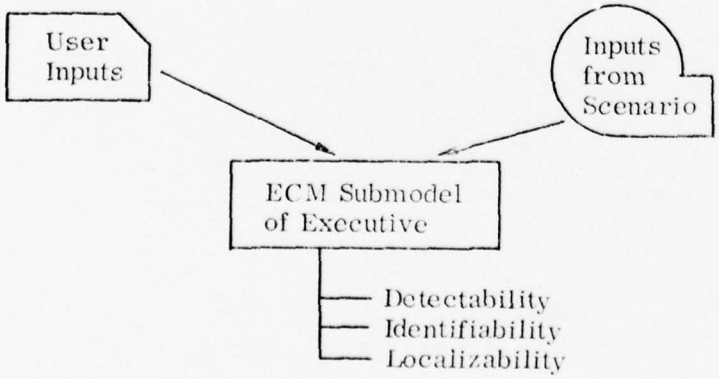

Paragraphs 3.2.6.1 and 3.2.6.2 discuss how detectability is found, Paragraph 3.2.6.3 discusses identifiability computation, and localizability (i.e., CEP) is discussed in Paragraph 3.2.6.4.

ECM is modeled in a unique way. First, since the inputs to this system are continuous over a long interval, single-look modeling is inadequate. Second, localization depends on passive ranging which, in this model, is assumed carried out essentially in an optimal manner via the on-board computer. To meet both these needs, the model assumes that there are precisely n independent receiver beams, corresponding to n antennas in the receiving array, disposed symmetrically about (but not including) the forward direction. A single possible detection event is recorded as the target passes through the center of each of these beams. Detectability arises from the conjunction of, in general, n/2 looks; identifiability (by assumption) from detection by at least 2 of the n/2 beams; and localizability by a probabilistic minimum-variance passive range calculation.

3.2.6.1 Single-Look Detectability. Detectability is computed for each of the ECM looks by first computing two values of interim single-opportunity detectabilities P_1 and P_2. P_1 is computed using the radar transmitter main lobe radiation, while P_2 is found by using the side lobe radiation. Both P_1 and P_2 are necessary because the aircraft sees the main and side lobes alternately. P_1 and P_2 are then combined, along with terrain masking and overload probabilities, to yield a single look detectability.

P_1 and P_2 are computed from the receiver signal-to-noise ratios as follows:

For main lobe radiation:

$$(S/N)_1 = \frac{P_T G_T G_R \lambda^2 Q}{(4\pi)^2 R^2 XN} \qquad (3.123)$$

$(S/N)_1$ = signal-to-noise ratio for the main lobe radiation.

where

P_T = peak transmitted power

G_T = transmitted gain -- main lobe

G_R = receiver antenna gain plus line losses, at the appropriate band

XN = 4×10^{-15} x bandwidth x receiver noise figure

R = slant range

λ = wavelength

Q = precipitation attenuation (see Paragraph 3.2.4.1.4)

(G_R, XN are functions of frequency by band, e.g., P, L, S, C, S, Ka, Kμ Band). For the side lobe radiation

$$(S/N)_2 = (S/N)_1 / K_A$$

where K_A = transmitter antenna front-to-back ratio ($K_A > 1.0$) in ratio units.

Using $(S/N)_1$ and $(S/N)_2$, two values of interim single-opportunity detectability P_1 and P_2 are calculated as in Paragraph 3.2.2.1.4.

The target main beam width Δ is estimated from

$$\Delta^2 = \frac{4\pi}{G_T} \tag{3.124}$$

and the fractional main beam time from

$$\alpha = \frac{\Delta}{2\pi} = \frac{1}{\sqrt{\pi G_T}} \tag{3.125}$$

except that $\alpha = 1$ for a locked-on tracking radar. The expected single-opportunity detectability for look (j) is

$$P^{(j)} = [\alpha P_1 + (1 - \alpha) P_2] P_3 P_4 \tag{3.126}$$

where P_3 is the terrain non-shadowing probability and P_4 the non-overload probability as defined in Paragraph 3.2.6.3. An assumption is made that the target passages cycle through the receiver lobes independently of target scan rate.

Overload Calculation. This paragraph defines P_4, the non-overload probability used in Paragraph 3.2.6.1. In the initial implementation, the entire overload section has been replaced by $P_4 = 1$ and the total Pulse Repetition Frequency (PRF) of targets in view have been separately accumulated by ten second intervals, computing the maximum and mean of this quantity at the end of mission. The following paragraphs discuss how overload should be implemented once there is sufficient empirical data.

Duty Factor Overload. Each frequency band (octave) accumulates duty factor (DF) as a function of time for all observable targets. Let the band have frequency ratios f_i, $2f_i$; then if f_o is the frequency discrimination of the broad-band receiver, compute and accumulate over the time of observation for each target:

$$X = (DF) \frac{f_o}{f_i} \tag{3.127}$$

as a function of time and octave band. This computation does not include the present target which is added to all appropriate ten second intervals after processing. Duty Factor is then:

$$DF = PW(PRF)\ (10^{-6}) \tag{3.128}$$

where PW is the pulse width in microseconds and PRF is in sec^{-1}.

PRF Overload. The variable Y, defined as $Y = (PRF)(P_d)$ (where P_d is the total detectability, from Paragraph 3.2.6.2) is accumulated over all bands as a function of time (tenth-second intervals). (Note that for this calculation the "present" target is not added in until after P_d is computed.)

The expectation of the total pulses per second, Z, being received by the ECM system at the time the present target is observed is:

$$Z = \begin{cases} 0 & \text{if } Y + PRF \leq K_{PRF} \\ \dfrac{PRF}{Y + PRF} & \text{if } Y + PRF > K_{PRF} \end{cases} \tag{3.129}$$

where K_{PRF} is the maximum PRF capability of the ECM system.

Computation of P_4. The non-overload probability, P_4, is estimated as follows:

$$\text{Let } \mu = 1 - X + DF$$

$$\text{except that } \mu \text{ is constrained by: } 1/2 \leq \mu \leq 1 \qquad (3.130)$$

$$\text{then } P_4 = \mu\ (1 - Z)$$

Updating of X and Y. After the ECM calculations are completed for a given target, its duty factor (DF) and PRF are used to update X and Y in the above discussion; at the same time the DF and PRF of those targets, which have passed out of radar range, are subtracted from X and Y.

This is a crude but pessimistic overload calculation, justifiable if X is small and if the radiating sources are on hilltops, keeping the terrain non-shadowing probability high.

3.2.6.2 Multiple-Look Detectability. If there are n independent samples available around the aircraft, n independent receiver beams are assumed whose centers are located at:

$$\psi_j = \frac{\pi}{n}(2j - 1); \qquad j = 1, \ldots, n \qquad (3.131)$$

Each passage of the target through a relative azimuth ψ_j is recorded and equation (3.126) separately applied, yielding for each target, a set of detectabilities $\{p(j)\}$ j = 1, . . , n. If, however, the target falls within the circle defined by a cone, with a side slope of 45 degrees directly below the aircraft, the total detectability and identifiability are taken as 1.0, and localizability (as circular error probibility) is taken as

$$CEP = 1.178H \tan 45^\circ$$

where H is aircraft altitude in feet above mean ground level. If the detectability and identifiability are both 1 as a result of this fact, no further computation need be made.

Having computed the set $\left\{P^{(j)}\right\}$ for each target the probability of detectability is

$$P_d = \left[1 - \prod_j (1 - P^{(j)})\right] P_{up} \tag{3.132}$$

where P_{up} is the probability that the ECM equipment is operable.

3.2.6.3 Identifiability. It has been assumed that (except for near-nadir passage, as noted in Paragraph 3.2.6.2) two looks are required for identification to assure that a triplet of noise pulses is not mistaken for a target. The conditional identifiability is then given by simple combinatorials:

$$P_I = 1 - \frac{P_{up}}{P_d} \sum_j P^{(j)} \prod_{i \neq j} \left(1 - P^{(i)}\right) \tag{3.133}$$

3.2.6.4 Localizability. Except for the near-nadir passage case, localizability is assumed to take the form of an optimal minimum-variance estimation procedure derived in Appendices D and E. In Appendix D, equations (10), (9), (17), (16), (24), and (25) are used in that order. From Paragraph D.4 it can be argued that the CEP is degraded by the fact that the expected number of detections is not n/2 but $P_d(n/2)$, in a proportional way. Then, to first order:

$$CEP = \frac{1.178n}{P_{dS}} \sqrt{\sigma\ (R)\, \sigma\ (X)} \tag{3.134}$$

where

CEP = localizability

n = number of looks

$P_{dS} = \sum_j P^{(j)}$ (eq. 3.126)

σ (R) = is standard deviation of estimation of target offset range

σ (X) = is standard deviation of estimation of target position along a line parallel to the aircraft flight path.

The last two data are computed in Appendix D, in equations (24) and (25), respectively.

Had it been assumed that the expected number of detection was n/2, the quantity P_d would not appear in equation (3.134).

3.2.7 Photo-TV Model

A single model is used for all optical sensors, e.g., photographic cameras and TV.* The main figure of merit of an optical sensor is its ability to detect targets and produce identifiable images of these targets on either film or a CRT. Optical sensors have a relative precision which is generally far greater than navigation errors in the aircraft, hence, the localizability problem is effectively ignored.

Following the established pattern, inputs to the Photo-TV portion of the Executive model are of two types: (1) data computed within Scenario and passed directly to the EXEC model, and (2) data input directly by the user.

INPUTS FROM SCENARIO

GEOMETRIC

- Aircraft height above mean ground level
- Depression angle to target
- Slant range to target
- Slant range of haze and/or rain traversed
- Probability of not being masked by terrain

WEATHER

- Prevailing visibility in clear weather and in rain
- Whether day or night mission
- Probability of no undercast clouds

TARGET/BACKGROUND

- Reflectivities of target and background

*The model does not incorporate a visual observer.

EQUIPMENT

- Probability that sensor equipment is operational
- Resolution required for 90% probability of detection

USER INPUTS

SENSOR DATA

- Film (and scanner) resolution
- Lens resolution and focal length
- Film (or display) gamma
- Logarithmic scale of the film (or display)
- Minimum detectable logarithmic contrast
- Processing levels at which cameras function

COMMUNICATIONS DATA

- Fraction of all keyed photos which are transmitted to ground

Outputs of the Photo submodel are, as in the case of all sensors, detectability, identifiability, and localizability. In block form:

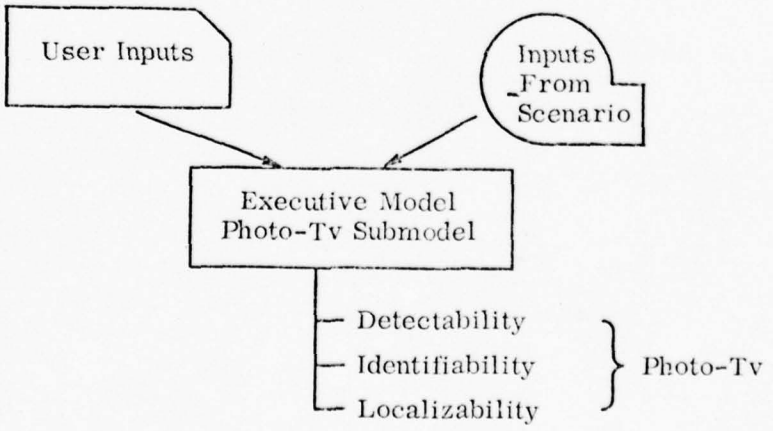

3.2.7.1 Target Detection. As one might expect, the computation of target detectability begins with an analysis of contrast; quite simply, if the contrast between the target and its background is not sufficient, no detection can occur. Contrast is a function of three basic parameters: (1) optical scattering, (2) target and background reflectivities, and (3) characteristics of the film being used. The latter two are user inputs, scattering is found by examining the effects of haze and rain on overall visibility.

The critical factor in detection is camera resolution. There are, of course, two components to this resolution -- tangential and radial -- each may be determined geometrically. Using these two components, an effective ground resolution may be computed. This effective resolution is then modified (empirically) to account for the contrast degradation.

Detectability may then be determined by using curves which give detectability as a function of the effective ground resolution relative to the resolution required for 90 percent probability of detection by an ideal observer (an input).

3.2.7.1.1 Target Contrast. The first step in the procedure is to compute the target contrast, assuming that the ground resolution cell is smaller than the target size. Let R_T and R_B be the reflectivities of the target and background, respectively. If S is the total scattering of target or background radiation of the optical path; then, by definition of logarithmic contrast:

$$C = \gamma \left| \log_{10} \left[\frac{(1-S)\ R_T + S}{(1-S)\ R_B + S} \right] \right| \qquad (3.135)$$

Where γ is the film or display gamma and the logarithmic contrast of the target is C.

The value of S can be estimated from the prevailing visibility, X_o, as discussed below. The prevailing visibility is generally defined as the distance corresponding to a reduction in contrast of a dark target against a light background to 60 percent. This corresponds approximately to S = 5/8 = 0.625.

Then, generally,

$$S = 1 - e^{-KX/X_o}, \tag{3.136}$$

and substituting,

$$0.625 = 1 - e^{-KX/X_o}$$

where X_o is the prevailing visibility in nautical miles (NM). Since visibility is usually given in statute miles (SM), and X, the slant range through haze is given in NM, the constant, K, becomes 1.13 yielding:

$$S = 1 - e^{\left(-1.13 \frac{X}{X_o}\right)} \tag{3.137}$$

The distance X used in the computation of scattering is not necessarily the total ray path distance because of the variation of visual scattering with altitude. Not knowing (and not being willing to predict) this variation, a constant scattering is assumed from ground level up to the prevalent haze level.

Let:

θ = the depression angle to the target

H_h = the haze level prevalent in the area of study (above mean sea level)

H_t = the target altitude above mean sea level (MSL)

H_a = the aircraft altitude above MSL

$$X = \begin{cases} \dfrac{H_h - H_t}{(\sin\theta)\ (6080)} & \text{if } H_a \geq H_h \\ \dfrac{H_a - H_t}{(\sin\theta)\ (6080)} & \text{if } H_a < H_h \end{cases}$$

The above scattering equation does not take into account scattering due to precipitation, therefore, the scattering equation is amended as follows:

$$S = 1 - e^{\left(-1.13\left(\frac{X}{X_o} + \frac{X'}{X'_o}\right)\right)} \tag{3.138}$$

and

S' = width of precipitation traversed

R = the fractional ground area upon which precipitation is falling

$$X' = \left\{\text{MIN}\left[\frac{S'}{\text{Cos}\,\theta}, \frac{H_h - H_t}{\text{Sin}\,\theta}\right]\right\} R \tag{3.139}$$

X'_o = the prevailing visibility in precipitation.

X_o = the prevailing visibility in haze.

The variable X' reflects the fact that precipitation can occur only below H_h.

The final value of S given by equation (3.138) is used in the contrast equation.

A simple test is now made: If the contrast, C, is less than the minimum contrast for detection, C_o (an input to the program) then no detection is possible.*

3.2.7.1.2 Local Illumination. If local illumination is employed for the photosensor rather than ambient illumination, the following procedure is used: assume that the film or display is correctly exposed at maximum density for the nearest point of the picture, i.e., the nadir point H'_a (AGL). Then if D is the total logarithmic scale of the film or display and R is the target slant range in nautical miles

$$R_{max} = \left(\frac{H'_a}{6080}\right)(10)^{D/2} \tag{3.140}$$

*In practice, C_o is a function of the characteristics of the film and the reconnaissance observer and has been determined experimentally. Reference (6), BETARS Report.

Then if,

$$R \geq R_{max}$$

no detection (or, consequently, identification) is possible. *

3.2.7.1.3 Calculation of Resolution. From a calculation of the system angular resolution, the ground resolution is approximated by the root mean square (rms) of the radial and tangential ground projection resolutions. The ground resolution is then corrected to account for the degradation effects due to low contrast.

The angular resolution of the system is given by geometry as

$$\rho = \frac{\left[\left(\frac{1}{L_o}\right)^2 + \left(\frac{1}{L_2}\right)^2\right]^{1/2}}{25.4F} \tag{3.141}$$

where

$$L_o = \begin{cases} L_1 & \text{when film is being used} \\ L_1' & \text{when considering the scanner or display} \end{cases}$$

and L_1 is the film resolution in lines/millimeter, L_1' is the scanner or display resolution in line pairs per millimeter, and L_2 is the effective lens resolution in lines per millimeter. The radial ground resolution is:

$$\rho_x = \frac{R\rho}{(6080)\ (\sin\theta)} \tag{3.142}$$

where R is the slant range in nautical miles and θ is the depression angle. The tangential ground resolution is simply

$$\rho_y = (R\rho)\ (6080) \tag{3.143}$$

then the effective ground resolution is the rms:

$$\bar{\rho} = \sqrt{\frac{\rho_x^2 + \rho_y^2}{2}} = 6080\ R\rho \sqrt{\frac{1 + \sin^2\theta}{2\ \sin^2\theta}} \tag{3.144}$$

* Day and night correspond respectively to ambient and local illumination.

This data must now be corrected for contrast degradation, from curve-fits by the authors to actual reconnaissance film data (12).

$$\bar{\rho}' = \frac{\bar{\rho}}{1 - e^{-2C}} \tag{3.145}$$

where C is the contrast and is given by equation (3.135).

Note, however, that in practice ρ' is constrained by

$$\bar{\rho}' \leq 3\rho' \tag{3.146}$$

3.2.7.1.4 Detectability. From curve-fits, taken by the authors on certain reconnaissance data (12) the detectability PD of the target on a given frame is now computed as

$$P_T \; P_{up} \; P_{NC} \; e^{-0.1 \, (\bar{\rho}'^2/\rho_T^2)} \tag{3.147}$$

Where ρ_T is the ground resolution required for 90% probability of detection by an ideal observer, P_T is the non-shadowing probability of the terrain, P_{up} is the probability that the equipment is operative, and P_{NC} is the probability that the line of sight is not obscured by undercast clouds. The variable $\bar{\rho}'$ is given by equation (3.145).

The above expression (3.147) is computed once per target and once per frame. However, in general, there are several frames associated with a given target. Therefore, it is necessary to accumulate the independent detectabilities for each frame. Let PD_j be the detectability on frame j. Let P_{kj} be the keying probability for the j^{th} frame and let $P_D^{(L)}$ be the detectability at Level L.
Then, at Level 1

$$PD^{(1)} = 0 \tag{3.148}$$

Level 2 allows both keying and transmission of data in that the detectability is given by

$$PD^{(2)} = \left[1 - \frac{j}{77}(1 - P_{dj} \; P_{kj} \; T)\right] P_{up} \tag{3.149}$$

where P_{dj} is the probability of detecting the target on frame j and T is the fraction of all keyed frames that are transmitted to the ground station.

Level 3 allows keying but no transmission, therefore:

$$P_D^{(3)} = \left[1 - \prod_j (1 - P_{dj}\, P_{kj})\right] P_{up} \tag{3.150}$$

At Level 4 there is neither keying nor transmission of data and detectability is:

$$P_D^{(4)} = \left[1 - \prod_j (1 - P_{dj})\right] P_{up} \tag{3.151}$$

3.2.7.2 Identifiability. Based on the assumption that one needs five times the detection resolution for identification:[12]

$$P_{Ij} = e^{-2.5\,(\bar{\rho}'^2/\rho_T^2)} \tag{3.152}$$

where P_{Ij} is the identifiability of the target on frame j.

Letting $P_I^{(L)}$ be the identifiability probability for Level L:

$$P_I^{(1)} = 0 \tag{3.153}$$

$$P_I^{(2)} = 1 - \prod (1 - P_{Ij}\, P_{kj}\, T) \tag{3.154}$$

over all j containing the target

$$P_I^{(3)} = 1 - \prod (1 - P_{Ij}\, P_{kj}) \tag{3.155}$$

over all j containing the target

$$P_I^{(4)} = 1 - \prod (1 - P_{Ij}) \tag{3.156}$$

over all j containing the target

where, as before, T is the fraction of all keyed frames transmitted; P_{kj} is the probability that frame number j is keyed.

3.2.7.3 Localizability. Since navigation errors dominate any optical sensor errors, the relative CEP is taken as equal to 0. Admittedly, geodetic techniques can be used (and indeed, the geodetic reconstruction probability is estimated in the program), in which case the sensor errors are not insignificant. However, this feature was not analyzed. For program stability purposes, a low value of CEP (50 ft. or 100 ft., depending on the sensor type) has been arbitrarily assigned to each of the optical sensors.

3.2.8 Forward Looking Infrared Sensor (FLIR)

It is necessary to digress for a moment and discuss the modeling technique of the FLIR sensor in the Scenario Model. The reader will recall that FLIR is assumed to always have three "looks" at each target; the first two assume that the sensor is slewed while the third assumes the sensor is not slewed. However, it shall be pointed out that if FLIR sees the target in the non-slewed mode, it may also see the target in the slewed mode.

For each of the three looks and for each of the four processing levels, the FLIR model computes detectability, identifiability, and CEP using the same equations as the IR sensor (Paragraph 3.2.2).

Inputs to the FLIR submodel of the Executive Program are identical to those of the IR (see Paragraph 3.2.2), both user determined inputs and those supplied by the Scenario Model. The outputs differ only in that FLIR integrates the performance over three looks, whereas the IR only computes performance on a single look basis.

3.2.8.1 Detectability. Let TPD_{ij} be the probability of detection for look i at processing level j. TPD_{ij} is computed using the IR equation of Paragraph 3.2.2. The index i varies from 1 to 3. The overall conditional detection probability for FLIR at processing level j is given by:

$$PDC_j = 1.0-(1.0 - TPD_{3j})(1.0 - PS\ (TPD_{2j}))\ (1.0 - PS\ (TPD_{1j})) \qquad (3.157)$$

where PS is the probability that the sensor is slewed. The total detectability is given by:

$$PD_j = PDC_j\ P_T\ K_L \qquad (3.158)$$

where

P_T is the probability that the target was not blocked by terrain;

K_L is the probability that the FLIR sensor operates in level j (1 or 0).

PS remains to be computed.

Slewing can occur in one of two ways: the target can be preplanned, or the target can be sensed by a different sensor which, in turn, directs the FLIR to point towards the target. In the preplanned mode, the system receives coordinates of known or suspected targets at the time of mission initiation. For the second mode the sensors must be considered which may reasonably be expected to pick up a target in time to direct the FLIR toward the target. The target must be sensed while still in front of the aircraft since FLIR looks only in a forward direction, and the target sensing must be in real time, i.e., Level 1 processing. Only the ECM and MTIFLR sensors can meet these criteria; each can detect targets in front of the aircraft and each operates in Level 1. The only other sensors which "see" in a forward direction are the cameras, but they do not function in Level 1. Therefore, PS, the probability of slewing, can be taken as:

$$PS = 1.0 - PP\,(1 - PD_{x,1})\,(1 - PD_{y,1}) \tag{3.159}$$

where

PP is equal to 0 if the target is preplanned and 1 if it is not;

$PD_{x,1}$ is the probability of detecting the target in Level 1 for the ECM sensor;

$PD_{y,1}$ is the probability of detecting the target in Level 1 for the MTIFLR sensor.

3.2.8.2 Identifiability. Let TPI_{kj} be the conditional identifiability of the target on look k at level j. TPI_{kj} is computed using the IR equations in Paragraph 3.2.2. Then PI_j, the system conditional identifiability, is given by:

$$PI_j = 1.0 - (1.0 - PS\,(TPI_{1,j}))\,(1.0 - PS\,(TPI_{2,j}))\,(1.0 - TPI_{3,j}) \tag{3.160}$$

3.2.8.3 Localizability. If the FLIR sensor is slewed, looks 1 and 2 are valid (look 3 may or may not be valid); when FLIR is unslewed, only look 3 is valid. Consider each case.

For each processing level j, if slewing occurs, the error in localization is taken to be:

$$CEP_j = MIN\left[TCEP_{2,j};\ TCEP_{1,j}\right] \tag{3.161}$$

where

CEP_j = CEP of FLIR at Level j

$TCEP_{i,j}$ = CEP given by look i at Level j *

Choosing the minimum of the two CEP's was felt to be as realistic as attempting to combine them by some averaging technique.

In the unslewed case:

$$CEP_j = TCEP_{3,j} \tag{3.162}$$

3.3 DATA COMBINING MODEL

This model operates separately for each target and simultaneously for all sensors. It presupposes all sensor calculations complete for the target being considered. Some of the calculations shown below are redundant with those in the sensor model sections; however, in the implementation they are not repeated.

The variables that are used in this paragraph are defined below:**

PDC_{ij} = Conditional detectability for sensor i level j.

PNS_i = Probability that sensor i is not shadowed by terrain.

PCC_i = Probability that sensor i is not obstructed by weather. This probability is 1.0 if the sensor is a non-visual sensor.

---

* Note that $TCEP_{i,j}$ is computed for each i and j using the IR equations of Paragraph 3.2.2.

**The difference between conditional and total probabilities are discussed at length in Paragraph 3.2.

K_{ij} = Equals 1 if i^{th} sensor operates at the j^{th} processing level. If the sensor does not operate at level j, $k_{ij} = 0$.

PUP_i = The probability that the sensor i equipment is up.

PD_{ij} = PNS_i PCC_i PUP_j PDC_{ij} K_{ij} (the total detectability provided by sensor i level j).

PI_{ij} = Conditional identifiability given by sensor i level j.

P_K = Alerting probability (see Paragraph 3.3.1).

CEP_{ij} = CEP given by sensor i level j (in feet).

The outputs are as follow (again for each target), where the subscript j refers to the level, i.e., j = 1, 2, 3, or 4.*

PD_j = Conditional detectability of the target over all sensors.

PDT_j = Total detectability of the target over all sensors.

PI_j = Conditional identifiability of the target over all sensors.

PIT_j = Total identifiability of the target over all sensors.

PG_4 = Probability of successful geodetic localization at Level 4

CEP_j = Relative localizability; i.e., assuming A/C coordinates are known

$CEPT_j$ = Total localizability; i.e., the uncertainity of A/C coordinates are taken into account

3.3.1 Alerting Probability

Let:

D_1 = the Level 1 IR detectability

D_2 = the MTISLR detectability at Level 1

D_3 = the MTIFLR detectability at Level 1

* PD with a single subscript refers to the conditional detectability over all sensors; with two subscripts, it pertains to a given sensor; PI is analogous.

D_4 = the ECM detectability at Level 1

D_5 = 1 if the target was preplanned, 0 if not.

Then the overall alerting probability for a given target is

$$P_k = 1 - \prod_{g=1}^{5} (1 - D_g) \tag{3.163}$$

This formula states that a target is keyed if any of the four sensors (IR, MTISLR, MTIFLR, or ECM) see the target and/or if the target was preplanned. The keying probability is just the conjoined probabilities that the target was seen by the relevant sensors or was preplanned.

3.3.2 Integrated Detectability

The conditional detectability for level j, PD_j is given by

$$PD_j = 1 - \prod^{i} (1 - PDC_{ij}) \tag{3.164}$$

Whereas the total detectability, PDT_j, is

$$PDT_j = 1 - \prod^{i} (1 - PD_{ij}), \tag{3.165}$$

A word of explanation is in order. By conditional detectability (i.e., PDC_{ij}) is meant the probability that sensor i sees the target (in Level j) given that:

(1) The sensor operates in Level j with certainty (i.e., with probability of 1.0).

(2) The target is not obscured by weather with probability 1.0.

(3) The target is not masked by terrain with probability 1.0.

(4) The sensor is in an "up" or operable condition with probability 1.0.

On the other hand, total detectability (i.e., PD_{ij}) does not constrain these factors to be one; that is, the conditional detectability is multiplied by the non-masking probability, the non-weather obscured probability, the probability that the sensor is up, and the probability that the sensor has an output at the level being considered.

3.3.3 Identifiability

Conditional identifiability is analogous to conditional detectability insofar as it assumes that the target is not masked by terrain, obscured by weather, and that the equipment is up and gives an output at the level being considered. This conditional identifiability is

$$PI_j = 1 - \prod_i (1 - PI_{ij}) \tag{3.166}$$

The total identifiability is

$$PIT_j = 1 - \prod_i (1 - (PI_{ij})\ (PD_{ij})) \tag{3.167}$$

3.3.4 Localizability

Estimating the CEP of integrated data is highly dependent upon the precise operational method employed for resolving target positions among several sets of data. One is forced to assume that this will be done in an optimal way; hence, the minimum-variance optimization criterion was used throughout this analysis. In the following discussion, two cases are treated: (1) where in the absence of knowledge of the a priori probabilities associated with individual sensor detectabilities they are assumed equiprobable, and (2) where the computed detectabilities will be employed to compute the minimum-variance CEP. In both cases it is assumed that the algorithim for operational data combining takes into account the a priori sensor CEP's, and that the resulting combined data CEP's reflect this weighted processing.

Though method (2) was actually employed in the program, a discussion of method (1) will provide some necessary groundwork.

3.3.4.1 Equiprobable Detections. Operationally, it is assumed that the position data relative to aircraft position are averaged subject to a weighting which minimizes the CEP. Assuming the problem to be symmetric on the x and y axes, a pessimistic estimate (i.e., worst case estimate) of the localizability can be made.

In actuality, the on-board computer will dynamically estimate x and y separately for each source of position data, and combine the x and y estimates separately, independently weighted — thereby yielding relative position estimates better than our analysis predicts.

Once relative position is determined, target position by time is obtained by combining with navigational data.

In Level 4, however, if photos are available, it is possible via geodetic rectification to further reduce target errors by mapping in relation to a geodetic control point. For all intent and purposes this error can be set to zero relative to map accuracies, which themselves are fixed relative to system design. This possibility will be indicated by a probability output, P_{G4}, which is simply estimated by

$$P_{G4} = 1 - \prod_{g}^{g} (1 - PD_{g4}) \tag{3.168}$$

where the index g ranges over the non-panoramic cameras.

For other cases, assumptions are: circular symmetry, independence, and small deviations. A linear unbiased estimator function is used for x and y:

$$\hat{Y}_j = \sum_i K_{ij} Y_{ij} \qquad \text{subject to} \sum_i K_{ij} = 1 \text{ for normalization} \tag{3.169}$$

and similarly for $\hat{X}_j$:

$$\hat{X}_j = \sum_i K_{ij} X_{ij} \tag{3.170}$$

The K_{ij} for which the estimator is minimum variance and maximum liklihood is

$$K_{ij} = \frac{1}{CEP_{ij}^2 \sum_i (CEP_{ij}^{-2})} \tag{3.171}$$

(by the formulae in Appendix E).

Now

$$CEP_{(j)}^2 = \left[\sum_i (CEP_{ij}^{-2}) \right]^{-1} \tag{3.172}$$

$$CEP_{(j)} = \left[\sum_i (CEP_{ij}^{-2}) \right]^{-1/2}$$

which is correct unless some $CEP_{ij} = 0$.

Note, however, that if any $CEP_{ij} = 0$ then, letting a bar over a quantity be the expected value of that quantity:

$$\overline{CEP}_{(j)} = 0. \tag{3.173}$$

The above $\overline{CEP}_{(j)}$ values are relative to the aircraft, and should be reported as such. In addition, for each j,

$$\overline{CEPT}_{(j)} = \sqrt{CEP^2_{(j)} + NAV\ CEP^2} \tag{3.174}$$

Where $NAVCEP^2$ is the squared CEP of the navigational system.

3.3.4.2 Combining Non-Equiprobable Detections. In "real life" the data from each sensor are assumed combined not knowing the "true" detectabilities. The precise estimation of the resulting target localizability was a horrendous calculation, so a recursive approximation was devised.

Let CEP_i be the CEP given by the i^{th} sensor. With each CEP_i is associated a p_i, the detectability of the i^{th} sensor*. There are N such pairs of numbers, where N is the number of sensors. Further, let $f_i = (CEP_i)^2$.

The procedure involves an iteration on i, the index of the sensors $i = 1, \ldots, N$. In general, let

$$q_i = 1 - p_i$$

$$Q_j = \prod_{i=1}^{j} q_i$$

$$P_j = 1 - Q_j$$

Then P_N is the net detectability of the target. Let F_i be the estimate of integrated $(CEP)^2$ at the ith iteration. Clearly $F_1 = f_1$, $P_1 = p_1$. Focus now on the $(i + 1)^{th}$ iteration. Four cases are shown:

		Did one of the first i sensors see the target?	
		Yes	No
Did the $(i + 1)^{st}$ sensor see the target?	Yes	Case 1, 1	Case 0, 1
	No	Case 1, 0	Case 0, 0

*Pairs of data for which the CEP_i has been computed as "infinite" are not used. P_i may, however, be equal to zero without adversely affecting the algorithms.

Case 1, 0: Prob (case 1,0) = $P_i\, q_{i+1}$

$$F_{i+1} = F_i \tag{3.175}$$

Case 1, 1: Prob (case 1,1) = $P_i\, p_{i+1}$

$$F_{i+1} = \left[F_i^{-1} + f_{i+1}^{-1} \right]^{-1} \tag{3.176}$$

Case 0, 1: Prob (case 0,1) = $Q_i\, p_{i+1}$

$$F_{i+1} = f_{i+1} \tag{3.177}$$

Case 0, 0: Prob (case 0,0) = $Q_i\, q_{i+1}$

F_{i+1} meaningless (3.178)

(Note: programmatically F_{i+1} is set to a very large number)

Thus, since the four cases are exhaustive and exclusive:

$$P_{i+1} = p_{i+1} + P_i - p_{i+1}\, P_i \tag{3.179}$$

$$F_{i+1} = \frac{1}{P_{i+1}} \left[p_{i+1}\,(1 - P_i) f_{i+1} + P_i\, F_i \left(1 - \frac{p_{i+1}\, F_i}{f_{i+1} + F_i} \right) \right] \tag{3.180}$$

The iteration is carried out for $i = 1, \ldots, (N-1)$. This approximation is best when the table of p_i, f_i is sorted in order of decreasing p_i/f_i with any unfilled array elements at the end. Then

$$CEP = \sqrt{F_N} \tag{3.181}$$

3.4 ORGANIZATION OF THE COMPUTER MODEL

Figure 3-6 shows the structure and interrelationships of the programs which implement the Executive Model. There are four logical groupings in the diagram:

(1). The main program.

(2). Housekeeping subroutines called upon by the main program.

(3). Sensor subroutines called upon by the main program.

(4). Utility subroutines used by the sensor subroutines.

The main program, called EXEC, serves as an event regulator, as well as handling all input. Each time an event (i.e., a target sighting by a particular sensor)

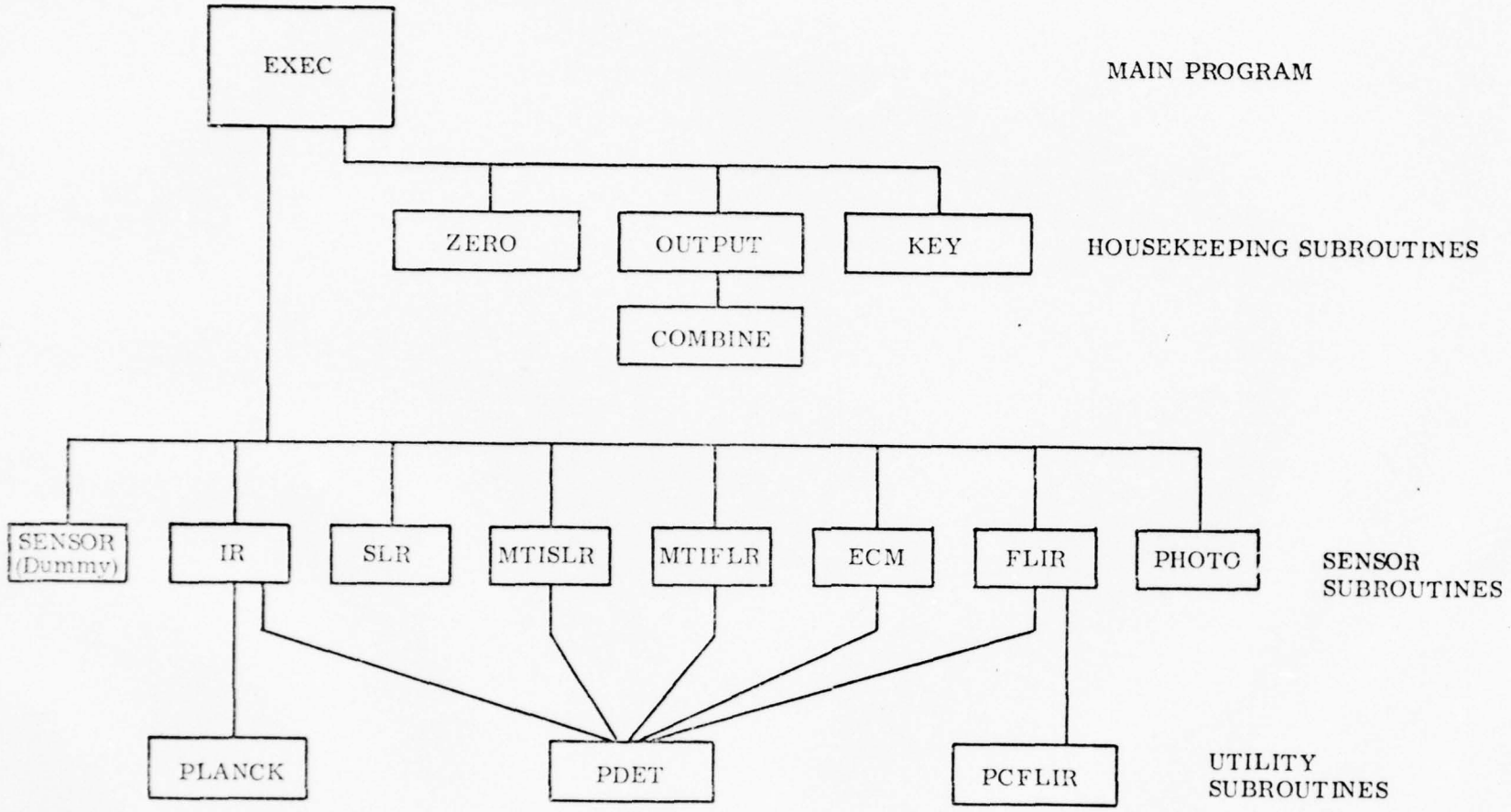

Figure 3-6. Executive Model Program and Subroutines

occurs, the EXEC program calls upon the relevant sensor subroutine. Whenever a given target has been considered for all sensors which saw it, the EXEC program calls upon the housekeeping functions which, in turn, prepare output pertaining to that target. The following paragraphs contain brief discussions of the three groups of subroutines.

3.4.1 Sensor Subroutines

Each sensor subroutine computes detectability, identifiability, and localizability (CEP) for its respective sensor. The methodology for computing these statistics formed the basis for Paragraph 3.2 of this report and will not be repeated here.

3.4.2 Utility Subroutines

Utility subroutines were written to be used with repetitious computations. Brief descriptions of these subroutines are given in the following paragraphs.

3.4.2.1 PLANCK. As shown in Figure 3-6, this subroutine is called by the IR sensor subroutine. Its purpose is to compute radiated power intensity in watts-per-square-meter as a function of band limits, temperature, and emissivity. In summary, this subroutine computes equation (3.3) in Paragraph 3.2.2.

3.4.2.2 PDET. As shown in Figure 3-6, subroutine PDET is called by the IR, MTISLR, MTIFLR, ECM, and FLIR subroutines. The function of this subroutine is to compute the probability of detection for each of these sensors. This detection probability is a function of the signal-to-noise ratio and assumes a false alarm rate of 10^{-8} per bit.

3.4.2.3 PCFLIR. The FLIR subroutine calls PCFLIR. It is identical to PLANCK in that it computes radiated power intensity in watts-per-square-meter as a function of band limits, temperature, and emissivity.

3.4.3 Housekeeping Subroutines

3.4.3.1 Zero. This subroutine is called by the EXEC program whenever a new target is about to be analyzed. It initializes all arrays which pertain to sensor-target combinations:

Set to zero

PDC(I)	the conditional detectability of the current target, sensor I

Set to zero (Contd.)

PD(I)	the total conditional detectability of the current target, sensor I
PI(I)	the conditional identifiability of the current target, sensor I
PR1(I)	the terrain shadowing probability for the current target, sensor I
PR2(I)	the probability that sensor I is up
PR3(I)	the probability that the current target is not blocked by clouds, sensor I

Set to 9999

CEP(I)	the CEP for the current target as given by sensor I

3.4.3.2 Key. Subroutine KEY computes the keying probability for the Photo Model. If the target is preplanned, the keying probability is taken as 1.0.* If the target is not preplanned, the keying probability is a function of the total detectabilities and CEP's given by the IR, MTISLR, MTIFLR, and ECM sensor models (see Paragraph 3.3.1). The KEY subroutine is called by the EXEC once for each target-pass combination just before the first call to the Photo model for that target on that pass.

3.4.3.3 Output. As the name suggests, this subroutine handles the output function of the Executive program. Within a given pass, after each target has been considered, OUTPUT is called by the EXEC which then sets up the output. Some computations pertaining to the FLIR sensor are done within the OUTPUT subroutine, namely:

(1). Computing the slewing probability for the FLIR sensor.

(2). Computing the final detectability, localizability, and identifiability of the FLIR sensor.

The computations are made by the OUTPUT routine because FLIR computes detectabilities, identifiabilities, and CEP's for each of three looks (see Paragraph 2.3.2) during a time in which it cannot be determined if slewing occurs. This determination can only be made after all sensors are considered for the target, and OUTPUT is the logical

*The probability of not flying past a preplanned target is not considered. This is proper because modern navigation systems have errors generally smaller than typical fields of view of reconnaissance sensors.

place for this to be done. In short, equations (3.157), (3.160), and (3.161) in Paragraph 3.2.8 are computed within OUTPUT.

Part of the output for each target is the capabilities of the overall reconnaissance system vis-a-vis the target, e.g., how well the system as a whole detected, identified, and localized the target. The OUTPUT subroutine computes these statistics by calling in the Combine subroutine.

3.4.3.4 Combine. This subroutine implements the data-combining algorithm given in Paragraph 3.3. Using this algorithm, this subroutine computes, for each target within a given pass, the detectability, identifiability, and localizability of the overall reconnaissance system vis-a-vis that target.

3.5 INPUTS TO THE EXECUTIVE PROGRAM

The input to the Executive Program consists of a tape and a deck of cards. The input tape is produced by the Scenario program; the card deck, which defines the parameters for each sensor, is prepared by the user.

3.5.1 Tape Input

The tape produced by the Scenario program (Output Tape 1) is not modified before being used as input to the Executive Program. Hence, the reader is referred to Paragraph 2.7.2 for a discussion of the data stored on this tape.

3.5.2 Card Input

Table 3-1 gives the form of the input deck by card number, variable name, variable definition, and format. There are 28 cards in the input deck, and each card(s) pertains to a specific sensor as follows:

Cards	Sensor
1, 2, and 3	IR
4, 5, and 6	SLR
7, 8, and 9	MTISLR
10, 11, and 12	MTIFLR
13, 14, and 15	ECM
16 to 24	Photo-TV
25 to 27	FLIR
28	Control card for hard copy output

TABLE 3-1. INPUT TO EXECUTIVE MODEL

CARD NUMBER	VARIABLE	DEFINITION	FORMAT
1	RES(1)	Angular resolution for Band 1 of the IR in radians	8F10.5
	RES(2)	Angular resolution for Band 2 of the IR in radians	
	ALAM22(1)	Highest wavelength of Band 1 of the IR in microns	
	ALAM22(2)	Highest wavelength of Band 2 of the IR in microns	
	ALAM21(1)	Lowest wavelength of Band 1 of the IR in microns	
	ALAM21(2)	Lowest wavelength of Band 2 of the IR in microns	
	DTEMP(1)	Thermal resolution of Band 1 of the IR in degrees Kelvin	
	DTEMP(2)	Thermal resolution of Band 2 of the IR in degrees Kelvin	
2	SIGTH1(1)	Variance in angle measurement of Band 1 of the IR	4F10.5
	SIGTH1(2)	Variance in angle measurement of Band 2 of the IR	
	GAMMA2	IR system film gamma	
	CØ2	Minimum detectable logarithmic contrast for the IR sensor	
3	IFALS2	Probability of false alarm coefficient. This is $-\text{Log}_{10}$ of the noise induced false alarm rate per unit detection time. It should be between 5 and 12.**	6I5
	ILEVEL(J, L)* L=1, 4	This variable gives the levels of processing desired (1 if desired, 0 if not). For those levels of interest, a probability of target detection at that level is computed.	
	JIR	If JIR=1, a diagnostic printout will be generated in the IR subroutine. If JIR≠1, no printout is generated.	

TABLE 3-1. INPUT TO EXECUTIVE MODEL (Contd.)

CARD NUMBER	VARIABLE	DEFINITION	FORMAT
4	HLITS	Range resolution in nautical miles.	8F10.5
	AJ	Cross range resolution in nautical miles.	
	PHEMIS	Depression angle in radians.	
	ALAMDS	Radar wavelength in centimeters.	
	GAMMAS	System gamma, including film gamma.	
	CØS	Minimum detectable logarithmic contrast.	
	AL1S	Film resolution in lines/millimeter.	
	AL1PS	Display resolution in line pairs.	
5	D1	Width of film in meters.	5F10.5
	RMAX	Maximum slant range covered by film in meters.	
	RMIN	Minimum slant range covered by film in meters.	
	R1P	Width of range displayed in the display in meters.	
	SIGTSS	$\sigma^2(\theta)$ in radians^2 (θ is the perceived azimuth angle.)	
6	ILEVEL (J, L)*, L=1,4	ILEVEL (J, L) is 1 if PD appears in Level L; it equals Ø if otherwise. Levels 1 to 4.	515
	JSLR	If JSLR=1, a diagnostic printout will be generated in the SLR subroutine. If JSLR = 1, no printout will be generated.	

TABLE 3-1. INPUT TO EXECUTIVE MODEL (Contd.)

CARD NUMBER	VARIABLE	DEFINITION	FORMAT
7	DX	Forward resolution in meters.	8F10.5
	DR	Slant range resolution in meters.	
	PRE4	Depression angle in radians.	
	ALAMD4	Radar wavelength in cm .	
	SCØ4	Signal-to-clutter for standard target under standard conditions in db.	
	SNØ4	Signal-to-noise for standard target under standard conditions in db.	
	SIGØ4	Size of standard target in square meters	
	HØ4	Difference in altitude between A/C and target under standard conditions in feet.	
8	RØ4	Reflectivity, backscatter coefficient of standard background.	5F10.5
	RANGØ4	Slant range of standard background.	
	VRMIN4	Threshold velocity above which target is detectable in knots.	
	SIGTS4	$\sigma^2(\theta)$(radians^2.) (θ is the perceived azimuth angle.)	
	PDC4	Threshold detectability probability below which target is unidentifiable.	
	IFALS4	Probability of false alarm coefficient. This is $-\text{Log}_{10}$ of the noise induced false alarm rate per unit detection time. **	
9	ILEVEL(J, L)*, L=1, 4	The levels in which PD (output variable) appears; 1 if it appears, 0 if not. Levels are L=1, L=2, L=3, and L=4.	6I5
	JMSLR	If JMSLR = 1, a diagnostic printout will be generated in the MTISLR subroutine. If JMSLR ≠ 1, no printout is provided.	

TABLE 3-1. INPUT TO EXECUTIVE MODEL (Contd.)

CARD NUMBER	VARIABLE	DEFINITION	FORMAT
10	VRMIN	Threshold velocity above which target is detectable in knots.	8F10.5
	SCØ	Signal-to-clutter for standard target under standard conditions (db).	
	RØ	Reflectivity, backscatter coefficient for standard background.	
	SIGMAØ	Size of standard target in meters.	
	RANGEØ	Slant range of standard target in NM.	
	SNØ	Signal-to-Noise for standard target under standard conditions (db).	
	HØ	Difference in altitude between A/C and target under standard conditions (ft.)	
	SIGT	Standard deviation of θ, the perceived azimuth angle (radians).	
11	HLIT	Size of the (rectangular) resolution scale in NM.	4F10.5
	PHEMIN	Depression angle in radians.	
	ALAMDA	Radar wavelength in centimeters.	
	PDC5	Threshold detectability probability below which target cannot be identified.	
12	IFALSE	$-\text{Log}_{10}$ of the noise induced false alarm rate per unit detection time (must be between 5 and 12).**	6I5
	ILEVEL(J, L)*, L=1, 4	For Level L (L=1, 2, 3, 4), the value is 1 if the level is to be considered and Ø otherwise.	
	JMFLR	If JMFLR=1, a diagnostic printout will be generated within the MTIFLR subroutine. If JMFLR $\neq$ 1, no printout will be generated.	

TABLE 3-1. INPUT TO EXECUTIVE MODEL (Contd.)

CARD NUMBER	VARIABLE	DEFINITION	FORMAT
13	A	Measurement of the angular measurement precision (sigma) relative to beam width (typically 1/6).	6F10.5
	SIGTS	Variance of the aircraft position (from the actual) as given by the aircraft avionic systems.	
	SIGVS	Variance of (true) velocity as given by the avionic systems in knots squared.	
	FREQ1	Threshold frequency in megahertz, above which it is possible to get an angular fix on the target.	
	ANF	Receiver noise figure in db	
	BAND	Receiver bandwidth in megahertz.	
14	NBEAM	Number of beams.	7I5
	ITABM	The number of entries in the table (i.e., the number of type 15 cards)	
	ILEVEL (J, L), * L=1, 4	The levels of processing for which a probability of detection should be computed 1=yes, 0=no.	
	JECM	If JECM=1, a diagnostic printout will be generated in the ECM subroutines. If JECM≠1, no printouts will be provided.	
15 (There are "ITABM" of these cards)	XTAB	The frequency associated with "YTAB" in megahertz.	2F10.5
	YTAB	This is the receiver antenna gain plus line losses experienced at frequency "XTAB". Units are in db.	
16	Q(1) Q(2) . . . Q(8)	Q(I) is the fraction of keyed photos which are transmitted to the ground station by sensor number I + 6	8F10.5

TABLE 3-1. INPUT TO EXECUTIVE MODEL (Contd.)

CARD NUMBER	VARIABLE	DEFINITION	FORMAT
17	ALIP(1) ALIP(2) . . . ALIP(8)	ALIP(I) is the display (or scanner) resolution for sensor I + 6. The units are display line pairs per millimeter	8F10.5
18	AL1(1) AL1(2) . . . AL1(8)	ALI(I) is the film resolution, in optical lines per millimeter for sensor I + 6.	8F10.5
19	AL2(1) AL2(2) . . . AL2(8)	AL2(I) is the lens resolution, in optical lines per millimeter for sensor I + 6.	8F10.5
20	F(1) F(2) . . . F(8)	F(I) is the lens focal length (in inches) for sensor I + 6	8F10.5
21	D(1) D(2) . . . D(8)	D(I) is the logarithmic scale of film (or of the display if TV) of sensor I + 6	8F10.5
22	CØ(1) CØ(2) . . . CØ(8)	CØ(I) is the minimum detectable logarithmic contrast. It is equal to $\log_{10}$ (minimum target to background brightness ratio detectable) for sensor I + 6	8F10.5

TABLE 3-1. INPUT TO EXECUTIVE MODEL (Contd.)

CARD NUMBER	VARIABLE	DEFINITION	FORMAT
23	GAMMA(1) GAMMA(2) . . . GAMMA(8)	GAMMA(I) is the film (or display if TV) GAMMA for sensor I + 6	8F10.5
24	ILEVEL(J,1)* ILEVEL(J,2) ILEVEL(J,3) ILEVEL(J,4) ILEVEL(J,1) . . . ILEVEL(J,4) ILEVEL(J,1) . . . ILEVEL(J,4) JPHOTO	ILEVEL(J,L) is equal to 1 if detection is possible at Level L. If this is not the case, ILEVEL(J,L) = 0. The first four ILEVEL values are for camera #1, the next four for camera #2,..the last four for camera #8. If JPHOTO=1, a diagnostic printout is generated within the photo subroutine. If JPHOTO ≠1, there will be no printout.	33(I2)
25	ANGRES(1) ANGRES(2) HLAMDA(1) HLAMDA(2) BLAMDA(1) BLAMDA(2) TEMRES(1) TEMRES(2)	Angular resolution for Band 1 of the FLIR in radians Angular resolution for Band 2 of the FLIR in radians Highest wavelength of Band 1 of the FLIR in microns Highest wavelength of Band 2 of the FLIR in microns Lowest wavelength of Band 1 of the FLIR in microns Lowest wavelength of Band 2 of the FLIR in microns Thermal resolution of Band 1 of the FLIR in degrees Kelvin Thermal resolution of Band 2 of the FLIR in degrees Kelvin	8F10.5

TABLE 3-1. INPUT TO EXECUTIVE MODEL (Contd.)

CARD NUMBER	VARIABLE	DEFINITION	FORMAT
26	ANGVAR(1)	Variance in angle measurement of Band 1 of the FLIR in radians^2.	4F10.5
	ANGVAR(2)	Variance in angle measurement of Band 2 of the FLIR in radians^2.	
	SYSGAM	IR system film gamma.	
	MDLC	Minimum detectable logarithmic contrast for the FLIR sensor.	
27	IFAL15	Probability of false alarm coefficient. This is $-\text{Log}_{10}$ of the noise induced false alarm rate per unit detection time. It should be between 5 and 12. **	6I5
	ILEVEL(J, L)* L=1 to 4	This variable gives the levels of processing desired (1 if desired, 0 if not). For those levels of interest, a probability of target detection at that level is computed.	
	JFLIR	If JFLIR=1, a diagnostic printout will be generated within the FLIR subroutine. If JFLIR $\neq$ 1, there will be no printout.	
28	JEXC1	If JEXC1 = 1, a hard copy of EXEC is prepared. If JEXC1 $\neq$ 1, no hard copy.	2I5
	JEXC2	If JEXC2 = 1, the phrase "official use only" will be printed on each sheet of the hard copy output. If JEXC2 $\neq$ 1, no official phrase is printed.	

*For the variable ILEVEL(J, L) the index J is a code number for the sensor number — these code numbers are given in Appendix I (Vol III) of this report.

**The quantity is computed as $-\frac{1}{n}\text{Log}_{10}\left(\frac{F}{B}\right)$, where B is the system bandwidth which is equivalent to the product of display frequency and the number of distinguishable spots on the screen, n is the number of consecutive false alarm spots constituting a false alarm, F is the acceptable false alarm rate measured in false alarms per second.

3.6 EXECUTIVE PROGRAM OUTPUT

The Executive program prepares two output tapes: Output Tape 1 describes, on a pass-target basis, the detectability, identifiability, and localizability statistics

for each of the sensors. This tape serves as input to the Evaluation Model discussed in Section IV. The second tape (Output Tape 2) contains information computed within the Executive program which is used by the PI-Q model discussed in Section V.

In addition, if the user so desires, a hard copy of the information recorded on Output Tape 1 is prepared.

3.6.1 Output Tape 1

This tape, also called the Target/Sensor Output Tape, is written in binary form and is organized on a pass basis. Within each pass, each target is considered in order (up to a maximum of 200 targets) and a group of 20 records for each target generated.

The 20 records for each target can be logically divided into three groups:

- Group 1 consists of the first 15 records. Record 1 contains general header information, true target data (e.g., actual time of beam passage), and various system parameters (e.g., navigational or speed errors). This information is in reality the statistics provided by the Dummy Sensor. The remaining 14 records contain, for each of the four levels of processing, statistics on the 14 other sensors — ordered by sensor number*. These statistics include detectability, identifiability, and localizability as well as terrain shadowing probability for the sensor and target being considered.

- Group 2 contains, in logical records 16 through 19, the combined data from all sensors on each level of processing for the given target. This data describes, for the overall system of sensors, how effectively the target was detected, identified, and localized.

- Group 3 consisting of record 20, contains the geodetic probability and localizability for the target.

Table 3-2 defines these records in greater detail. Figure 3-7 shows the logical grouping of records on the tape.

After the last pass, target, and sensor have been analyzed, an end-of-file record, which does not contain data, is placed at the end of the tape.

*See Appendix I, for the number associated with each sensor. Appendix I is contained in Volume III.

TABLE 3-2. RECORDS ON OUTPUT TAPE 1

Group 1 Record 1 Word Number	Name	Definition
1-20	IALPHA(J) J=1, 20	Header information, obtained from Scenario tape
21	ITARG	Target ID = YYXXX where YY is the pass index and XXX is the target index
22	ITTYPE	Target type code
23	ITPP	Time of passage (tenths of seconds)
24-25	PK(I)	Probability of automatic keying
26-27	CEPKEY	CEP of automatic keying
28-29	XOFFG	Ground offset range (NM)
30-31	EN1	Error in heading
32-33	EN2	Error in speed
34-35	EN3	CEP NAV (NM)
36	ITKEY	Code denoting if target is keyed to air-to-air communications (1=no, 0=yes)
Records 2 through 15		
1	I1	Sensor Number
2	NSEN(I1)	Indicates whether the sensor saw target (1 = yes, 0 = no)
3-4	PRI(I1)	Terrain shadowing probability (probability target is not shadowed)
5-6	PR2(I1)	Probability that equipment is up
7-8	PR3(I1)	Probability of no undercast cloud, fraction not observed
9-10	PDC(I1, 1)	Conditional Detectability for Level 1
11-12	PDC(I1, 2)	Conditional Detectability for Level 2
13-14	PDC(I1, 3)	Conditional Detectability for Level 3
15-16	PDC(I1, 4)	Conditional Detectability for Level 4

TABLE 3-2. RECORDS ON OUTPUT TAPE 1 (Contd.)

Word Number	Name	Definition
17-18	PD(I1, 1)	Total Detectability for Level 1
19-20	PD(I1, 2)	Total Detectability for Level 2
21-22	PD(I1, 3)	Total Detectability for Level 3
23-24	PD(I1, 4)	Total Detectability for Level 4
25-26	PI(I1, 1)	Conditional Identifiability for Level 1
27-28	PI(I1, 2)	Conditional Identifiability for Level 2
29-30	PI(I1, 3)	Conditional Identifiability for Level 3
31-32	PI(I1, 4)	Conditional Identifiability for Level 4
33-34	CEP(I1)	Conditional CEP
Group 2 Records 16 through 19		
1	L	Level Number
2-3	PRC	Conditional Detectability
4-5	PR	Total Detectability
6-7	PRI	Conditional Identifiability
8-9	PRIT	Total Identifiability
10-11	CEPR	Relative Localizability
12-13	CEPT	Total Localizability
Group 3 Record 20		
1-2	PG4	Geodetic Probability
3-4	CEPG4	Geodetic Localizability

3.6.2 Output Tape 2

Output Tape 2 is written in BCD, with the header information identifying the run located in record 1. The second record gives, for each of the photo cameras, the fraction of keyed photos that are actually transmitted to the ground station.

Next, each target (within a given pass) is considered in order. N + 1 records are generated for each target, where N is the total number of photographic frames containing the target. The first N records give data relating each frame to

Pass 1 Target 1	Header Information, target and system parameters	(Record 1)
Sensor 2	How well did sensor 2 do vis-a-vis target on pass 1	(Record 2)
.		.
.		.
.		.
Sensor 15	How well did sensor 15 do vis-a-vis target 1 on pass 1	(Record 15)
System Performance, Level 1	How well did the system as a whole do against target 1 pass 1	(Record 16)
.		.
.		.
.		.
System Performance, Level 4	How well did the system as a whole do against target 1 pass 1	(Record 19)
Geodetic Information	What was the geodetic localizability and probability of the target	(Record 20)
Pass 1 Target 2		
.		
.		
.		
Pass 2 Target 1		
.		
.		
.		

Figure 3-7. Form of Output Tape 1

the target; the N + 1st record contains a number specifying the total number of frames containing the target, i.e., N. These records follow, on a pass-target basis, Record 2. (N may be zero, in which case only 1 record is generated.)

The forms of Records 1 and 2, which appear only once at the start of the tape, are given in Table 3-3. Form for the succeeding records is shown in Table 3-4.

TABLE 3-3. RECORDS 1 AND 2 OF OUTPUT TAPE 2

Record	Name of Variable	Definition	Format
1	IALPHA(I), I=1, 20	This record contains an alpha-numeric header which identifies the run.	20A4
2	Q(1) Q(2) . . .. Q(8)	Q(1) is the fraction of keyed photos taken by sensor (I+6), i.e., camera I, which are actually transmitted to the ground station	8F10.5

3.6.3 Hard Copy Output

As an option, a printout of the contents of Output Tape 1 can be produced*. This output is easily interpreted since all the variables are labeled. An example of such an output is given in Appendix H, Volume III.

3.7 OPTIMIZATION ROUTINES FOR EACH SENSOR TYPE

It was previously stated that the following sensor types are considered in the AIRS Simulation model:

(1). Dummy Sensor
(2). Infrared (IR)
(3). Side Looking Radar (SLR)
(4). Side Looking Radar with Moving Target Information (MTISLR)
(5). Forward Looking Radar with Moving Target Information (MTIFLR)
(6). ECM Sensor
(7). Photographic Cameras (Forward Looking Panoramic, Side Looking Frame, and Forward Looking Frame)
(8). Forward Looking Infrared (FLIR)

*Hard copy output is produced if sense switch 1 on the CDC 3200 console is turned on.

TABLE 3-4. OUTPUT TAPE 2 RECORDS

Record Type		Variable Name	Format
This record is repeated once for each camera frame for the target being considered. (Targets are considered in order within a given pass — passes are considered in order.)	ITKEY	This variable is equal to 0 if the target is keyed air-to-air.	I5
	ITPP	This is the time of target passage in tenths of seconds.	I10
	ITARG	A five digit integer; the first two digits are the pass number, the last three are the target number.	I10
	PK	The probability that the camera which generated this frame was automatically keyed.	E15.7
	XOFFS	The slant offset range to the target at the time this frame was was taken.	E15.7
	ITTYPE	An index which gives the type of target.	I5
This record is generated once per target and follows all frame records (the record above) for that target.	JFRAM	The number of camera frames on which the current target appears.	I10

As now programmed, the AIRS Simulation Model can handle 15 sensor types: one each of the first six sensors on page 3-97, eight of the photo cameras (the seventh sensor), and one of the eighth sensor. During any given run, the sensors of interest are placed in an "on" mode, and those of no interest are turned "off". Hence, it is possible to use the model to study the effectiveness of a single sensor (i.e., turning the other 14 off). However, in practice, this technique is simply to inefficient. These inefficiencies are obvious in two areas:

(1). Data preparation

(2). Parametric representation of the sensor

Each area is briefly discussed below.

First, when running the overall model, sensor data must be provided for all 15 sensors, even those placed in an "off" mode. This data is hard to find and time consuming to prepare. For example, an IR specialist who wished to test the effect of changing the capabilities of this sensor would have to prepare meaningful data for all other sensors; if the data isn't meaningful, the program may abort.

Second, for a single run the parameters affecting the performance of a given sensor are fixed, and cannot be changed. Among these parameters are geographic data (e.g., aircraft altitude) weather data (e.g., rain), and sensor data (e.g., resolution). If a designer wishes to optimize a sensor over a wide range of conditions he must make a separate run of approximately 20 minutes for each combination of parameters.

In short, the above discussion indicates that the overall AIRS Simulation Model cannot be reasonably used to study a single sensor.

To solve this problem, it was decided to develop a separate computer program for each of the seven types of sensors of interest. (The dummy sensor is of no interest because it is a perfect sensor and is used only as a basis for performance comparison in the AIRS Simulation Model.)

The seven programs utilize the following three classes of user-input data:

(1) Sensor characteristic data

(2) Geographic and weather data

(3) Target characteristic data.

The logic which converts the input data to a set of performance statistics, including probabilities of detecting and identifying the target at each of the four levels, is identical to that of the EXEC program of the AIRS Model for each of the sensors.

A separate document describing these programs has been submitted to the Naval Air Development Center.[9]

SECTION IV.
EVALUATION MODEL

4.1 INTRODUCTION

The Evaluation Model (EVAL routine) was written jointly by Analytics, Inc. and Kettelle Associates, Inc. Its purpose is to produce a report of sensor effectiveness within a number of different target classifications. More specifically, EVAL provides detectability, identifiability, localizability, and redundancy measures for a given sensor and target configuration. These measures are computed target-by-target for all 15 sensors.

Following these computations, the detectability, identifiability, and localizability figures are integrated over all targets of the same target type to produce 30 summary tables (one for each different target type), and are also integrated over every target to produce total system results. The redundancy measures are integrated only in this final summary.

The user, through the use of input parameters, has control over what processing actually takes place. It is through such control that EVAL gains its flexibility. The user can exclude certain targets and any target type he wishes from consideration. Also, he can amalgamate target types into target groups and obtain an abbreviated summary table for such a group. User options are described in detail in Paragraph 4.2. A flowchart of the EVAL routine is shown in Figure 4-1.

4.2 INPUTS

Two types of inputs are used for EVAL: user option parameters, and target/sensor data. User option parameters are card inputs and are described in Table 4-1. The target/sensor data is the Target/Sensor Output Tape (Output Tape 1 generated by the EXEC model). Basically, the tape consists of records containing the necessary data for each target sighting.

4.3 PROCESSING

The EVAL Routine produces output via the following series of steps:

Step 1:

The Target/sensor Output Tape is positioned and all variables and accumulating arrays are initialized.

Step 2:

A target-sighting record is read in. A check of the user-defined (see Table 4-1) ROFFMX, IHOLD, NONPRE, and IPREPL is made against the appropriate target-sighting data. If the target sighting is not to be considered, the record is skipped and the sensor performance measures are not affected. Step 2 is then repeated. If, on the other hand, the sighting is to be considered, processing continues with Step 3.

Step 3:

Input data for multiple-sighted targets are conjoined into one set of figures per target. For each target the following eight quantities are calculated for every sensor.

The derivations, except for item (8), are straightforward. They merely require multiplication of scalars, i.e., a particular number of sensors, by probabilities.

(1) The number of times the target fell within the field of view (FOV) of that particular sensor.

(2) The number of times the target was expected to fall within FOV and was not masked by terrain.

(3) The expected number of times the target fell within FOV, was not masked by terrain, and the sensor was operational.

(4) The expected number of times the target fell within FOV, was not masked by terrain, equipment was operational, and there was no obscurity due to clouds.

(5) The expected number of times the target was detectable at processing Level i (i=1, 2, 3, 4).

(6) The expected number of times the target was identifiable at processing Level i (i=1, 2, 3, 4).

(7) The relative target CEP in feet, computed as an arithmetic mean over all sightings of the target in question.

(8) Measures of sensor redundancy denoted by α_{ij} and β_{ij} as defined in Appendix F; these are known as the "unscaled" and "scaled" contributions, respectively.

After computing the eight quantities, individual sensor data is integrated for each target to yield overall system measures:

(a) Total target detectability at each processing level. This is the conjoined* probability over all 15 sensors.

(b) Total target identifiability at each processing level. This is also conjoined.

(c) Relative target CEP at each processing level. The method for integrating CEP's over sensors is given in Data Combining, Paragraph 3.3.4.2.

(d) Total target CEP at each processing level. This is a combination of relative and mean navigational target CEP.

Step 4:

For all target types not excluded from processing by the input value of IHOLD, an integration (over the targets in that type) of all quantities calculated in Step 3, except item (8), is performed. This yields a summary table for each valid type. The integration process is as follows: quantities (1), (2), (3), (4), (5), and (6), are summed; quantities (7), (a), (b), (c), and (d), are averaged. Finally, the summary data for each target type is integrated over types to yield final performance measures for the overall system. Added to this set of final measures are the integrated α and β redundancy measurements derived from (8) as explained in Appendix F.

Step 5:

In accordance with the group numbers assigned by the input values of NTY, the quantities (a), (b), and (c), are integrated over target types belonging to a particular group. These are the only target group statistics computed.

Step 6:

If an end-of-file mark is the next character on the System Input Tape, processing is concluded, the EVAL routine ends, and control is returned to the monitor. Otherwise, the program returns to Step 1 so that the same EXEC-generated tape may be processed with a different set of user-input variables.

*Total conjoined probability is, of course, computed by $P_{conj} = 1 - \prod_{i=1}^{n} (1-P_i)$ where n=15 and i ranges over the sensors. The sensors are assumed statistically independent; this assumption is discussed in Appendix F.

4.4 OUTPUT

The printed materials generated by an EVAL routine* (execution of Steps 1 through 6) are:

(1) Pages of tables containing the target type summary statistics for each type considered.

(2) A one-page** table containing the overall system performance measures with the exception of the next item.

(3) A page containing the overall system redundancy measure for each level of processing and a similar page for the measure.

(4) A two-page table of the group (a user-defined set of target types) statistics.

(5) Header material containing the numbers of the target types being considered, the maximum offset distance, and a flag indicating whether preplanned, non preplanned, or both kinds of targets, are being included in the analysis.

(6) A message indicating how the β redundancy measure should be interpreted.

(7) Several of the EVAL table-pages contain the following auxiliary information which is useful in interpreting the tables:

   (a) The number of target-sightings per target type.

   (b) The number of targets per target type.

   (c) The number of targets per target group.

   (d) The target types included in each target group.

   (e) The total number of target sightings.

   (f) The total expected number of target sighting detections for each processing level.

*A sample EVAL output is given in Appendix H, Volume III.

**This page is labeled Target Type 31; Type 31 cannot be excluded.

4.5 SUMMARY

Great flexibility can be achieved when using EVAL because the EVAL routine is coded as a loop around the processing phase. The user may evaluate a particular simulation result (as recorded on the Target/Sensor Output Tape) in many ways by stacking, one behind the other, sets of user option parameter cards (3 per run).

By using the ROFFMX (see Table 4-1), the user can determine the effects of varying maximum offset distances on system performance in terms of target types and groups. Moreover, the user can evaluate system performance with respect to any collection of target types. For a quick look at system performance (i.e., total system detectability, identifiability, and localizability at each processing level), the user groups the relevant targets together through the use of the input variable NTY and then reads the target group output table. For a more detailed breakout he simply "turns off" the target types he is not interested in (through the use of IHOLD) and receives the total EVAL output with only the right types considered. The user input variables IPREPL and NONPRE similarly provide flexibility. This flexibility is summarized in Table 4-2.

TABLE 4-1. USER OPTION PARAMETERS

CARD NUMBER	NAME	DESCRIPTION	FORMAT	COLUMN
1	NTY(J)	NTY(J) = Group Number (from 1 to 5) of Target Type J. $1 \leq J \leq 30$. Leave blank if no grouping of target J is desired.	30I1	1-30
2	IHOLD(J)	IHOLD(J) = 1 if Target Type J is to be considered on this EVAL run; 0 otherwise. $1 \leq J \leq 30$.	30I1	1-30
	NONPRE	NONPRE = 1 if non-preplanned targets are being counted on this run; 0 if not.	I1	45
	IPREPL	IPREPL = 1 if preplanned targets are being counted on this run; 0 if not. Note that it is permissible for both NONPRE and IPREPL to = 1.	I1	46

TABLE 4-1. USER OPTION PARAMETERS (Contd.)

CARD NUMBER	NAME	DESCRIPTION	FORMAT	COLUMN
	LABELS(I)	$1 \leq I \leq 5$ up to 20 characters of alphanumeric header information printed at the top of every Target Type output page	5A4	47-67
3	ROFFMX	ROFFMX = maximum allowed target offset distance. The value may be punched anywhere in the first ten columns with any number of digits before and after the decimal point as long as the decimal point itself is punched.	F10.0	1-10

TABLE 4-2. USER FLEXIBILITY

DESIRED OUTPUT	RELEVANT VARIABLE*
Only targets within a specified offset distance from the aircraft are considered	ROFFMX
Only preplanned, or non-preplanned, targets are considered	IPREPL NONPRE
Only targets of a certain type (e.g., revetted aircraft) are considered	IHOLD
Summary tables for groups of target types (e.g., all types of radar may form one group) are produced	NTY

*See Table 4-1 for additional information on variable setting.

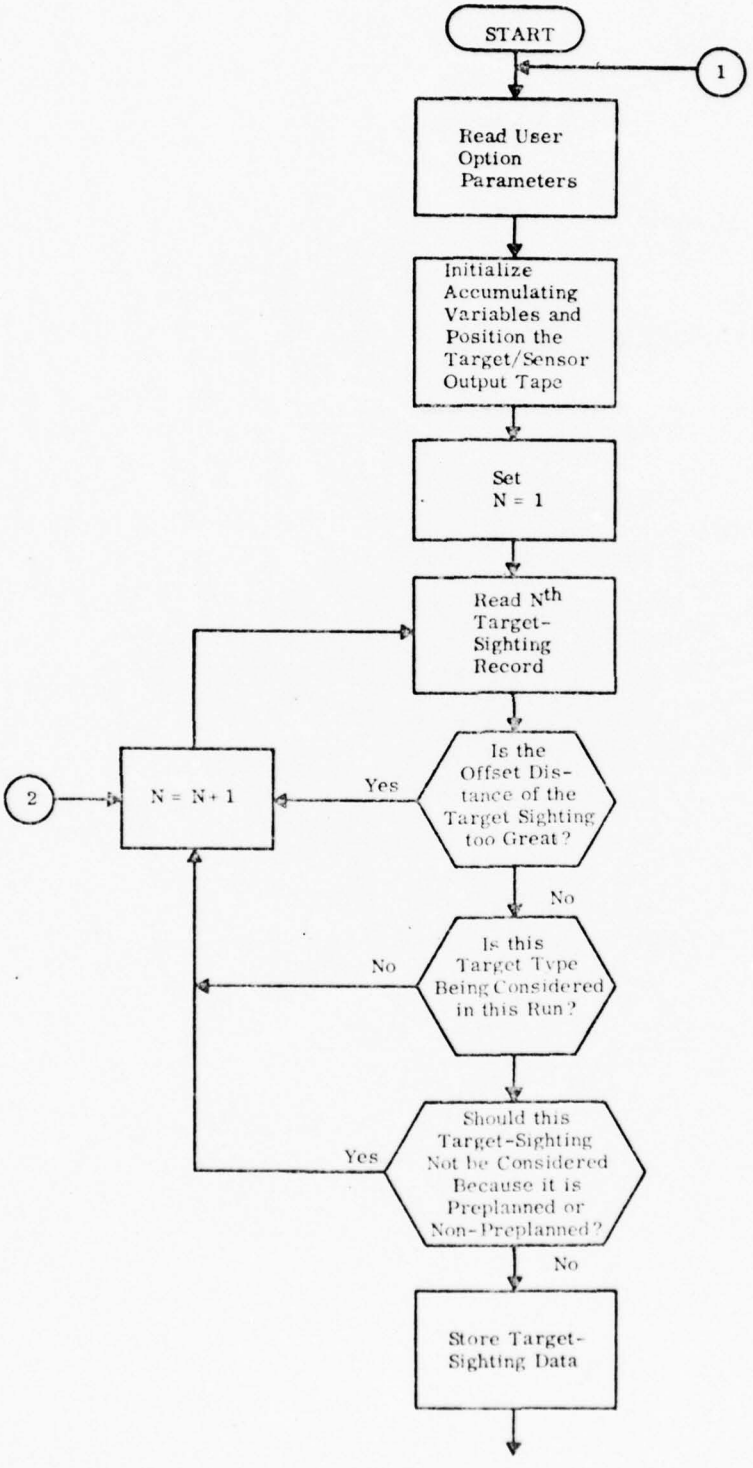

Figure 4-1. EVAL Routine (Sheet 1 of 3)

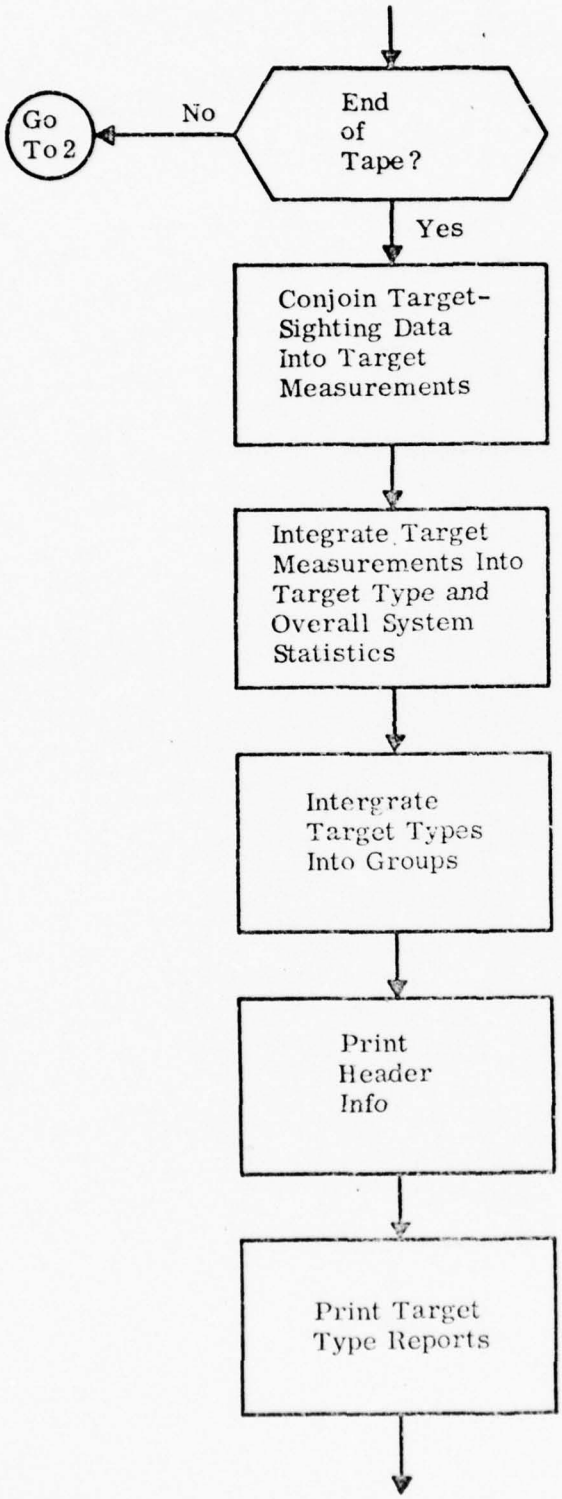

Figure 4-1. EVAL Routine (Sheet 2 of 3)

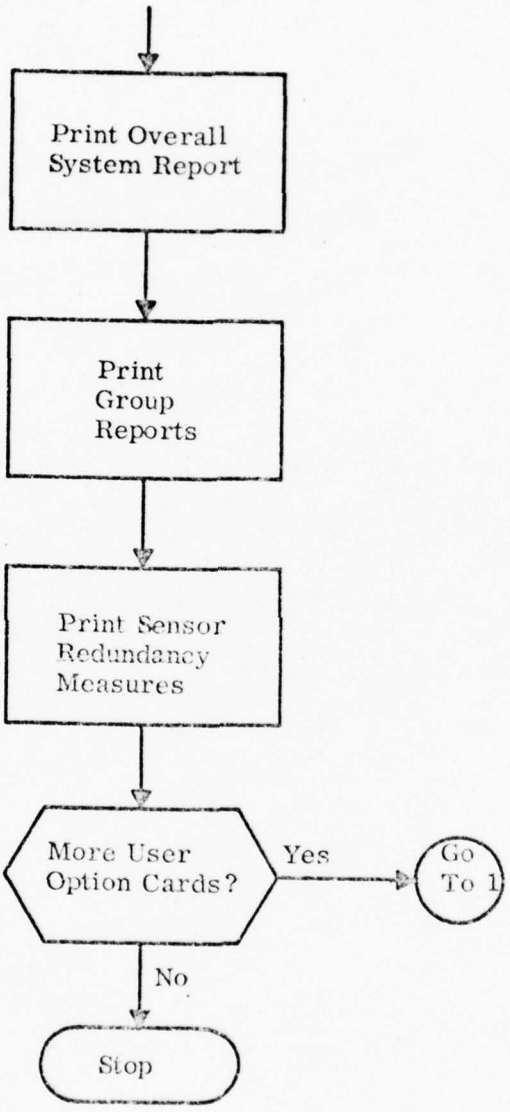

Figure 4-1. EVAL Routine (Sheet 3 of 3)

SECTION V.
PHOTO INTERPRETER AND QUEUEING MODEL

5.1 INTRODUCTION: SYSTEM TIME-LATE

The Photo-Interpreter and Queueing Model (PI-Q) is used in estimating system time-late. PI-Q is a composite of two models which have been separated from the main stream of the AIRS simulation model for programmatic purposes and have been combined into one computer program because they share many common inputs. Their purposes are also related functionally: to develop data necessary for estimation of the system time-late characteristics of the reconnaissance system under investigation.

System time-late is generally regarded as the most significant parameter governing the decision to develop a new reconnaissance system. The driving force behind data integration, real-time data analysis, on-board processing, and direct data communications all relate primarily to this parameter, the requirements for which are dictated by a series of target characteristics relating to the time decay of information regarding such targets. For moving targets, the "half-life" of any reconnaissance data may be measured in fractions of a minute; for highly mobile targets, the half-life of the data might be measured in minutes. In the case of fixed installations, the data half-life is of no consequence in a dynamic conflict scenario.

System time-late is defined as the distribution of the time difference between presentation of a reconnaissance opportunity (defined as the time at which the aircraft first passes abeam the target) and completion of data analysis. This means that command-decision and command-communications time is not charge to the reconnaissance system, but data transport and interpretation time are. Also, it means that the quality of the data analysis varies with time late (simply, given more time, the precision of the interpreted reconnaissance data increases). Within the AIRS model, the relation between data quality and time-late is expressed by considering performance (i.e., detectability, identifiability, and localizability) at four levels of operation, and estimating (by means of the PI-Q model) the time-late characteristics associated with the data available at each of these levels. This yields a four-point estimate of the tradeoff of data quality with time-late, and affords a significant output to the overall system effectiveness evaluation.

Time-late, as defined above, is composed of the following major contributions:

(1) On-board processing delay (usually insignificant)

(2) Queueing of data to the on-board operator (Level 1).

(3) Queueing of data communications to the Integrated Operational Intelligence Center (IOIC) (Level 2).

(4) Physical data transport via the vehicle to the IOIC (Levels 3 and 4).

(5) Queueing and interpretation delays at the IOIC (Levels 3 and 4, but different for each).*

Of these major contributions, Item (1) is inferred via engineering considerations. Item (4) can be estimated from the specification of the aircraft mission, and allowances for physical delays between landing and beginning of processing. The other contributions depend upon queueing of data which are, in general, received at a much higher average rate than they can be processed. The need arises for a queueing model which can be used to estimate the delays (and the associated data storage requirements) attendant with the buildup of such queues. The Queueing Model in the present program serves these needs, being designed for use, with different parameters for Items (2) and (3) above. Queueing with respect to IOIC processing is a simple matter since, in effect, all the data relating to one mission are given to the IOIC at one time (or at least far more rapidly than they are processed). Thus, no queueing calculation beyond simple arithmetic is required for Item (5), once the sequence in which the data are interpreted is decided.

The operational differences between Levels 3 and 4 relate to the keying of potentially significant data; data which are so keyed are processed by the IOIC ahead of other data. If the alerting and keying subsystem perform according to expectations, the Level 3 data processed by the IOIC ahead of the Level 4 data will be relatively richer in target images, thereby yielding a reduction in the average time-late for these target data. The purpose of the Photo-Interpreter Model is to estimate this

*To review, Level 1 constitutes real-time processing, Level 2 involves communication via data links to the IOIC, Level 3 comprises data carried back and annotated as potentially interesting by the alerting and keying subsystem, and Level 4 constitutes all data processed conventionally.

enrichment, thereby allowing an estimate of the time-late improvement due to the alerting and keying subsystem.

Thus, the Photo-Interpreter and Queueing Model comprises two logically independent programs:

(1) The Photo-Interpreter part estimates the degree of discrimination provided by the automatic alerting and keying capabilities of the system in selecting, for early photo-interpretation, those photographic frames which are relatively rich in target content.

(2) The Queueing part estimates the length and time delays of the data queues which form in front of

   (a) the on-board display system, and

   (b) the data communication circuits.

The outputs of these two models are then used to estimate the time-late for the system. Paragraph 5.2 discusses the PI model, and in Paragraph 5.3 the Queueing Model is discussed. The outputs generated by the PI and Queueing models, which are used to ascertain time-late statistics, are discussed in Paragraph 5.4.

5.2 PHOTO-INTERPRETER MODEL

The PI model provides sufficient information to estimate the performance of the system in selecting, for early interpretation, those frames that were relatively rich in target content. This was accomplished by developing three measures, namely:

X_L The expected number of frames presented to PI at Level L.

Y_L The expected number of targets (contained on X_L frames) presented to the PI model at Level L.

Z_L A measure of target content per frame at Level L, the ratio of Y_L to X_L.

Thus, Z_L is a measure of the richness of target content per frame. (Hopefully, a reconiassance system would have a high Z_1 and Z_2.)

As discussed in Paragraph 5.4, these measures also provide the data necessary in a time-late analysis. Looking forward, the Y_L's tell how many targets are processed at each level; recalling that Level 1 data is processed before Level 2, Level 2 before Level 3, and Level 3 before Level 4, it is now possible to answer such questions as: "What percent of all targets are processed in Levels 1 and 2 combined?".

The three measures which have just been discussed will now be developed.

A number of targets appear on a given photo frame, associated with each of these targets is a photo detectability and a target alerting probability. Let the subscript i denote the frame number and the subscript j denote the target number within that frame. Then the photo detectability of target j on the i^{th} frame is PD_{ij} and the keying probability for the j^{th} target is PK_j. It is assumed that a fraction, T, of all alerted frames is transmitted.

Let P_{im} be the probability that frame i contains precisely m detectable targets. Then

$$P_{i0} = \prod_{j=i}^{n} (1 - PD_{ij})$$

$$P_{i1} = \sum_{j=1}^{n} \prod_{\substack{K=1 \text{ and} \\ K \neq j}}^{n} PD_{ij} \; (1 - PD_{iK}) \qquad (5.1)$$

$$P_{i2} = \sum_{\ell=1}^{n} \sum_{\substack{j=1 \\ j \neq \ell}}^{n} \prod_{\substack{K=1 \\ \text{and} \\ K \neq i \text{ or } j}}^{n} PD_i \; PD_{ij} \; (1 - PD_{iK})$$

It can be seen that this series becomes extremely complex, and therefore, another way to compute P_{im} for any m would be more desirable. To this end, the following exact iterative technique was developed.

Let ${}_{(g)}P_{im}$ be the g^{th} iteration calculating P_{im}. First, observe that:

$$
\begin{aligned}
{}_{(1)}P_{i0} &= 1 - PD_{i1} \\
{}_{(1)}P_{i1} &= PD_{i1}
\end{aligned}
\tag{5.2}
$$

Then, for j = 2, 3, ...n, the following iterative is computed until j = n.

$$
{}_{(j)}P_{i0} = {}_{(j-1)}P_{i0} \ (1 - PD_{ij}) \tag{5.3}
$$

$$
{}_{(j)}P_{im} = {}_{(j-1)}P_{im} \ (1 - PD_{ij}) + {}_{(j-1)}P_{i\,(m-1)} \ PD_{ij} \qquad m = 1,2, \ldots (j-1)
$$

$$
{}_{(j)}P_{ij} = {}_{(j-1)}P_{i\,(j-1)} \ PD_{ij}
$$

where n is the maximum number of targets on frame i.

Now, let $P_{mi}^{(L)}$ be the contribution of frame i to the total expected number of frames containing m detectable targets at processing Level L:

Level 4 contains no keying or transmitting of data. Therefore:

$$
P_{mi}^{(4)} = P_{im} \tag{5.4}
$$

Level 3 considers keying, but no transmission. Therefore:

$$
P_{mi}^{(3)} = P_{im} R \tag{5.5}
$$

where R is given by the following equation:

$$
R = 1 - \prod_{j=1}^{n} (1 - PK_j) \tag{5.6}
$$

which is, of course, the probability that the frame is keyed. This is because only 1 of the j targets needs to be keyed for the whole frame to be keyed.

Level 2 considers both keying and transmission. Therefore:

$$P_{mi}^{(2)} = P_{im} RT \tag{5.7}$$

where, as defined above, T is the fraction of all alerted frames transmitted.

Let $N_m^{(L)}$ be the number of targets at Level L which contain m targets.

Then

$$N_m^{(L)} = \sum_i P_{mi}^{(L)} \tag{5.8}$$

except that

$$N_0^{(4)} \equiv \sum_i P_{01}^{(4)} + W \tag{5.9}$$

where W is the total number of frames containing no possible targets.

The expected number of frames presented to the PI model at Level L, call this value X_L, is just

$$X_L = \sum_m N_m^{(L)} \tag{5.10}$$

Y_L, the expected number of detectable target images presented to the PI model at Level L is

$$Y_L = \sum_m m N_m^{(L)} \tag{5.11}$$

A measure can be developed to express the "richness" of detectable targets per frame at Level L. This measure Z_L (which is not equal to the expected values of the number of targets per frame) is:

$$Z_L = \frac{Y_L}{X_L} \tag{5.12}$$

5.3 QUEUEING MODEL

The Queueing model was developed to study:

(1) The transmission delay from the aircraft and how this delay is affected by the communication bandwidth.

(2) How far behind the display rate the airborne operator falls (at Level 1, real time) in processing the information which appears on his display, as a function of the display rate.

Rather than use classical queueing models, the Scenario output generated queues, and a separate Monte-Carlo simulation was utilized to determine the probabilities, sizes, and waiting times of the communication queues. This technique was necessary because the communication queues are not in equilibrium; no closed-form solution can be computed.

Computationally, three separate cases are analyzed to determine queue length and waiting times:

Case A: Worst case analysis - every possible keyed event is assumed keyed with a probability of 1.00.

Case B: Mean case analysis - each event having a non-zero keying probability is assumed transmitted with certainty; however, the size of the data package containing the event is decreased by the factor of the computed keying probability.

Case C: Monte-Carlo analysis - queue length and waiting times are determined by Monte Carlo techniques using keying probabilities (i.e., an event either does or does not enter the queue, the decision is made by using the keying probability and the Monte Carlo distribution).

In each of these cases the mean, maximum, and standard deviation of the queue length and wait times are computed.

The definitions listed below are used in the following paragraphs:

N = the total number of events considered

T_i = the time of alerting (event i) $\quad i = 1, \ldots, N$

P_i = the probability of alerting for event i $\quad i = 1, \ldots, N$

K_i = binary event marker; 0 if air-to-air communications are not present for event i, 1 if present* $\quad i = 1, \ldots, N$

B = system bandwidth in units/sec.

R_o = continuous output rate in units/sec.

X = size of event data package in units

Y = size of incremental data package in units when air-to-air communications are used (i.e., total package size when air-to-air keyed is $X + Y$).

Q_i = queue length after occurrence of event i $\quad i = 1, \ldots, N$

Δ_i = waiting time to finish transmitting the i^{th} data package

$$\phi_i = \begin{cases} 1 & \text{when studying case A} \\ P_i & \text{when studying case B} \\ [0,1] & \text{A Monte-Carlo distribution is entered with } P_i\text{; 0 or 1 is the output} \end{cases}$$

Further, let:

$$Z_i \equiv [X + Y(K_i)]\,\phi_i$$

$$t_i \equiv T_{i+1} - T_i$$

$$T_N \equiv T_{N+1} - T_N$$

$$T \equiv T_{n+1} - T_1$$

$$R \equiv B - R_o$$

5.3.1 Computation of Queue Lengths

This paragraph discusses the manner in which the queue lengths and associated waiting times are computed for each of the three cases previously discussed.

*K_i for each event is an input from the Executive Model; see in particular Table 3-2 Variable Name ITKEY (Record 1 word 38)

The queue length, Q_i, immediately following each event is given by.

$$\left.\begin{aligned} Q_1 &= Z_1 \\ Q_i &= \text{MAX } [(Z_i) \text{ or } (Q_{i-1} + Z_i - Rt_{i-1})] \end{aligned}\right\} \quad (5.13)$$

The maximum queue size encountered is just the maximum value of Q_i over all i: $Q_{MAX} = \text{MAX } [Q_i]$.

The times of the events, T_i are inputs except in the case of T_{N+1}. This is defined to be

$$T_{N+1} = T_N + \frac{Q_N}{R}$$

Let Q_i' be the integral contribution of the interval $[T_i, T_{i+1}]$ to the mean value of Q_1 denoted by $\overline{Q}$. Let Y be the instantaneous height of the queue. The equation for Y is simply*:

$$Y = \left\{\begin{array}{l} Q_i - Rt_i \text{ so long as } Q_i - Rt_i \geq 0 \\ 0 \text{ when } Q_i - Rt_i < 0 \end{array}\right\} \quad (5.14)$$

Y is set to zero, when appropriate, to reflect the fact that there is no such thing as a negative queue.

It must be noted that two cases exist as shown in Figures 5-1a and 5-1b. In Figure 5-1a, the queue built up at time T_i is completely processed before event i + 1 occurs. That is, $Q_i - Rt_i < 0$. When this occurs, Q_i' is given by the shaded area of Figure 5-1a.

$$Q_i' = \int_{T_i = 0}^{T_{i+1}} Y \, dt = \int_0^{\frac{Q}{R}} (Q_i - Rt_i) \, dt$$

$$= \frac{Q_i^2}{2R}$$

*Taking the occurrence of event i at time zero, i.e., $T_i = 0$.

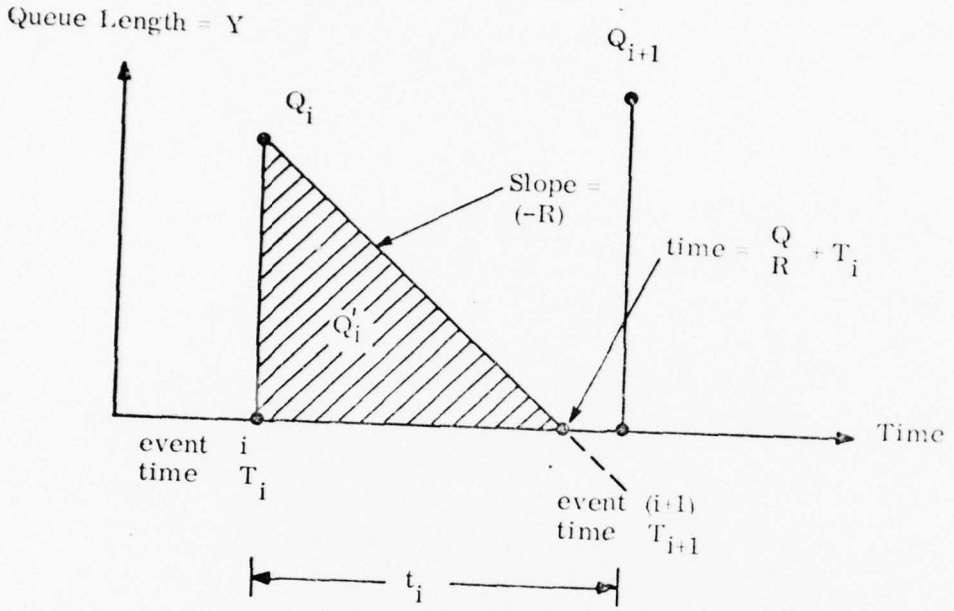

Figure 5-1a. Case 1 — Queue Length Vs. Time

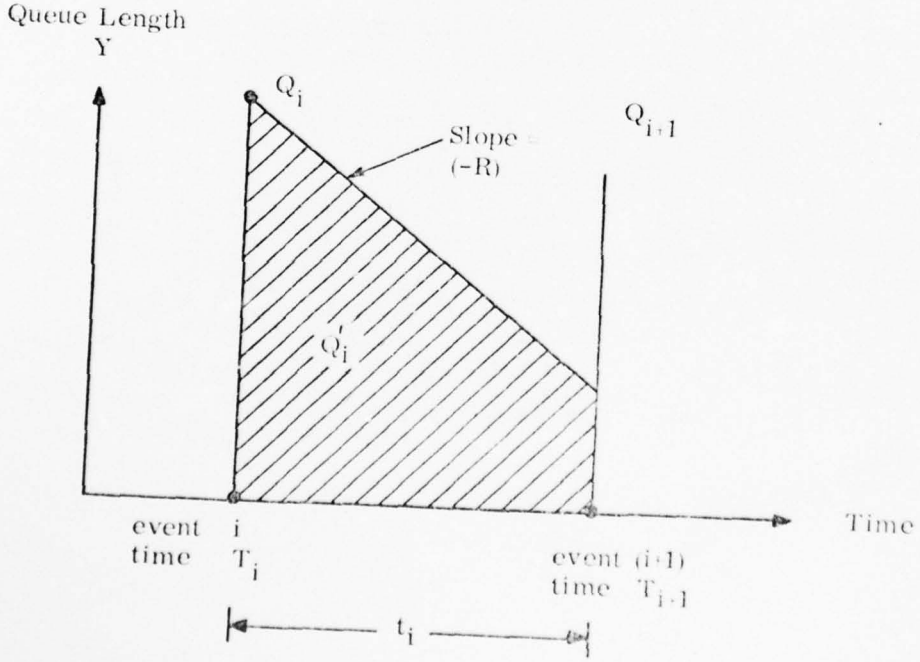

Figure 5-1b. Case 2 — Queue Length Vs. Time

The second case exists when, as shown in Figure 5-1b, the queue built up at time T_i is not completely processed by the time event i + 1 occurs. In this case

$$Q_i' = \int_0^{t_i} Y\,dt = \int_0^{t_i} (Q_i - Rt_i)\,dt$$

$$= \left(\frac{t_i}{2}\right)\left(2\,Q_i - R\,(t_i)\right)$$

Summarizing,

$$Q_i' = \begin{cases} \frac{t_i}{2}\,(2\,Q_i - R\,t_i) & \text{if } Q_i - R\,t_i \geq 0 \\ \frac{Q_i^2}{2R} & \text{if } Q_i - R\,t_i < 0 \end{cases} \qquad (5.15)$$

For completeness, Q_N' is defined as

$$Q_N' = t_N\left(\frac{Q_N}{2}\right) \qquad (5.16)$$

$\overline{Q}$, the mean queue length, is then given by

$$\overline{Q} = \frac{1}{T}\sum_{i=1}^{N} Q_i' \qquad (5.17)$$

Let Q_i'' be the integral contribution of the interval $[T_i, T_{i+1}]$ to the variance of Q, $\sigma^2(Q)$. For i = 1, . . . , N:

$$Q_i'' = \int_{T_i}^{T_{i+1}} Y^2\,dt$$

Keeping in mind the two cases discussed in computing Q_i'.

$$Q_i'' = \begin{cases} Q_i^2 t_i + \dfrac{R^2 t_i^3}{3} - Q_i R t_i^2 & \text{if } Q_i - Rt_i \geq 0 \\ \dfrac{Q_i^3}{3R} & \text{if } Q_i - Rt_i > 0 \end{cases} \tag{5.18}$$

Then, as usual:

$$\sigma^2 (Q) = \frac{1}{T} \sum_{i=1}^{N} Q_i'' - \overline{Q}^2 \tag{5.19}$$

and the standard deviation is just $\sqrt{\sigma^2 (Q)}$.

5.3.2 Computation of Waiting Times

The waiting time of the i^{th} event is given by

$$\Delta_i = \frac{[Q_i - Z_i + X + Y K_i] \phi_i}{R} \tag{5.20}$$

The maximum waiting time is: $\Delta_{MAX} = MAX (\Delta_i)$, and the mean wait time $\overline{\Delta}$ is given by

$$\overline{\Delta} = \frac{1}{N} \sum_{i=1}^{N} \Delta_i \tag{5.21}$$

The variance of the wait time $\sigma^2 (\Delta)$ is

$$\sigma^2 (\Delta) = \frac{1}{N} \sum_{i=1}^{N} (\Delta_i)^2 - \overline{\Delta}^2 \tag{5.22}$$

and the standard deviation of wait time is $\sqrt{\sigma^2 (\Delta)}$

5.3.3 Notes on the Monte-Carlo Analysis

Case A and Case B each require only a single run as the analysis is not problematic in the sense of a Monte Carlo.

Case C, however, requires a number of runs to ensure that the results become relatively stable.

A problem arises in computing the number of runs necessary to reach a relatively stable state.

Since Q_{MAX} is probably the "Nosiest" variable, at each run (denoted by j) a measure, S_j, of the fractional variance of its mean is computed as follows:

After the j^{th} Monte-Carlo iteration, the variance of the mean is estimated using the normal approximation to the distribution of variance (which is valid when j is large). The unbiased estimator of the variance is well known:

$$V_j = \frac{1}{j\,(j-1)} \sum_{i=1}^{j} \left[\overline{Q_{MAX\,(j)}} - Q_{MAX\,(i)} \right]^2 \tag{5.23}$$

The value $\overline{Q_{MAX\,(j)}}$ *is the current mean value of the variable* Q_{MAX}. This mean is now assumed to vary only slowly with increasing j, for j sufficiently large.* Then since

$$V_{j-1} = \frac{1}{(j-1)\,(j-2)} \sum_{i=1}^{j-1} \left[\overline{Q_{MAX\,(j-1)}} - Q_{MAX\,(i)} \right]^2 \tag{5.24}$$

by substituting (5.24) in (5.23), the incremental formula for the variance is:

$$V_j = \left(\frac{j-2}{j} \right) V_{j-1} + \frac{1}{j\,(j-1)} \left[\overline{Q_{MAX}} - Q_{MAX\,(j)} \right]^2 \tag{5.25}$$

Computing the fractional variance of the mean, S_j, requires dividing V_j by $\overline{(Q_{MAX})}^2$ to preserve consistency of units:

$$S_j = \left(\frac{j-2}{j} \right) S_{j-1} + \frac{1}{j\,(j-1)} \left[1 - \frac{Q_{MAX\,(j)}}{\overline{Q_{MAX}}} \right]^2 \tag{5.26}$$

*Precisely, $\overline{Q_{MAX\,(j+1)}} = \left(\frac{j}{j+1} \right) \overline{Q_{MAX\,(j)}} + \left(\frac{1}{j+1} \right) Q_{MAX\,(j)}$. Since j will be constrained to be greater than 100, these approximations are valid.

For completeness, $S_0 = 0$.

This incremental formula offers a measure of the degree of stability of the averaged results of the first j Monte-Carlo iteration. A practical stop rule is

$$j \geq 100 \text{ and } S_j \leq 10^{-6} \tag{5.27}$$

5.4 THE PI-Q PROGRAM

Figure 5-2 presents a flowchart of the overall program. Boxes numbered 1 through 9 comprise the Photo Interpreter portion of the model, and the Queueing portion consists of boxes 10 through 24.

Paragraphs 5.4.1 through 5.4.4 discuss the four utility subprograms: PROBD, SORT, RUN, and RN used by the PI-Q program. Paragraph 5.5 discusses the inputs to the PI-Q Program and Paragraph 5.6 the program's outputs.

5.4.1 PROBD1

This subroutine computes the recursion formula for the probability, P_{im}, that exactly m targets appear on frame i (see Paragraph 5.2). This subroutine is called whenever needed by the main PI-Q Program.

5.4.2 SORT

This subroutine accepts the data read from the tape discussed in Paragraph 5.5.2, and reorders the data in a manner easily handled by the PI-Q Model.

5.4.3 RUN

This subroutine is at the heart of the Queueing Model, computing the queue lengths and wait times.

5.4.4 RN

This function supplies random numbers to the Monte-Carlo simulation in the PI-Q Model.

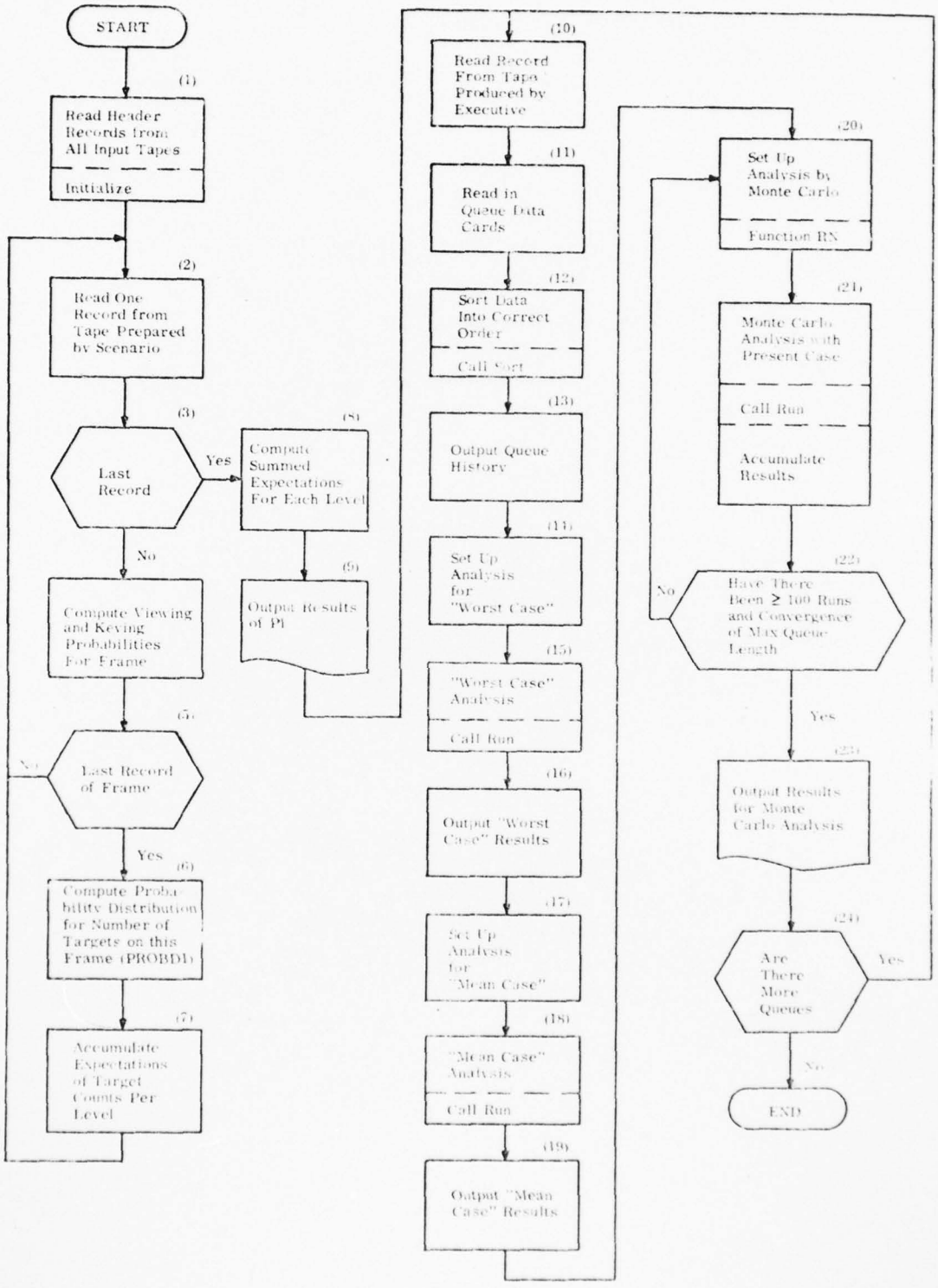

Figure 5-2. Flowchart of the PI-Q Model

5.5 PROGRAM INPUTS

The inputs to the PI-Q Model are provided by two tapes and a deck of cards.

Input Tape 1, which is generated by the Scenario Program (see Paragraph 2.7.3), contains the data used by the Photo Interpreter Model. Input Tape 2, which is generated by the Executive Program (see Paragraph 3.6.2), contains the data used by the Queueing Model.

The Card Deck, which is prepared by the user for use by the Queueing Model, defines the parameters of the transmission system on board the aircraft.

5.5.1 Input Tape 1

The information stored on Tape 1 is produced by the Scenario and sorted* by camera, frame, and target, before being passed to a program called TAPEQNT,** which computes the number of targets seen on each camera frame.

The resultant tape contains a header record (Table 2-5) and a series of sighting records (Table 2-6). This tape is read by the PI model and used to compute the data discussed in Paragraph 5.2.

5.5.2 Input Tape 2

Input Tape 2 is prepared by the Executive Program and is not modified before being used as input to the PI-Q model. The content of this tape, along with formats and definition, are given in Tables 3-3 and 3-4.

Tape 2 inputs coupled with the card inputs discussed in Paragraph 5.5.3, form the data base for the Queueing Model.

---

* This is the standard CDC 3200 library sort routine. Its use (i.e., how to set up control cards) is discussed in Appendix G, Volume II.

**The TAPEQNT program prepared by Kettelle Associates, is discussed in Appendix G, Volume II.

5.5.3 Card Input

The input cards contain information which defines the parameters of the transmission system. This data, together with that provided on Input Tape 2, allow the Queueing Model to compute waiting times and queue lengths for the transmission of data to the ground station.

In order that the user have maximum flexibility in studying a wide range of conditions, more than one set of parameters for the transmission system can be considered on any one run. Each such parameter set is processed sequentially.

Table 5-1 lists and defines the input cards.

TABLE 5-1. CARD INPUT DECK FOR THE PI-Q MODEL

CARD NUMBER	CONTENT	DEFINITION	FORMAT
1	JEXC1	Always set to 1	2I5
	JEXC2	If = 1, a "secret" label is printed on each page. (Set = 0 if not desired)	
2	IA(I) I = 1, 20	An alphanumeric name which describes or identifies the set of parameters to be considered. This is a user convenience - the program itself only prints this data.	20A4
3	B	Channel bandwidth for data transmission in units/record	4F10.4
	RO	Channel baseload data rate in units per record.	
	X	Basic data package size in units.	
	Y	Incremental data package size in units.	
Note: Cards 2 and 3 are repeated any number of times. Each such pair of cards defines a parameter set for the data transmission system. A blank card should follow all such pairs.			

5.6 OUTPUT OF THE PI-Q MODEL

5.6.1 Output of the Photo-Interpreter Model

The output of the PI is a table for each number of targets that can appear in a single frame and the expected number of frames containing that number of targets for each level of processing (other than Level 1 which is real time processing). Table 5-2 represents a hypothetical set of results.

TABLE 5-2. SAMPLE OUTPUT OF PI MODEL

	LEVEL		
N	2	3	4
0	1.0	1.1	500.0
1	0	1.0	8.0
2	3.2	4.3	10.0
3	4.5	7.2	20.0
4	7.9	19.0	11.0
5	10.0	7.0	9.0
6	16.0	3.2	6.0
7	4.0	1.5	0
8	1.0	0	2.1
9	.5	.5	0
10	0	0	0
Expected number of frames	48.9	44.8	366.1
Expected number of targets	238.0	176.5	229.8

As an illustration, there is an expected number (19.0) of frames which contain four targets at Level 3.

5.6.2 Output of the Queueing Model

The Queue output is a table of mean, maximum, and the standard deviation of queue lengths and associated waiting times for three cases: case A, worst case; case B, mean case; and case C, based on a Monte-Carlo Simulation. (See Paragraph 5.3 for a detailed discussion of the three cases.)

AD-A039 578 ANALYTICS INC WILLOW GROVE PA F/G 15/4
SIMULATION OF ADVANCED INTEGRATED RECONNAISSANCE SYSTEMS. VOLUM--ETC(U)
APR 69 S W LEIBHOLZ, S F MARTIN N62269-68-C-0441
UNCLASSIFIED 1004-1 NL

3 OF 3
AD A039 578

END

DATE
FILMED
6-77

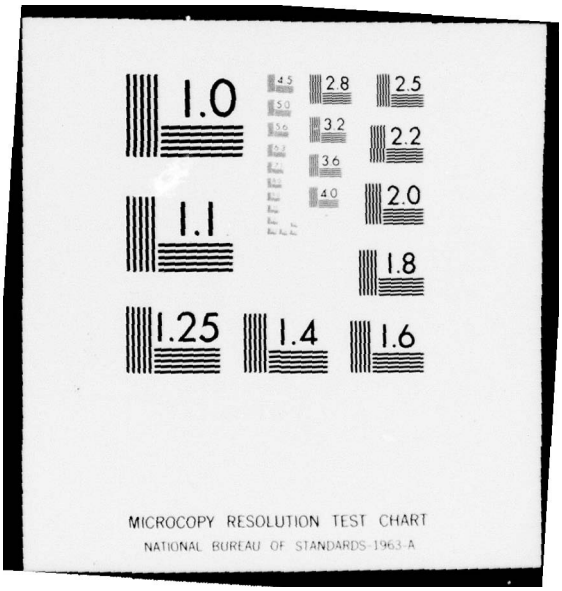
1.0
1.1
1.25
1.4
1.6
1.8
2.0
2.2
2.5
2.8
3.2
3.6
4.0
4.5
5.0
5.6
6.3
MICROCOPY RESOLUTION TEST CHART
NATIONAL BUREAU OF STANDARDS-1963-A

Table 5-3 presents a hypothetical set of results generated by Queue Models.

TABLE 5-3. SAMPLE OUTPUT OF THE QUEUE MODEL

	QMAX	QME	QSIG	DMAX	DME	DSIG
Run A	10	6	5	40	25	25
Run B	8	5	4	30	15	20
Run C	9	5	4	34	21	17

Notes for Table 5-3:

QMAX = Maximum Queue length in units
QME = Mean Queue length in units
QSIG = Standard Deviation of Queue length in unit
DMAX = Maximum wait time in minutes
DME = Mean wait time in minutes
DSIG = Standard deviation of wait time in minutes

Run A is the worst case, Run B the mean case, and Run C the Monte-Carlo case.

5.6.3 Computation of Time Late

An important part of this model involves manual computation. Using the outputs of the PI Model, a graph which portrays "time-late" can be constructed; this graph plots the percent of all targets (or alternatively, the number of targets) processed versus time.

An assumption is that it takes $K_1 + K_2$ N seconds to process (on the ground) each photo frame where K_1 and K_2 are empirically determined constants and N is the number of targets on that particular frame.

As an illustration, consider the example given in Table 5-2. In Level 2 there are 238 targets on 48.9 frames. Therefore, it takes $238K_1 + 48.9K_2$ minutes to process all frames. Let K_1 = 3 minutes and K_2 = 0.2 minutes. (Level 3 and 4 computations are analogous.) The result is the graph shown in Figure 5-3. Level 2 is always processed first because the ground station receives these frames before the end of the mission. Level 3 frames are next processed, because the "good" frames are keyed. Only after all other frames are processed are those in Level 4 considered.

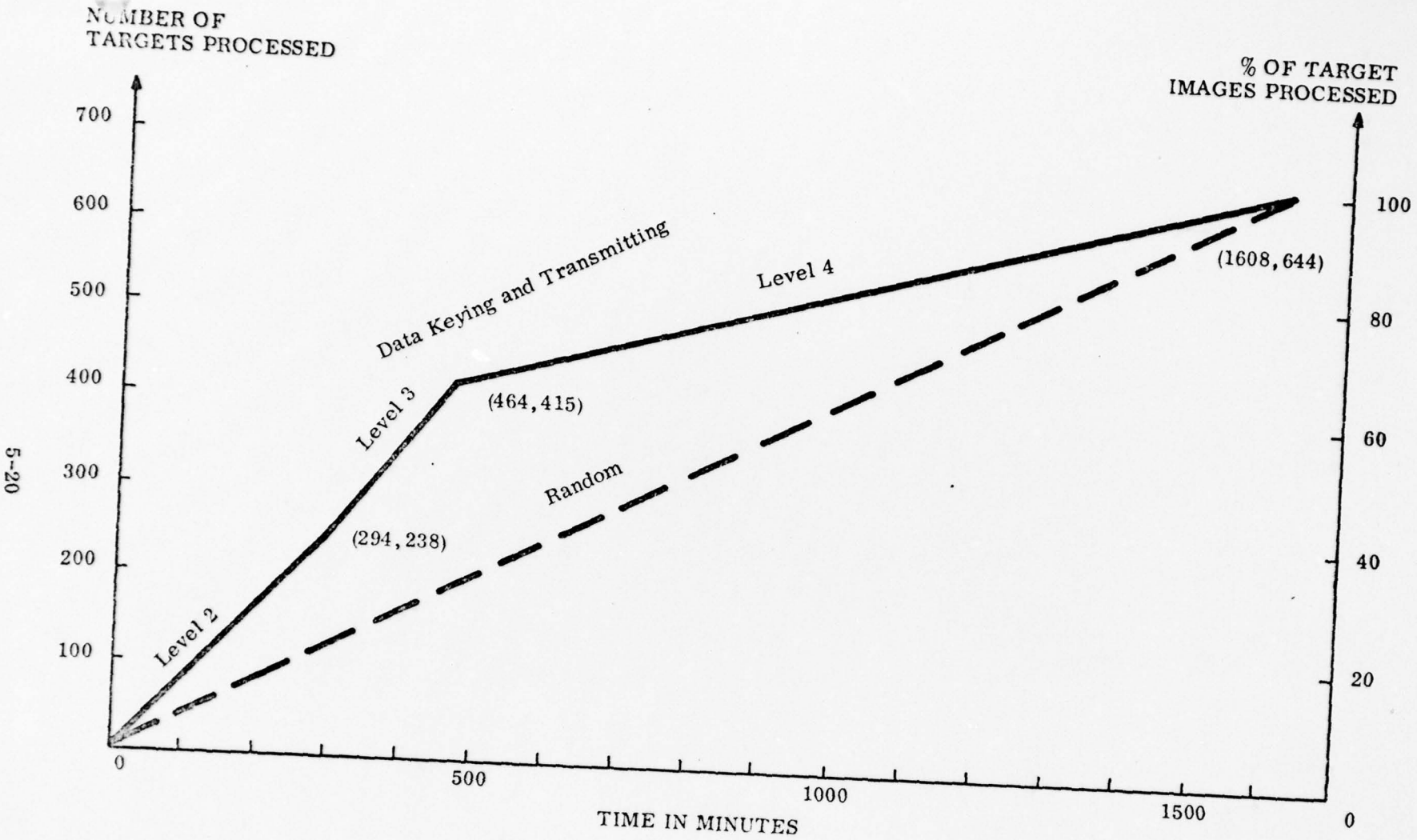

Figure 5-3. Target Processing Rates for Random Frame Selection and Data Keying Techniques

In Figure 5-3 the heavy dashed line shows the time to process, assuming a random selection of frames (i.e., no keying or transmitting). The amount that the actual curve lies above the dashed curve is an indication of the improvement in timeliness brought about by using data keying and transmitting techniques.

series of decision rules; such rules could include priorities associated with certain targets, consideration of queue length at the particular time, probability of identifying the target, and other such factors.

SECTION VI.
RECOMMENDATIONS

6.1 INTRODUCTION

It is recommended that the AIRS model be amended to include consideration of:

(1) A visual detection model

(2) An automatic topographical mapping capability

(3) Automatic detection capability

These three recommendations are discussed in more detail in the following paragraphs.

6.2 VISUAL DETECTION MODEL

As now programmed, the AIRS model does not include a visual observer. This has not been a problem since, in general, the reconnaissance operators have been found to have almost no slack time. Nevertheless, such a model would allow studying the value of visual observation, especially from the point of view of trade-offs with other sensors for overall system optimization.

6.3 TOPOGRAPHICAL MAPPING

The possibility of including another "sensor" should be considered. In particular, a tactical laser could be used for topographical mapping of the terrain. Though not strictly a sensor, this would certainly be a valuable output of the reconnaissance system.

6.4 AUTOMATIC DETECTION

Through operational use of the model it became clear that the on-board reconnaissance operator cannot keep up with the flood of information presented to him by the system for analysis. As he falls behind he keys less and less data; system performance correspondingly decreases. It is recommended that a study be made on the feasibility of incorporating an adaptive, automatic, detection capability. Such a capability would enable the system to present to the operator only that data actually known to contain target information. The adaptability would arise from exercising a

APPENDIX A. INTERSECTION OF TARGET PATH COMPUTATION

Points (X_1, Y_1) and (X_2, Y_2)

$$X^2 + Y^2 = R_2^2$$

$$Y = Y_o + (X_o - X)g$$

where

$$g = \tan \delta$$

$$Y^2 = Y_o^2 + [X_o^2 - 2X_o X + X^2]g^2 + 2 Y_o g X_o - 2 Y_o gX$$

$$X^2 + Y_o^2 + g^2 X_o^2 - 2g^2 X_o X + g^2 X^2 + 2 Y_o g X_o - 2 Y_o gX - R_2^2 = 0$$

$$X^2 [1 + g^2] + X [-2 g^2 X_o - 2 Y_o g] + [Y_o^2 + g^2 X_o^2 + 2 Y_o g X_o - R_2^2] = 0$$

Let:

$$a = 1 + g^2$$

$$b = -2 g^2 X_o - 2 Y_o g$$

$$c = Y_o^2 + g^2 X_o^2 + 2 Y_o g X_o - R_2^2$$

If

$b^2 - 4ac$ is negative, there is no real solution.

If

$b^2 - 4ac > 0$:

$$X_1 = \frac{-b + \sqrt{b^2 - 4ac}}{2a} \; ; \; Y_1^2 = R_2^2 - X_1^2$$

$$X_2 = \frac{-b - \sqrt{b^2 - 4ac}}{2a} \; ; \; Y_2^2 = R_2^2 - X_2^2$$

If

$X_2 > X_1$, interchange X_1 and X_2; Y_1 and Y_2.

Point (X_3, Y_3)

$$Y = Y_o + (X_o - X)\,g \qquad g = \tan \delta$$

$$Y = -\frac{X}{f} \qquad f = (\pi/2 - \beta)$$

$$-\frac{X}{f} = Y_o + g\,X_o - Xg$$

$$X\left[g - \frac{1}{f}\right] = Y_o + g\,X_o$$

$$X_3 = \frac{[Y_o + g\,X_o]\,f}{[fg - 1]} \qquad Y_3 = -\frac{[Y_o + g\,X_o]}{[fg - 1]}$$

Point (X_4, Y_4)

$$Y = Y_o + (X_o - X)\,g$$

$$fY = X$$

$$X\left[g + \frac{1}{f}\right] = Y_o + g\,X_o$$

$$X_4 = \frac{[Y_o + g\,X_o]}{[fg + 1]}\,f \qquad Y_4 = \frac{[Y_o + g\,X_o]}{[1 + fg]}$$

Points (X_5, Y_5) and (X_6, Y_6)

Exactly the same technique is used as in computing (X_1, Y_1) and (X_2, Y_2); the only change is that R_1 replaces R_2.

APPENDIX B. COMPUTATIONS FOR DETERMINING COORDINATES OF A TARGET PASSING THROUGH A FIELD OF VIEW

Computation of (X_1, Y_1) and (X_4, Y_4):

$$Y = Y_o + (X_o - X) \tan \delta$$

$$X_1 = \text{constant} = X_a$$

$$Y_1 = Y_o + (X_o - X_a) \tan \delta$$

$$X_4 = \text{constant} = X_c$$

$$Y_4 = Y_o + (X_o - X_c) \tan \delta$$

Computation of (X_2, Y_2):

$$Y = Y_o + (X_o - X) \tan \delta$$

$$\frac{Y_2 - Y_c}{Y_a - Y_c} = \frac{X_2 - X_c}{X_a - X_c}$$

$$Y_2 = \left[\frac{X_2 - X_c}{X_a - X_c}\right] [Y_a - Y_c] + Y_c = Y_o + \tan \delta\, X_o - \tan \delta\, X_2$$

$$Y_2 - X_2 \left[\frac{Y_a - Y_c}{X_a - X_c}\right] - X_c \left[\frac{Y_a - Y_c}{X_a - X_c}\right] + Y_c = Y_o + X_o \tan \delta - X_2 \tan \delta$$

$$X_2 \left[\frac{Y_a - Y_c}{X_a - X_c} + \tan \delta\right] = Y_o - Y_c + X_o \tan \delta + X_c \left[\frac{Y_a - Y_c}{X_a - X_c}\right]$$

$$X_2 = \frac{Y_o - Y_c + X_o \tan \delta + X_c \dfrac{Y_a - Y_c}{X_a - X_c}}{\tan \delta + \left[\dfrac{Y_a - Y_c}{X_a - X_c}\right]}$$

and finally

$$Y_2 = Y_o + \tan \delta\, (X_o - X_2)$$

Computation of (X_3, Y_3):

Following the same technique (subscript b replaces subscript a, and subscript d replaces subscript c) as in the computation of (X_2, Y_2) yields:

$$X_3 = \frac{Y_o + X_o \tan\delta - Y_d + X_D \left[\frac{Y_B - Y_D}{X_B - X_D}\right]}{\tan\delta + \left[\frac{Y_B - Y_o}{X_B - X_o}\right]}$$

$$Y_3 = Y_o + \tan\delta \ (X_o - X_3)$$

APPENDIX C. MONTE-CARLO GENERATION OF TERRAIN SAMPLES

C.1 GENERATION OF A TERRAIN SAMPLE z (x)

The main loop involves the computation of z_n according to equation (1) below and the computation of u according to equation (2) below.

z_n is the terrain elevation at the nth sampling point. Using the difference-equation, approximation to the desired terrain function expressed in Paragraph 2.4 is computed according to the difference equation

$$z_n = 3bz_{n-1} - 3b^2 z_{n-2} + b^3 z_{n-3} + cR_n \qquad (1)$$

where

$$b = 1/(1 + hr)^3 = 1/1.1^3 = 1/1.331000\ldots$$

$$c = (1 - b^2)^2 \sqrt{3\ (1 - b^2)/(1 + 4_b{}^2 \times b^4)}$$

σ = an input constant, the rms value of z (about its mean zero),

R_n = a random number evenly distributed over the interval (-1, 1)

h = 0.1/r is the horizontal distance between sampling points, and is the breakpoint "frequency", in radians/foot.

At any iteration of the main loop, u is the largest value of z_n/nh so far encountered. That is, if $z_n/nh \leq u$, replace u by the current z_n/nh; if $z_n/nh = u$, let the current value of u remain.

Or:

$$u = \text{Max} \left\{ z_i/h_i \right\}$$
$$K < i \leq n \qquad (2)$$

There are no printouts in the main loop.

To start the process, set

$z_{-12} = z_{-11} = z_{-10} = 0$ (This lets the main loop begin with the digital filter at a steady-state.)

and use equation (1) to compute

$z_{-9}, z_{-8}, z_{-7} \cdots z_{-2}, z_{-1}$.

The value of z_0 is a preassigned constant (z^*) representing target height. However, it cannot be inserted into the sequence z_{-2}, z_{-1}, z_0, and continue with the main loop. First, test to see whether z_0 fits the values z_{-3}, z_{-2}, z_{-1}.

The test is as follows:

Set $R^* = (z_0 - 3bz_{-1} + 3b^2 z_{-2} - b^3 z_{-3})/c$,

where z_0 is the preassigned value and z_{-3}, z_{-2}, z_{-1} have just been computed using equation (1).

If $-1 \leq R^* \leq 1$, set z_0 to its preassigned value and enter the main loop.

If $R^* < -1$ or $R^* > 1$, discard $z_{-9}, z_{-8}, \ldots, z_{-1}$ and return to the beginning "To start the process . . ."

To stop the process, there is a preassigned value N of main loop iterations. A stop rule has been written that can be used, if necessary, to save computer time but for now N is an input constant. The entire procedure is repeated a predetermined number of times (at least 30).

C.2 SAMPLE RESULTS

A Monte-Carlo analysis of the actual terrain model was made to check the arithmetic and to investigate the effects of quantization at steps of 10 per unit distance. For 5000 tries, σ (h) = 1.52, $\overline{X}$ = 1.86, where $\overline{X}$ is the mean distance between zero crossings of the terrain.

Thus, $u = \frac{(h - z)\overline{X}}{\rho\sigma} \quad \frac{1.52}{1.86}$

Note that $\overline{X}$ corresponds to a "half wavelength" estimate since it measures the mean distance from a positive-going zero to the next negative-going zero.

"Elevation" is defined as aircraft distance above mean terrain, i.e. above the point z = 0.

If a target is at elevation z* and an aircraft at elevation H, the ground range is ρ.

Because of this scaling algorithm, proceed as indicated in Paragraph 2.4. Basically, to simplify matters, it was only computed for values of z_0/σ equal to (-3, -2, -1, 0, 1, 2, 3). While the results indicated that geometric interpolation could be employed for other values of z (linear interpolation being not as useful according to the results), actual implementation was initially restricted to these seven integers above.

The results of the Monte-Carlo simulation were fitted with curves on a least-squares basis, and the resulting terrain-shadowing alogrithm implemented in the main simulation.

The procedure developed for programming in the Scenario Model is as follows. Referring to Table C-1 and letting P equal the cumulative shadowing probability:

(1) Select a target height relative to terrain sigma (z_o/σ) from Column A.

(2) Compute the current value of u, the corrected line of sight tangent given above.

(3) If u is less than the value in Column B, set P = 0 and exit.

(4) If u is not less than the value in Column B, but is iess than the value in Column C, then set

$$P = D \left[\frac{u - B}{C - B} \right]^2$$

where the values B, C, D are given in the respective columns; then exit.

(5) If u is not less than the value in Column C, but less than the value in Column F,

set $P = E_1 + E_2u + E_3u^2 + E_4u^3$, where E_1 through E_4 are the four values in Column E for any z_o/σ value in Column A.

(6) If u is not less than the value in Column F, set P = 1.0.

The resulting algorithm is considered good to at least two significant figures (although the long coefficients need to be retained for precision in the third-order approximation). This is more precise than any physical uncertainties associated with particular terrain samples.

TABLE C-1. COEFFICIENTS FOR TERRAIN SHADOWING ALGORITHM

A	B	C	D	E	F
-3	6.47098E01	6.6090342E01	5.6148369E-02	7.7343042723E01 -3.0561841003E00 3.9659267829E-02 -1.6808448134E-04	9.060563E01
-2	3.441621E01	4.459798E01	1.0681267E-01	1.615280661616E01 -1.0618857914E00 2.2319714703E-02 -1.4747275965E-04	6.351531E01
-1	1.563301E01	1.60589E01	6.4571343E-02	1.2971606791E00 -1.9056697404E-01 8.7192342903E-03 -1.0162780732E-04	3.52894E01
0	1.4323E-01	4.2012E-01	2.0586496E-01	6.6064529761E-02 3.534096155E-01 -5.010330503E-02 2.282623723E-03	1.119466E01
1	0.0	7.837E-02	5.9392306E-02	-3.0981982706E-01 5.2429194628E00 -7.0243511596E00 3.0479551228E00	1.05959E00
2	0.0	5.3E-02	1.6064188E-01	-2.4836507897E-01 8.8312536038E00 -2.1976417416E01 1.8016748475E01	5.7648E-01
3	0.0	1.144E-02	1.9422261E-01	2.040956524E-02 1.6159293793E01 -8.6011972132E01 1.3854173354E02	3.2343E-01

APPENDIX D. ECM PASSIVE RANGING PRECISION

D.1 INTRODUCTION

In this appendix estimates are made of the precision of passive ranging from an aircraft assuming that it flies relatively quickly past a stationary target, inspecting its bearing as a function of time and performing the resultant analysis. By "quickly" is meant that the aircraft velocity navigation errors do not change significantly during the fly-by, hence the analysis can be divided into two parts: (1) estimation of baseline range and point-of-passage errors due to angular measurement errors, and (2) independent contributions of navigational position, course, and speed errors.

This analysis further assumes that the onboard computation of target position is optimal, i.e., the on-board computer performs an unbiased minimum-variance statistical analysis of the data; this is feasible in real time, but perhaps it is not currently done.

Additionally, this analysis assumes a straight aircraft path, but it is generally applicable to known curved paths, known up to the navigation error. Plus heavy use of assumptions is made of data independence and normality, whenever reasonable, without explicity calling them out.

Finally, it will be observed that considerable simplification of the results is obtained if the passive ranging is performed symmetrically with respect to the aircraft y (wing-to-wing) axis, because by taking "looks" in this manner the estimators for the target position variables become independent of each other. Consequently, this procedure is assumed for our results, which, e.g., is not valid for passive ranging from a forward looking radar alone.

D.2 ESTIMATION OF BASELINE SLANT RANGE

Consider the two-dimensional passive ranging problem. First studied is the error in baseline range, R.

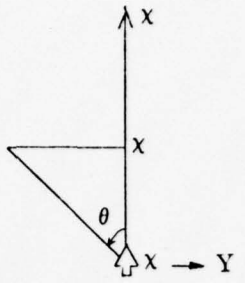

If there are n beams, in effect $\frac{n}{2}$ independent samples are taken at angles given by:

$$\theta_i = \frac{\pi}{n}(2i - 1) \qquad i = 1, \ldots \frac{n}{2} \tag{1}$$

Let

$$\sigma(\theta_i) = A\frac{2\pi}{n}$$

$$\sigma^2(\theta_i) = \sigma_o^2 = A^2\frac{4\pi^2}{n^2} \tag{2}$$

where $\frac{2\pi}{n}$ is the effective beam width and A is a measure of the angular measurement precision (sigma) relative to beam width (typically $\frac{1}{6}$).

Let:

R = true distance, target to flight-line

x = axis is flight-line, and x_o is true point of closest approach.

$R = (x - x_o)\tan\theta$, where θ is true target bearing.

Unknowns are R, x_o, and θ. However, there is an estimate $\hat{X}_o$ for the point of closest approach and the error-contaminated bearings are

$$\hat{\theta} = \theta + \delta\theta$$

Therefore target-to-flight-line distances, $\hat{R}_i$, have been estimated

$$\hat{R}_i = (X_i - \hat{X}_o)\tan(\theta_i + \delta\theta_i)$$

An estimator is required

$$\hat{R} = \sum_i C_i \hat{R}_i$$

that is unbiased and has minimum variance.

$$\hat{R} = \Sigma C_i (X_i - \hat{X}_o) \tan (\theta_i + \delta\theta_i)$$

$$= \Sigma C_i (X_i - X_o) \tan (\theta_i + \delta\theta_i) + (X_o - \hat{X}_o) \Sigma C_i \tan (\theta_i + \delta\theta_i) \qquad (3)$$

Since

$$E\,[\tan (\theta_i + \delta\theta)] = \tan\theta_i$$

$$E\hat{R} = \Sigma C_i (X_i - X_o) \tan\theta_i + (X_o - \hat{X}_o) \Sigma C_i \tan\theta_i = R \Sigma C_i$$

$$+ (X_o - \hat{X}_o) \Sigma C_i \tan\theta_i$$

In order for $\hat{R}$ to be an unbiased estimator independently of errors in $\hat{X}_o$, it is necessary and sufficient that $\Sigma C_i = 1$ and $\Sigma C_i \tan\theta_i = 0$. The θ_i is not known, so $\Sigma C_i \tan\theta_i = 0$ is not of practical value, but going back to equation (3) it can be seen that

$$\Sigma C_i \tan (\theta_i + \delta\theta_i) = 0$$

gives at once

$$\hat{R} = \Sigma C_i (X - X_o) \tan (\theta_i + \delta\theta_i)$$

$$E\hat{R} = \Sigma C_i (X - X_o) \tan\theta = R \Sigma C_i$$

so that

$$\Sigma C_i = 1, \quad \Sigma C_i \tan (\theta_i + \delta\theta_i) = 0$$

are the necessary and sufficient conditions for

$$\hat{R} = \Sigma C_i (X_i - \hat{X}_o) \tan (\theta_i + \delta\theta_i)$$

to be an unbiased estimator: $E\hat{R} = R$,

independently of errors in X_o.

The key expression $\hat{R} = \Sigma C_i (X_i - \hat{X}_o) \tan (\theta_i + \delta\theta_i)$ implies, if the $\delta\theta_i$ are independent with zero mean and common variance $\sigma^2(\theta)$, that

$$\sigma^2(\hat{R}) = \sigma^2(\theta) \Sigma \frac{C_i^2}{K_i} \tag{4}$$

where

$$K_i = \frac{\cos^4 (\theta_i + \delta\theta_i)}{(X_i - \hat{X}_o)^2}$$

It is then desirable to minimize $\Sigma C_i^2/K_i$ subject to $1 - \Sigma C_i = 0$ and $\Sigma C_i \tan (\theta_i + \delta\theta_i) = 0$:

Write

$$\hat{\theta}_i \text{ for } \theta_i + \delta\theta_i.$$

Considering

$$\Sigma \frac{C_i^2}{K_i} + \lambda_1 (1 - \Sigma C_i) + \lambda_2 (- \Sigma C_i \tan \hat{\theta}_i)$$

it can be seen that

$$\frac{2C_i}{K_i} - \lambda_1 - \lambda_2 \tan \hat{\theta}_i = 0$$

Multiplying by C_i and summing,

$$\Sigma \frac{2C_i^2}{K_i} - \lambda_1 = 0 \text{ or}$$

$$\frac{\lambda 1}{2} = \Sigma \frac{C_i^2}{K_i} = \frac{\sigma^2(\hat{R})}{\sigma^2(\theta)}$$

Multiplying by K_i and summing over i gives

$$2 - \lambda_1 \Sigma K_i - \lambda_2 \Sigma K_i \tan \hat{\theta}_i = 0.$$

Multiplying by $K_i \tan \hat{\theta}_i$ and summing gives

$$0 - \lambda_1 \Sigma K_i \tan \hat{\theta}_i - \lambda_2 \Sigma K_i \tan^2 \hat{\theta}_i = 0$$

first dividing each equation by 2,

$$\frac{\lambda_1}{2} = \frac{\Sigma K_i \tan^2 \hat{\theta}_i}{\Sigma K_i \Sigma K_i \tan^2 \hat{\theta}_i - (\Sigma K_i \tan \hat{\theta}_i)^2} \tag{5}$$

where:

$$K_i = \frac{\cos^4 \hat{\theta}_i}{(X_i - \hat{X}_o)^2}$$

The situation is: Whatever is used for $\hat{X}_o$ will give an $\hat{R}$ that is an unbiased estimator, but the variance of this estimator will depend on $\hat{X}_o$. Equation (5) shows how to select the c's for given $\hat{X}_o$ so as to minimize that variance, but that minimized variance will depend on $\hat{X}_o$. Equation (5) doesn't really explain how to select the c's; an additional step shows that

$$C_i = \frac{K_i \Sigma K_j \tan^2 \hat{\theta}_j - K_i \tan \hat{\theta}_i \Sigma K_j \tan \hat{\theta}_j}{\Sigma K_j \Sigma K_j \tan^2 \hat{\theta}_j - (\Sigma K_j \tan \hat{\theta}_j)^2}$$

but Equation (5) does tell us the resulting value of

$$\frac{\sigma^2 \hat{R}}{\sigma^2 \theta}$$

What has to be done is to select $\hat{X}_o$ so as to minimize (5). This presents problems, since

$$R = (X_i - X_o) \tan \theta_i$$

For each i, then approximately, if the errors in θ and in X_o are not too great,

$$R \cong \sin \hat{\theta}_i \frac{\lambda_i - \hat{X}_o}{\cos \hat{\theta}_i}$$

or

$$K_i \cong \sin^2 \hat{\theta}_i \cos^2 \hat{\theta}_i / R^2 \tag{6}$$

This removes $\hat{X}_o$ from consideration and no optimization with respect to $\hat{X}_o$ remains. In effect, what has been said is that near the best $\hat{X}_o$, which is near the correct X_o as well, the optimum is relatively flat. Then (5) becomes

$$\frac{\lambda_1}{2} = \frac{\sigma^2(\hat{R})}{\sigma^2(\theta)} = R^2 \frac{\sin^4 \hat{\theta}_i}{\Sigma \sin^2 \hat{\theta}_i \cos^2 \hat{\theta}_i \; \Sigma \sin^4 \hat{\theta}_i - (\Sigma \sin^3 \hat{\theta}_i \cos \hat{\theta}_i)^2} \tag{7}$$

This is the limit using actual values of bearing (observed) $\hat{\theta}_i$. Matters become simplified when assuming continuous or evenly-spaced looks. The squared term in the denominator of equations (7) or (5) is the square of a sum that goes to zero if the same looks are taken going and coming. That is, a look at $\hat{\theta}_i$ and one at $\pi - \hat{\theta}_i$ cancels each other in the sum. The squared term might be considered as a loss of precision due to failure to take advantage of some looks. Dropping this squared term

$$\sigma^2(\hat{R}) = \frac{\sigma^2(\theta) R^2}{\sin^2 \hat{\theta}_i \cos^2 \hat{\theta}_i} \tag{8}$$

or in terms of equation (5),

$$\sigma^2(\hat{R}) = \sigma^2(\theta) / \Sigma \frac{\cos^4 \hat{\theta}_i}{(X_i - \hat{X}_o)^2}$$

$$\sigma^2(\hat{R}) \cong \sigma^2(\theta) / \Sigma \frac{(X_i - X_o)^2}{(R^2 - (X_i - X_o)^2)^2}$$

Substituting in equation (2)

$$\sigma(R) = 2\pi AR\ \phi(n) \tag{9}$$

where

$$\phi(n) = \frac{1}{n}\left(\sum_{1}^{n/2} \sin^2\theta_i \cos^2\theta_i\right)^{-1/2} \tag{10}$$

and where

$$\theta_i = \frac{\pi}{n}(2i - 1) \tag{11}$$

The function $\phi(n)$ is tabulated in Table D-1.

D.3 ESTIMATION OF DOWN-RANGE POSITION

The following procedure is not necessarily optimum; it depends on the assumption that the value of R (namely $\hat{R}$) discovered is also optimum for estimating X_o. This obviously is not necessarily the case. As a matter of fact, finding R and X_o from the observations with the objective of minimizing their CEP could have been done, but the algebra would be extensive.

Using the same assumptions as in equation (2) and adding the selection of $\hat{R}$ as optimum.

$$\hat{X}_i - X_{oi} = \frac{R}{\tan\hat{\theta}_i} \tag{12}$$

Again

$$\hat{X}_o = \Sigma\, C_i\, X_{oi}$$

$$X_{oi} = X_i - \frac{R}{\tan\hat{\theta}_i}$$

TABLE D-1. COMPUTATION OF ϕ (n) FOR PASSIVE RANGING PRECISION

No. of Beams	Value of ϕ
4	.353553
6	.272165
8	.176777
10	.126491
12	.096225
14	.076360
16	.062509
18	.052378
20	.044721
22	.038764
24	.034021
26	.030172
28	.026997
30	.024343
32	.022097
34	.020176
36	.018519
38	.017076
40	.015811
42	.014696
44	.013705
46	.012821
48	.012028
50	.011314
52	.010667
54	.010080
56	.009545
58	.009056
60	.008607
62	.008194
64	.007812
66	.007460
68	.007133
70	.006830
72	.006547
74	.006284
76	.006037
78	.005807
80	.005590
82	.005387
84	.005116
86	.005015
88	.004845
90	.004685
92	.004533
94	.004389
96	.004253
98	.004123
100	.004000

$$\sigma^2 (X_{oi}) = \sigma^2 R \frac{1}{\tan^2 \hat{\theta}_i} + R^2 \sigma^2 (\hat{\theta}_i) \csc^4 \hat{\theta}_i$$

$$\sigma 2 (X_o) = \sigma^2 R \sum C_i^2 \frac{1}{\tan^2 \hat{\theta}_i} = R^2 \sigma^2 (\hat{\theta}_i) \Sigma C_i^2 \csc^4 \hat{\theta}_i \qquad (13)$$

Which must be minimized subject to the constraint $\Sigma C_i = 1$.

Reasoning from the results of equation (2), it is obvious that if the observations are symmetrically disposed about $\theta = \frac{\pi}{2}$ then, provided that C_i are likewise assigned symmetrically, the result will be unbiased by errors in R. In fact the precise condition is, by inspection, that

$$\sum \frac{C_i^2}{\tan^2 \theta_i} = 0.$$

Equation (13) can be simplified as well (interchanging θ_i and $\hat{\theta}_i$ to simplify the analysis)

$$\sigma^2 (X_{oi}) = R^2 \sigma^2 (\theta_i) \csc^4 \theta_i$$

$$\sigma^2 (X_o) = R^2 \sigma^2 (\theta_i) \Sigma C_i^2 \csc^4 \theta_i \qquad (14)$$

Referring to Appendix E*

$$K_i = R^2 \csc^4 \theta_i$$

and, directly

$$\sigma^2 (X_o) = \sigma^2 (\theta_i) \frac{1}{\sum \frac{1}{R^2 \csc^4 \theta_i}} \qquad (15)$$

Thus, combining the results with equation (1)

$$\sigma (X_o) = 2 \pi A R \psi (n) \qquad (16)$$

*Appendix E presents a technique for finding the minimum - variance estimate of a mean value.

where

$$\psi\,(n) = \frac{1}{n\,(\Sigma \sin^4 \theta_i)^{1/2}} \tag{17}$$

The function ψ (n) is tabulated in Table D-2.

D.4 SIMPLIFICATION FOR LARGE N

If n is large (say 8 or more) then the sums in Equations (10) and (17) may be replaced by integrals

$$\int_0^{\pi} \sin^2 \theta_i \cos^2 \theta_i \, \delta\theta_i = \frac{\pi}{8}$$

$$\int_0^{\pi} \sin^4 \theta_i \, \delta\theta_i = \frac{3\pi}{8}$$

So that, roughly,

$$\sigma R \cong \frac{2\pi AR}{n} \sqrt{\frac{8}{\pi}} = \frac{4\sqrt{2\pi}\,AR}{n} \tag{18}$$

$$\sigma X_o \cong \frac{2\pi AR}{n} \sqrt{\frac{8}{3\pi}} = \frac{1}{\sqrt{3}}\,\sigma R \tag{19}$$

Then

$$CEP \cong \frac{2\pi AR}{n} \frac{1}{\sqrt[4]{3}} \quad (1.178) \tag{20}$$

$$CEP \cong 5.63 \frac{AR}{n} \tag{21}$$

$$\cong 0.88\, R\, \sigma(\theta) \tag{22}$$

And, if P is the fractional number of times observed relative to the possible n/2 observations

$$CEP \cong \frac{0.88\, R\, \sigma(\theta)}{P} \tag{23}$$

TABLE D-2. COMPUTATION OF $\psi(n)$ FOR PASSIVE RANGING PRECISION

No. of Beams	Value of ψ
4	.353553
6	.157135
8	.102062
10	.073030
12	.055556
14	.044087
16	.036084
18	.030241
20	.025820
22	.022380
24	.019642
26	.017420
28	.015587
30	.014055
32	.012758
34	.011649
36	.010692
38	.009859
40	.009129
42	.008484
44	.007913
46	.007402
48	.006532
50	.006159
52	.006159
54	.005820
56	.005511
58	.005228
60	.004969
62	.004731
64	.004511
66	.004307
68	.004118
70	.003943
72	.003780
74	.003628
76	.003486
78	.003352
80	.003227
82	.003110
84	.003000
86	.002896
88	.002798
90	.002705
92	.002617
94	.002534
96	.002455
98	.002380
100	.002309

D.5 EFFECTS OF NAVIGATIONAL ERRORS

It has been assumed that the navigational errors are small and essentially constant over the time of target observation.

Let $\sigma^2(X)$ and $\sigma^2(y)$ be the variance of position navigation along and across the track, respectively.

(Approximately, $\sigma X = \sigma y = 0.849$ CEP (Nav)).

Let:

σ^2_v be the variance of ground speed estimation (v).

$\sigma^2_{\theta_n}$ be the variance of heading (θ_n).

It is assumed that the drift angle is small and that in the passive ranging calculations corrections were made for the predicted drift.

The effects are as follows:

(1) The navigation position variances simply add to the passive ranging position variances.

(2) The speed error causes an error in $(\hat{X}_i)$ proportional to $(\hat{X}_i - X_o)$, hence it is equivalent to a scale correction of $\Delta v/v$ as far as R-measurement goes. It has no first-order effect on X_o measurement in the symmetrical case, provided $\sigma x, \sigma y$ are taken at the point X_o.

The heading error enters in a complex way, if large. However, if small compared to θ_i, it has, by symmetry, no first-order effect on R, but displaces X_o by an amount R sin $(\Delta\theta_n) \cong R \Delta\theta_n$.

Thus,

$$\bar{\sigma}^2(X_o) \cong \sigma^2(X_o) + \sigma^2(X) + R^2\sigma^2(\theta_n) \tag{24}$$

$$\bar{\sigma}^2(R) \cong \sigma^2(R) + \sigma^2(y) + \frac{R^2}{v^2}\sigma^2(v) + \left[\left(\frac{H_T}{(H_A - H_T)}\right) DIS\right]^2 \tag{25}$$

where: DIS = ground range to the target
H_T = height of the target
H_A = height of the aircraft

Or, to use the simplified formulas

$$\bar{\sigma}^2 (X_o) = \frac{32\pi A^2 R^2}{3 n^2} + 0.72 \, [CEP(Nav)]^2 + R^2 \sigma^2 (\theta_n) \tag{26}$$

$$\bar{\sigma}^2 (R) = \frac{32\pi A^2 R^2}{n^2} + 0.72 \, [CEP (Nav)]^2 + \frac{R^2}{v^2} \sigma^2 (v) \tag{27}$$

Ignoring the CEP (nav) terms, assuming in effect that the position errors are removed via relative positioning, the navigational errors become dominant (i.e., cross over) when, roughly

$$\sigma(\theta_n) \geq \sqrt{\frac{8}{3\pi}} \, \sigma(\theta_i) \tag{28}$$

or

$$\sigma(v) \geq v \sqrt{\frac{8}{3\pi}} \, \sigma(\theta_i) \tag{29}$$

APPENDIX E. MINIMUM-VARIANCE ESTIMATE OF A MEAN VALUE

Consider a number of independent measurements x_i made on a quantity x to ascertain a best value for some function $y = f(x)$. Let

$$y_i = f(x_i) \tag{1}$$

Using small-error and independence assumptions, we have

$$\sigma^2 (y_i) = K_i \sigma^2 (x_i) \tag{2}$$

where $\sigma^2 (x_i)$, the variance of the i^{th} measurement, is assumed a constant for all i and

$$K_i = \left(\frac{\partial f}{\partial x_i} \right)^2 \tag{3}$$

Let us use a linear unbiased estimator $\hat{y}$. Hence,

$$\hat{y} = \Sigma P_i y_i \tag{4}$$

where for normalization we set

$$\Sigma P_i = 1$$

chosen for best fit, i.e., minimum variance. By standard formulae we have

$$\sigma^2 (\hat{y}) = \Sigma P_i^2 \sigma^2 (y_i). \tag{6}$$

Minimize equation (6) subject to the constraint equation (5) using a Lagrange multiplier λ.

Let

$$U = \Sigma P_i^2 \sigma^2 (y_i) + \lambda (1 - \Sigma P_i) \tag{7}$$

$$U = \sigma^2 (x_i) \Sigma P_i^2 K_i + \lambda (1 - \Sigma P_i) \tag{8}$$

and let

$$\sigma^2(x_i) = \sigma_o^2 \tag{9}$$

Hence,

$$\frac{\partial U}{\partial P_i} = \sigma_o^2\, 2\, P_i\, K_i - \lambda = 0 \tag{10}$$

and

$$\frac{\partial U}{\partial \lambda} = 1 - \sum P_i = 0 \text{ for minimization.} \tag{11}$$

Solving

$$P_i = \frac{\lambda}{2\sigma_o^2\, K_i} \quad , \text{ and}$$

$$\lambda = \frac{2\sigma_o^2}{\sum_\ell \frac{1}{K_\ell}}$$

substituting in equation (10)

$$2\sigma_o^2\, P_i\, K_i - \frac{2\sigma_o^2}{\sum_\ell \frac{1}{K_\ell}} = 0$$

$$P_i = \frac{1}{K_i \sum 1/K_\ell}$$

Then from equations (6) and (2)

$$\sigma^2(\hat{y}) = \sigma_o^2 \sum P_i^2\, K_i$$

$$\sigma^2(\hat{y}) = \sigma_o^2 \sum \frac{1}{K_i \left(\sum_\ell \frac{1}{K_\ell}\right)^2} = \frac{\sigma_o^2}{\sum_\ell 1/K_\ell} \tag{12}$$

We can also show that this linear unbiased minimum variance estimator is maximum likelihood. For a particular estimate

$$\hat{y} = \sum_j a_j y_j,$$

the value of the log-likelihood function is (letting $\sigma_i^{*2} = \sigma^2(y_i)$)

$$Q = \sum_i \log\left\{\sqrt{\frac{1}{2\pi\sigma_i^{*2}}}\, e^{-\left[\frac{(x_i - \sum_j a_j x_j)^2}{2\sigma_i^{*2}}\right]}\right\}$$

$$= \sum_i \left\{-\log\left(\sqrt{2\pi\sigma_i^{*2}}\right) - \frac{(x_i - \sum_j a_j x_j)^2}{2\sigma_i^{*2}}\right\}$$

Hence,

$$\frac{\partial Q}{\partial a_k} = x_k \sum_i \frac{2(x_i - \sum_j a_j x_j)}{2\sigma_i^{*2}} \qquad (13)$$

For maximum likelihood, equation (13) must be 0 for all k.

Hence, we must have

$$\sum_i \frac{x_i}{\sigma_i^{*2}} = \sum_i \frac{\sum_j a_i x_j}{\sigma_i^{*2}}$$

But this will be true only for

$$a_j = \frac{1/\sigma_i^{*2}}{\sum_\ell 1/\sigma_\ell^{*2}}$$

Now setting

$$\sigma_i^{*2} = K_i \sigma_o^2$$

and rewriting we get

$$a_i = \frac{1}{K_i \sum_{\ell} 1/K_{\ell}} = P_i$$

so our above estimate is maximum likelihood also.

APPENDIX F. INDIVIDUAL SENSOR PERFORMANCE MEASURE

F.1 INTRODUCTION

The EVAL routine computes a measure of individual sensor contribution to the overall effectiveness of the AIRS System.

F.2 DERIVATION

Two measures are derived of individual sensor contributions that are theoretically sound and computationally simple. One is called the "scaled" measure, and the other "unscaled". Each rests on different assumptions; hence, the analysis will result in two sets of M numbers: α_i and β_i. The numbers are between 0 and 1 and represent the unscaled and scaled contribution of sensor i, respectively; the larger the number, the larger the contribution. The input data for this problem consists of an M x N matrix P_{ij}, $1 \leq i \leq M$; $1 \leq j \leq N$. The input M represents the number of sensors; N represents the number of target sightings; and P_{ij} is the probability that sensor i detects target sighting j.

Consider a situation with just one target sighting, i.e., fix j constant. Let $P_{\bullet j}$ be the overall detection probability that at least one of the M sensors will detect the target. Then $P_{\bullet j}$ is precisely one minus the probability that all sensors see nothing.

The probability that sensor i does not detect the sighting is $1 - P_{ij}$. Hence, assuming the sensors operate independently, the probability that not a single sensor detects is

$$\prod_{i=1}^{M} (1 - P_{ij}) \tag{1}$$

Hence,

$$P_{\bullet j} = 1 - \prod_{i=1}^{M} (1 - P_{ij}) \tag{2}$$

Note: Cap P_{ij} and lower case p_{ij} are used interchangeably in this Appendix.

Let a particular sensor k be fixed and removed from the AIRS system. Let $p_{\bar{k}j}$ be the overall detection probability of target passage j for this new system of M-1 sensors. By the above argument,

$$P_{\bar{k}j} = 1 - \prod_{i \neq k} (1 - P_{ij}) \tag{3}$$

but

$$\prod_{i \neq k} (1 - P_{ij}) = \frac{\prod_{i=1}^{M} (1 - P_{ij})}{(1 - P_{kj})} \tag{4}$$

so

$$P_{\bar{k}j} = 1 - \frac{\prod_{i=1}^{M} (1 - P_{ij})}{(1 - P_{kj})} \tag{5}$$

$$= \frac{1 - P_{kj} - \prod_{i=1}^{M} (1 - P_{ij})}{(1 - P_{kj})}$$

or, simply,

$$P_{\bar{k}j} = \frac{P_{\bullet j} - P_{kj}}{1 - P_{kj}} \tag{6}$$

An excellent measure of the usefulness of sensor k is given by $p_{\bar{k}j}/p_{\bullet j}$, the ratio of total detectability without sensor k to total detectability with it. If this ratio is close to 1, sensor k is not very important; if it is near 0, k contributes quite a bit.

To make this a direct rather than inverse relationship let

$$x_{kj} = 1 - \frac{P_{\bar{k}j}}{P_{\bullet j}} \tag{7}$$

be defined as the fixed target contribution of sensor k to overall AIRS performance.

The case where $p_{\bullet i} = 0$ is an exception: x_{kj} does not exist. Sensor k could be assigned a measure of 0 (after all, the system loses nothing by eliminating k since it had nothing to begin with), but this would be unfairly prejudicing the measure; likewise a value of 1 is plausible (sensor k provides all the system capability - nothing is all of nothing), but for the same reasons is unfair. Hence, no assignment is made of any x_{kj} for all sensors k when $P_{\bullet j} = 0$.

An algebraic simplification of x_{ij} is shown below.

$$x_{ij} = 1 - \frac{P_{ij}}{P_{\bullet j}}$$

$$= 1 - \frac{P_{\bullet j} - P_{ij}}{\frac{1 - P_{ij}}{P_{\bullet j}}}$$

$$= 1 - \frac{P_{\bullet j} - P_{ij}}{P_{\bullet j} - P_{\bullet i} P_{ij}}$$

$$= \frac{P_{\bullet j} - P_{\bullet j} P_{ij} - P_{\bullet j} + P_{ij}}{P_{\bullet j} - P_{\bullet j} P_{ij}}$$

$$= \frac{P_{ij} - P_{ij} P_{\bullet j}}{P_{\bullet j} - P_{ij} P_{\bullet j}}$$

$$= \left(\frac{1 - P_{\bullet j}}{P_{\bullet j}}\right)\left(\frac{P_{ij}}{1 - P_{ij}}\right) \qquad (8)$$

Equation (8) is used to compute x_{ij}.

To derive the final measures the x_{ij}'s are combined over all target sightings j for which x_{ij}'s exist. Two different integration procedures are plausible; therefore, two different measures are found.

First, assuming all target sightings are equally important then a straight average will suffice; that is,

$$\alpha_i = \frac{1}{N'} \Sigma x_{ij} \tag{9}$$

where the sum is taken over all j such that $p_{\bullet j} \neq 0$ and N' is the number of such j's. This is called the unscaled measure.

However, it may be desired to assume that all detected target sightings are equally important. It is not known in advance whether or not a particular target will in fact be detected, but this can be taken care of by scaling the measure in proportion to expected target sighting detections. In other words, instead of a straight average over the x_{ij}'s a weighted average is formed with weights equal to the overall detection probability of sighting j. Thus,

$$\beta_i = \frac{P_{\bullet 1} x_{i1} + P_{\bullet 2} x_{i2} + \cdots + P_{\bullet N'} x_{\bullet N'}}{P_{\bullet 1} + P_{\bullet 2} + \cdots + P_{\bullet N'}}$$

$$= \frac{1}{\Sigma_j P_{\bullet j}} \Sigma_j P_{\bullet j} x_{ij} \tag{10}$$

where the sum is over all j such that $p_{\bullet j} \neq 0$ and N' is the same as before. This is called the scaled measure.

The difference between the two measures is easy to appreciate. Suppose one sensor provides 90 percent of a 0.01 system detectability for a given target and a second sensor provides 50 percent of a 0.99 detectability for another target. Relative to the two targets, the first sensor contributes more than the second to overall effectiveness if unscaled measures are used, while the reverse is true for a scaled analysis.

Using the above algebraic simplification, the final forms of the two measures are shown as.

$$\alpha_i = \frac{1}{N} \Sigma \frac{P_{ij}}{1 - P_{ij}} \times \frac{1 - P_{\bullet j}}{P_{\bullet j}} \tag{11}$$

$$\beta_i = \frac{1}{\Sigma P_{\bullet j}} \Sigma \frac{(P_{ij})\ (1 - P_{\bullet j})}{1 - P_{ij}} \tag{12}$$

F.3 CRITIQUE AND ANALYSIS

F.3.1 Introduction

This paragraph discusses several aspects of the measures that add to their usefulness and increase the reader's understanding. Included are three completely resolved numerical examples. Each example consists of two tables: the first gives the p_{ij} matrix, the $p_{\bullet j}$ vector, the overall expected detection values, and the $p_{\bullet j} / \sum_j p_{\bullet j}$ ratios; the second includes the x_{ij}'s, the α_i's, and the β_i's.

F.3.2 Expected Values

For a given sensor i, the sum of p_{ij} over all j gives the expected target sighting detection value, i.e., the expected number of passed over targets that sensor i will detect in a given aircraft run. It is important to note that neither α_i nor β_i are necessarily in proportion to this expected value. If several sensors have similar high detection probabilities over a set of sightings, then they all have large expected values but small α's and β's. This is for the simple reason that the system loses nothing if one of these sensors is removed, because individual contribution and importance, are measured, not frequency of detection. (See examples.)

However, the β measure for a sensor can be related to a meaningful expected value percentage. In the same way that $\sum_j p_{ij}$ is the expected detections for sensor i, $\sum_j p_{\bullet j}$ is the expected number of target sighting detections for the overall systems. (Hereafter denoted by ED.)

Hence,

$$\beta_i = \frac{1}{\sum_j P_{\bullet j}} \sum_j P_{\bullet j}\, x_{ij}$$

$$= \frac{1}{ED} \sum_j P_{\bullet j} \left(\frac{P_{\bullet j} - P_{\bar{i}j}}{P_{\bullet j}} \right)$$

$$= \frac{1}{ED} \left[\sum_j P_{\bullet j} - \sum_j P_{\bar{i}j} \right]$$

$$= \frac{ED - ED_{\bar{i}}}{ED} \qquad (13)$$

where Ex $D_{\bar{i}}$ is the expected target sighting detections with sensor i removed from the system. So therefore

$$\beta_i = 1 - \frac{ED_{\bar{i}}}{ED} \qquad (14)$$

In other words (interpreting equation (14), β_i is the expected percentage (decimal) of overall system target sighting detections that will be lost if sensor i is removed.

F.3.3 Marginal Contribution of Sensors

A brief defense of the methodology used in the construction of the measures is given.

Basically, it must be realized that a given sensor does not contribute its entire detection probability to the system effectiveness for a particular target. The addition law for independent events in probability theory guarantees that the whole is always less than the sum of its parts. For this reason using p_{ij} as the measure is unsatisfactory. In particular, the direct measure $p_{ij}/p_{\bullet j}$ overestimates contribution, while the inverse measure underestimates it.

To fairly construct a measure the marginal contribution of a sensor must be studied. It must be found what sensor i contributed to the system that it did not already have. It is precisely for this reason that $p_{\bar{ij}}$ was introduced (note that $p_{\bar{ij}} + P_{ij} \neq p_{\bullet j}$). Fair measures would then have the form $p_{\bullet j} - p_{\bar{ij}}$ (direct) and $p_{\bar{ij}}/p_{\bullet j}$ (inverse) which are precisely what the β and α measures, respectively, are based on.

F.3.4 Use of the Measures

It must be remembered that α and β are primarily measures of individual contribution compared to the overall system and should be interpreted in that light. In the case of the β measure (which has a direct expected value interpretation) intra-sensor scale comparisons can be made, i.e., sensor i is twice as important as sensor k, but, in general, results of the analysis should be stated in terms of the ranking induced on the sensors by the measures (sensor i is the most important, sensor k the least). The α induced ranking sometimes differs from the β induced ranking and sometimes does not. (Compare Examples 1 and 2.)

Any change whatsoever in the system can vastly change the values of the measures. Therefore it is erroneous to conclude that the two or three lowest valued sensors can be eliminated from the system without much effectiveness loss. Rather, only the least valuable sensor can be dropped and the measures must then be recomputed for the resulting system. It is possible that a previously low ranked sensor will be quite important in the new system. (Compare, using α measures, Examples 2 and 3.)

F.3.5 Independence

An assumption made in the derivation is that sensors are independent, thus allowing the combining of probabilities by taking products. Although it is assumed, it is not entirely obvious that it is a valid assumption. The fact that the sensors are physically independent is not enough to guarantee statistical independence. For instance, if one sensor works better at night and another during the day, then the two are not statistically independent even though there is no physical connection between them, i.e., knowing the performance of one of them helps in guessing the performance of the other.

If no independence is assumed, the measure can still be computed if all the conditional distributions are given. Of course, $p_{\bullet j}$ and $p_{\bar{i}j}$ would be calculated differently and x_{ij} would not algebraically simplify. *

F.3.6 Degeneracy

Looking at the simplified form for x_{ij}, it can be seen that degeneracy occurs when $p_{\bullet j} = 0$ or $p_{ij} = 1$. The former case has already been discussed; sensors are given no value for that target. If $p_{ij} = 1$, the value 1 is then assigned to x_{ij}. This is the obvious thing to do - sensor i provides all of the system capability.

That $x_{ij} = 1$ in this case can also be demonstrated formally. If $p_{ij} = 1$, then $p_{\bullet j} = 1$ so $p_{ij} = p_{\bullet j}$. Hence,

$$x_{ij} = \frac{p_{ij}}{1 - p_{ij}} \times \frac{1 - p_{\bullet j}}{p_{\bullet j}}$$

$$= 1$$

*However, it is certainly not possible to obtain these conditionals.

EXAMPLE 1

3 Sensors
3 Targets

p_{ij}

	Target 1	Target 2	Target 3	Sensor Expected Value
Sensor 1	0.9	0	0	0.9
Sensor 2	0.8	0	0	0.8
Sensor 3	0	0.1	0.2	0.3
$P_{\bullet j}$	0.98	0.1	0.2	
$P_{\bullet j}/\Sigma_j P_{\bullet j}$	0.765	0.078	0.157	

x_{ij}

	Target 1	Target 2	Target 3	α_i	β_i
Sensor 1	0.183	0	0	0.061	0.140
Sensor 2	0.081	0	0	0.027	0.062
Sensor 3	0	1	1	0.667	0.235

EXAMPLE 2

3 Sensors
2 Targets

p_{ij}

	Target 1	Target 2	Sensor Expected Value
Sensor 1	0.9	0	0.9
Sensor 2	0.8	0	0.8
Sensor 3	0	0.1	0.1
$p_{\bullet j}$	0.98	0.1	
$p_{\bullet j} / \Sigma p_{\bullet j}$	0.907	0.093	

x_{ij}

	Target 1	Target 2	α_i	β_i
Sensor 1	0.183	0	0.092	0.166
Sensor 2	0.081	0	0.041	0.074
Sensor 3	0	1	0.5	0.093

EXAMPLE 3

2 Sensors
2 Targets

	Target 1	Target 2	Sensor Expected Value
Sensor 1	0.9	0	0.9
Sensor 2	0	0.1	0.1
$p_{\bullet j}$	0.9	0.1	
$p_{\bullet j}/\Sigma p_{\bullet j}$	0.9	0.1	

x_{ij}

	Target 1	Target 2	α_i	β_i
Sensor 1	1	0	0.5	0.9
Sensor 2	0	1	0.5	0.1